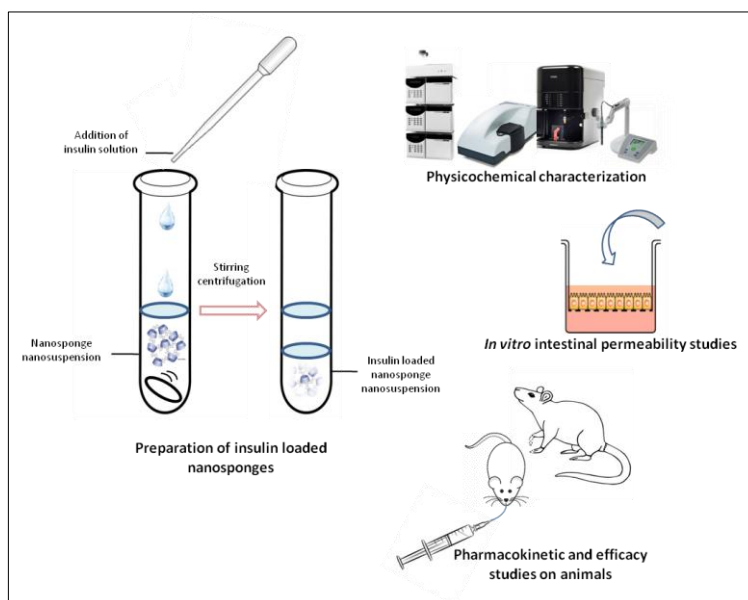## Università degli Studi di Torino

Doctoral School of the University of Torino

PhD Programme in Chemical and Materials Sciences XXXIV Cycle

Polysaccharide-based biomaterials for controlled protein delivery applications

Silvia Lucia Appleton

Supervisor:
Prof. Francesco Trotta
Co-Supervisor:
Prof.ssa Roberta Cavalli

Università degli Studi di Torino

Doctoral School of the University of Torino

PhD Programme in Chemical and Materials Sciences XXXIV cycle

Polysaccharide-based biomaterials for controlled protein delivery applications

Candidate:　　　　**Silvia Lucia Appleton**

Supervisor:　　　　Prof. **Francesco Trotta**
Co-Supervisor:　　　Prof.ssa **Roberta Cavalli**

Jury Members:　　　Prof. **Andrea Mele**
　　　　　　　　　Polytechnic University of Milan
　　　　　　　　　Department of Chemistry, Materials and Chemical Engineering "Giulio Natta"

　　　　　　　　　Prof.ssa **Fabiana Quaglia**
　　　　　　　　　University of Naples Federico II
　　　　　　　　　Department of Pharmacy

　　　　　　　　　Prof. **Marco Zanetti**
　　　　　　　　　University of Turin
　　　　　　　　　Department of Chemistry

Head of the Doctoral School:　　Prof. Alberto Rizzuti
PhD Programme Coordinator:　　Prof. Bartolomeo Civalleri

Torino, 2022

Abstract

Peptides and proteins have recently attracted a great deal of attention due to an increased awareness of their therapeutic potential.

Despite this, significant limitations have restricted their use in medicine due to their low bioavailability, thus necessitating the search for adequate drug carriers.

This PhD project aims to develop drug delivery systems suitable for proteins, with insulin chosen as a case study for its relevance to diabetes treatment and its oral formulation is still greatly desired.

As the nanoporous structure of starch nanosponges (NS) has proven to be suitable for various classes of drugs, cyclodextrin and linecaps-based hyper-crosslinked polymers were thought to be promising for the delivery of macromolecules like proteins as well, and thus herein proposed.

In detail, the formulation of three kinds of nanosponges (industrial NS, pyromellitic dianhydride crosslinked β-cyclodextrin NS and citric acid crosslinked Linecaps NS) was fine-tuned by adopting a top-down approach in order to obtain stable blank nanosuspensions, which were then loaded with bovine insulin and characterized from a physicochemical point of view.

They were nanometric with high negative zeta potential, mucoadhesion and swelling properties, good loading capability and encapsulation efficiency. The *in-vitro* release of insulin was negligible at a gastric pH while sustained at an intestinal pH, thus showing a pH-sensitive behaviour of the nanosponges. The Caco-2 cell permeability assay proved that the intestinal permeation of insulin was enhanced when loaded inside nanosponges. The *in-vivo* studies confirmed the presence of insulin in rat plasma and a marked hypoglycaemic effect in 2 diabetic mice models (non-obese diabetic mice and streptozotocin-induced diabetic mice) after duodenal and oral administrations, respectively.

Table of contents

1. Drug delivery

Drug delivery refers to the methods and approaches for administering pharmaceutical compounds with the goal of achieving a therapeutic effect. Indeed drug delivery has improved the ability of a variety of drugs to overcome the challenges faced in the route of administration and reach the absorption sites, where they carry out their therapeutic effect[1].

Drug delivery is successful when it prevents drug degradation, allows for dose reduction due to the ability to localize a therapeutic molecule to specific tissues, avoiding toxic levels, and also high costs due to overdosing[2]. Last but not least, it enables drug administration via more appropriate routes, thereby improving patients' quality of life.

The routes of administration are generally divided into two groups: enteral routes, which include oral, sublingual, buccal and rectal routes, and parenteral routes, which include intravenous, intramuscular and subcutaneous routes[3]. The oral route is preferred, due to better patient compliance.

The route of administration is crucial because it has a significant impact on drug bioavailability and thus requires specific delivery strategies[4].

The first controlled drug delivery devices and implants were developed in the 1960s and 1980s, and they included mucosal inserts, skin patches, subcutaneous and intramuscular implants, and capsules for gastrointestinal delivery[5]. Drug delivery systems (DDS) evolved from macroscopic to microscopic in the 1980s and 1990s with the introduction into clinical practice of degradable polymers used as microscopic depot delivery systems for the sustained delivery of steroids, peptides and proteins[5].

The discovery of PEGylation, as well as active and passive targeting, which are defined below, changed the nature of drug delivery systems dramatically with a further size reduction from micro to nano scale, which triggered intense research over the years and made nanomedicine a key science of the 21st century[6,7].

PEGylation, or the conjugation of polyethylene glycol to drugs, ensured a prolonged circulation time as well as stability against enzyme action and immunogenic recognition.

Active targeting entails assisting the drug molecule in reaching the desired site (cell/tissue/organ) by conjugating biological ligands capable of binding to specific receptors on the surface of target cells, thus increasing cellular uptake[8].

Hiroshi Maeda's discovery of the enhanced permeation and retention effect (EPR) gave nanoparticles a great opportunity for a fundamental application, that of cancer treatment. In fact,

nanocarriers reach and accumulate in solid tumours via passive diffusion due to the leaky blood vessels of rapidly-growing tumour tissues[8].

The following paragraph discusses how nanoparticles emerged in drug delivery due to their unique properties, allowing the evolution from "conventional" DDSs to "smart" systems[9] capable of controlled and stimuli responsive delivery with improvements in solubility, pharmacokinetics, distribution, sustained release, and drug targeting[7].

1.1 Nanocarriers

Lipid-based nanoparticles (liposomes) were the first nano-DDS to be discovered, and they were used as drug and protein carriers in the 1960s[9]. Since then, an increasing number of materials have been investigated for nanoparticle production and used as DDSs. According to Bobo et al. in 2016 the FDA approved 51 nanomedicines and 77 were under investigation in the clinical field, which explains the pharmaceutical industry's growing interest[10].

Nanoparticle DDSs consist of particulate dispersions or solid particles of a nanometric size, i.e. less than 1000 nm and with several morphologies[11]. Drugs are generally dissolved, encapsulated or attached to the nanoparticle matrix.

Nanocarriers are classified into three groups on the basis of their nature: organic, inorganic and hybrid nanoparticles[12].

Organic nanoparticles include solid lipid nanocarriers, liposomes, dendrimers, polymeric nanocarriers, micelles and viral nanocarriers. They have a wide range of applications and are particularly suitable for drug delivery due to their low toxicity.

Gold, magnetic nanocarriers, quantum dots, and mesoporous silica are examples of inorganic nanoparticles. They are used in biosensing, cell labelling, targeting, imaging, and diagnostics due to their traceability. They may also have synergistic therapeutic effects. However, using heavy metals as inorganic nanocarriers would cause long-term health problems.

Hybrid nanoparticles are a combination of the aforementioned nanocarriers, organic and inorganic, and thus have a dual nature, which can be successful in some cases. For example organic nanocarriers, such as liposomes, suffer from internal solution leakage and instability, but the addition of another type of nanocarrier may improve the delivery system's stability[12].

Nano-DDSs emerged because they responded to the need to overcome the limits of current conventional therapies in which high dosages of drugs, their effects also on healthy cells and burst release caused severe side effects, especially in cancer treatment. Hence the need for smart delivery systems able to protect the drug from degradation, release it gradually with no burst effect and reach the target without being harmful to healthy cells[12].

Nanoparticles have been found to meet these requirements due to their unique properties, such as the ability to pass through capillary vessels however small and a prolonged presence in the bloodstream as they are generally not removed by phagocytes[2]. They can also penetrate into cells and intercellular spaces to reach target organs[11].

They have allowed the encapsulation of a great variety of drugs, with both low and high molecular weights, improved pharmacokinetics and limited toxic side effects[11]. In addition they can have controlled-release properties due to their biodegradability, pH, ionic nature and temperature[12].

1.2 Polymeric nanocarriers

Nanoparticles for drug delivery can be prepared using polymeric materials, which must be at least biocompatible if not biodegradable.

Use has been made of many different polymeric materials, such as polylactic and polyglycolic acids, polycaprolactone, polysaccharides, polyacrylic acids, proteins and polypeptides (gelatin), etc.[11].

Among them, both natural and synthetic polysaccharides are the most popular in drug delivery[13].

1.3 Polysaccharide nanoparticles

Polysaccharides are complex carbohydrates made up of monosaccharides joined together by glycosidic bonds (e.g. D-glucose, D-fructose, D-galactose, L-galactose, D-mannose, L-arabinose, and D-xylose).

Like proteins and lipids, they have a natural origin. Many are derived from plants or marine organisms, making them less likely to cause adverse immunological reactions than proteins[2]. They are inexpensive, widely available, and often biodegradable and biocompatible[2].

Interestingly, they are particularly suitable for pharmaceutical applications because they are expected to be degraded inside the body into small sugar units that integrate endogenous metabolic processes, allowing elimination or reabsorption and thus limiting potential toxicity[14].

Because of their ionic nature, cationic, anionic, and neutral polysaccharides exist, making electrostatic interaction a possible drug-loading strategy[15,16].

An important advantage of using polysaccharides is that they can be easily chemically modified due to the presence of derivable groups on molecular chains with the introduction of ionic or hydrophobic groups, degradable bonds, spacers, or targeting moieties to achieve advanced delivery systems with controlled or triggered release and targeted delivery[13].

In addition, the presence of simple sugar acids such as glucuronic and iduronic acids, as well as amino sugars such as D-glucosamine and D-galactosamine, and derivatives, on the side chain of carbohydrate polymers, make them suitable for targeted delivery via carbohydrate recognizing cell receptors[13].

Last but not least, the hydrophilic groups found in most natural polysaccharides, such as hydroxyl, carboxyl, and amino groups, can form non-covalent bonds with biological tissues (primarily epithelia and mucous membranes), resulting in bioadhesion and increased residence time, which favours drug absorption[2].

1.4 Starch derivatives

Among polysaccharides, starch derivatives have received a great deal of attention for pharmaceutical applications[17].

Starch is one of the most abundant biomass materials in nature, as it is produced as a source of energy by many plants, including cereals (which contain the largest amount of starch), roots, tubers, legumes, and fruit[17].

Because of its natural origin, the composition may differ from one source to another.

It is produced in two forms: amylopectin (70–80%) and amylose (20–30%).

While amylose is a non-branching helical polymer of (1,4)-linked D-glucose monomers, amylopectin is a branched molecule with 1,6 branch points every 24–30 glucose residues on average.

Starch is extracted from plants via wet grinding, sieving, and drying.

Important starch derivatives are cyclodextrins, which have made an important contribution to drug delivery and are now well known ingredients of pharmaceuticals[18].

1.4.1 Cyclodextrins

Cyclodextrins (CDs) were discovered accidentally by Villiers in the 1890s during experiments on the degradation and reduction of carbohydrates under the action of ferments[19].

They are oligosaccharides with a truncated cone shape composed of (1,4) linked glucose units.

The CD ring is an amphiphilic conical cylinder with a hydrophilic outer layer formed by the hydroxyl groups and a lipophilic cavity[20].

Natural α, β and γ CDs contain six, seven, and eight glucose units, respectively[21] (Figure 1).
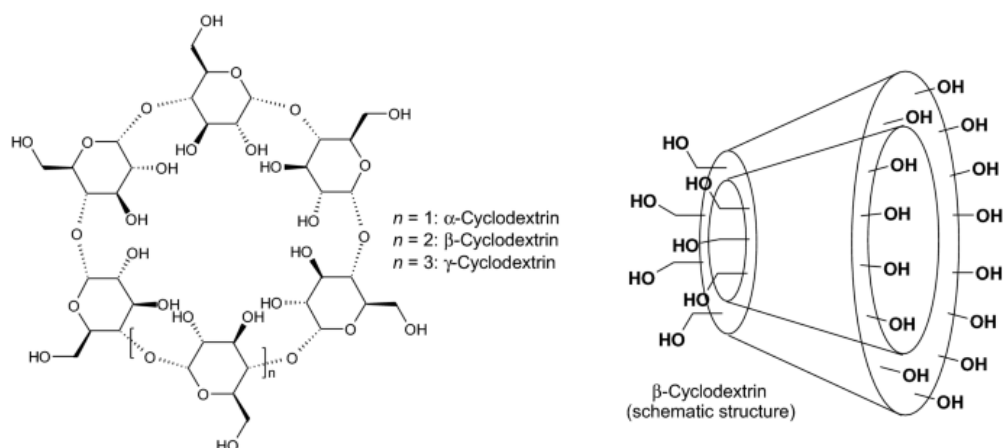
Figure 1. Structure of natural cyclodextrins[21].

Their industrial scale production of highly pure forms at an affordable cost made a significant contribution to their development.

Furthermore, the use of natural molecules rather than toxic solvents to increase drug solubility was a new trend that began to take hold in the pharmaceutical industry, and CD popularity grew as a result[19]. Indeed, the amphiphilic behaviour of cyclodextrins, attributable to the hydrophobic cavity and the hydrophilic surface, enabled hydrophobic drugs to be encapsulated forming inclusion complexes, thus enhancing the dissolution of scarcely water-soluble drugs[22].

Cyclodextrins were found to improve the stability of pharmaceutical formulations and to be suitable for a variety of routes of administration, including oral, parenteral, rectal, cutaneous, ocular and sublingual, with improved drug pharmacokinetic profiles[23].

Nowadays, CDs are the most versatile tools in pharmaceutical technology, ranging from classical dosage forms to the most recent innovative drug delivery systems[24] with at least six types available on the market used to improve the water-solubility and bioavailability of medicinal products[20].

2. Cyclodextrin-based nanosponges

Cyclodextrins have been the subject of intense research to optimise their formulation due to the limitations associated with their intrinsic structure, which requires interaction with and fitting inside the CD cavity, with the result that hydrophilic or high molecular weight drugs are not suitable for complexation with CDs[25]. Supramolecular structures have therefore been developed (e.g. self-assembled systems, crosslinked polymers, drug-conjugates), to improve the limits of single CDs and transform them into advanced drug delivery systems[24]. One of the strategies proposed is reacting native cyclodextrins with a crosslinking agent to form insoluble polymers, called nanosponges (NSs)[25] Figure 2.
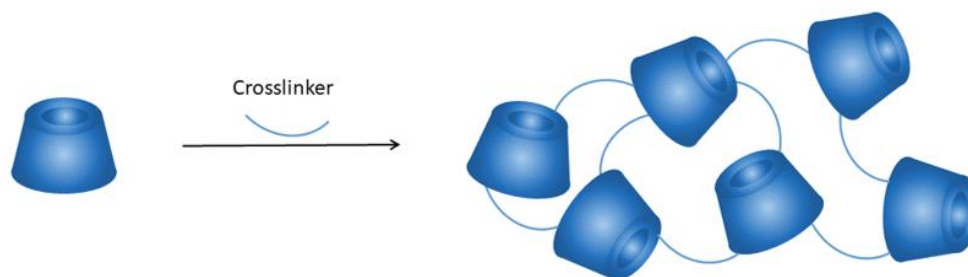
Figure 2. Graphic representation of the formation of NSs through CD-crosslinker interaction.

Because of the exceptional properties attributable to their peculiar structure, cyclodextrin-based nanosponges have piqued the interest of researchers in drug delivery[26]. Alongside the common polysaccharide features, such as the presence of tunable functional groups and their ability to interact with biological tissues, thus giving rise to bioadhesion, what makes CD NSs unique is their three-dimensional network made up of crosslinked cyclodextrin units. In fact, the main advantage of polymerizing cyclodextrins (CDs) is the formation of a complex network in which host molecule complexation may occur not only inside the internal cavities of CDs, but also in the interstitial spaces between them. Hence, nanosponges can entrap both hydrophobic and hydrophilic molecules[27].

In addition, the polymeric structure surrounding each CD contributes to prolong the time for which the entrapped guest molecules remain inside the CD cavity[28]. The release of the encapsulated molecules can also be modulated due to the presence of functional groups, which are responsive to external stimuli[29].

CD NSs are generally classified into four generations[29]:

The 1st generation comprises urethane, carbonate, ether and ester NSs synthesized by reacting CDs with a crosslinking agent.

The 2nd generation includes polymers with specific properties e.g. fluorescence or charged side chains.

The 3rd generation consists of stimuli-responsive NSs modifying their behaviour according to changes in the environment, such as pH, temperature gradients or oxidizing/reducing conditions.

The 4th generation includes molecularly imprinted NSs with high selectivity towards specific guest molecules.

Moreover, efforts are currently being made to develop nanosponges that can reach their target through the interaction of biological ligands grafted on the NS surface and cellular receptors.

These NSs pave the way for the 5th generation[26].

2.1 History of Nanosponges

To understand how nanosponges emerged over the years and be aware of their role today, their historical development has been herein explored, focusing on the origin and key points of NS research in the last 50 years, progressing from relatively simple crosslinked networks in the 1960s to today's multifunctional polymers.

2.1.1 Early years: from the 1960s to the new millennium

The first polymers that resemble the structure of what we call nanosponges today appear in an article of the 1960s, described as simple network polymers made up of crosslinked CDs, the binding properties of which were investigated[30]. This study suggested a possible application in separation techniques, which was further developed in the 1970s with the production of stationary phases for nucleic acids, etc[31].

However, various decades passed before their huge potential as drug delivery systems was widely recognised[26].

In the 1980s, research explored new polymers and made efforts to understand their properties alongside their binding ability. The influence of the crosslinker and the degree of crosslinking on guest-binding properties of CDs were investigated for the first time[32].

In the 1990s, CD polymers found application as debittering agents and food component carriers (e.g. caffeine, vanillin and theobromine)[33]. Moreover, in the water remediation field, they overcame the limits of purification methods used up to then, due to their high adsorption capacity, tunability and low cost[26].

At the end of this decade they were called "nanosponges" for the first time due to their nanoporous sponge-like structure[34].

2.1.2 The new millennium: the entry of nanosponges into the drug delivery field

New opportunities for nanosponges were studied in the new millennium, above all in the pharmaceutical field.

Cavalli et al. (2006) made the first attempt, using nanosponges to deliver different types of drugs, both lipophilic (dexamethasone and flurbiprofen) and hydrophilic (doxorubicin), and achieving drug encapsulation and sustained release[27]. The promising results obtained prompted extensive research from 2010 to 2015, lengthening the list of drugs delivered, such as anticancer drugs, polyphenols, NSAIDs, and gases of pharmaceutical interest (i.e. oxygen and carbon dioxide).

2.1.3 From 2010 to 2015: focus on nanosponges as delivery systems

The need to improve conventional anticancer chemotherapeutic therapies, which have severe side effects and limited efficacy, triggered research for suitable nanoparticulate delivery systems[35], and CD NSs were proposed as a promising solution in the studies discussed below.

Ansari et al. (2011) developed various β-CD NSs crosslinked with diphenylcarbonate (DPH) with ratios 1:2, 1:4 and 1:8 to find the best carrier for loading paclitaxel[36].

Another attempt was made by Mognetti et al. who developed fluorescent NSs for the delivery of paclitaxel. *In-vitro* studies on cancer cells showed that the anticancer activity of paclitaxel was enhanced, it was thus assumed that the nanosponges interacting with the cell membrane facilitated drug release[37].

Camptothecin, which is used in the treatment of hematological and solid tumours, was encapsulated in DPH-linked NSs and tested on human prostate cancer cells. β-CD NS carriers were able to overcome the drug's chemical limitations and improve *in-vitro* anti-tumour efficacy[38].

Nanosponges were also studied for the delivery of antioxidants, which have low solubility and physicochemical stability, limiting their use.

CDI-linked β-CD NSs have been proposed as a means of delivering resveratrol and polyphenols found in apples (rutin, phloridzin and chlorogenic acid)[39]. Having significantly enhanced the photostability and antioxidant activities, NSs offered a potential oral and topical drug delivery system[40,41].

Furthermore, gamma-oryzanol (GO), a ferulic acid ester mixture commonly used to stabilize food and pharmaceutical raw materials as a sunscreen in cosmetic formulations, was loaded in NSs. The photodegradation of GO after UVA or UVB irradiation was slowed when it was included in nanosponges, but the antioxidant effect remained. In-vitro experiments on porcine ear skin also revealed an accumulation of GO[42].

Interesting results were also achieved with anti-inflammatory drugs, such as non-steroidal anti-inflammatory drug (NSAIDs) and steroids. β-CD/PMDA nanosponges were investigated by Shende et al. (2015) to deliver meloxicam in order to improve its solubility and bioavailability as well as to prolong its release for anti-inflammatory and analgesic effects. Furthermore, efforts were made to extend the duration of the drug release[43].

Positive results were also achieved with ibuprofen. This drug was loaded inside β-CD/ethylenediaminetetraacetic acid (EDTA) dianhydride nanosponges. The dynamic properties of ibuprofen, especially in the gel state, were studied for advanced formulations using high resolution magic angle spinning (HRMAS) NMR spectroscopy. The polymeric network was believed to affect the diffusive regimes of ibuprofen[44].

Dexamethasone, a steroidal anti-inflammatory drug, was encapsulated within β-CD NSs prepared with DPH as a crosslinker. This study suggested that nanosponges could be used for ocular administration. The drug was actually retained in the eye for a longer period of time, increasing its corneal permeability[45].

Alongside ocular delivery, nanosponges were used in drug delivery through skin. Imiquimod, which is used to prevent and treat post-burn hypertrophic scars, was loaded into β-CD/PMDA nanosponges[46].

Conte et al. (2014) studied the same type of nanosponge for the first time as a multifunctional ingredient in semisolid formulations for drug delivery to the skin[47]. The NS was tested for its role in the solubilization and stabilization of benzoporphyrin-derivative monoacid ring A, all-trans retinoic acid and diclofenac skin permeation.

Another extremely interesting property of NSs, as demonstrated by Lembo et al. (2013), is the ability to make them fluorescent, which is particularly useful for cellular trafficking studies[48]. The method involved adding a pre-formed carbonate NS to a fluorescein isothiocyanate solution in DMSO and incubating for 3 hours at 90°C. After recovering the solid through filtration, it was reacted with succinic anhydride to produce fluorescent NSs.

As mentioned previously, nanosponges have been found to be suitable for gases such as oxygen and carbon dioxide. The former can resolve tissue hypoxia, while the latter has beneficial physiological effects such as blood vessel dilation, improved blood circulation, and activation of gastrointestinal movement. The ability of NS constituents, such as cyclodextrins, to store gases in their cavity has long been known, dating back to 1987, when the encapsulation of carbon dioxide with CDs was patented in Japan, anticipating its use in cosmetics, cleansing, and personal care

products[49]. As gases have a low molecular weight and a small size, α-cyclodextrins were preferred to β-cyclodextrins, which have a larger inner cavity dimension and thus cannot host gases.

For the first time, it was demonstrated that crosslinked cyclodextrins, including β-CDs, were not only capable of hosting gases, but were also particularly advantageous in this regard[49,50]. In particular, Cavalli et al. (2010) investigated the ability of nanosponges synthesized using various types of cyclodextrins, α, β, γ-CD crosslinked with 1,1'-carbonyldiimidazole (CDI) to deliver oxygen[50]. These nanosponges, particularly β-CD NSs, were found to be capable of encapsulating, storing, and releasing oxygen for an extended period of time, which could be enhanced in an *in-vitro* environment by using ultrasound as an external stimulus.

To summarize, a number of NSs-based drug delivery systems with different types of CDs and crosslinkers have been developed since the first study on NSs in the pharmaceutical field.
Their ability to improve solubility and stability and achieve sustained release, as well as increase permeability and thus improve drug bioavailability, has been widely studied.
Furthermore, attention has been given to their suitability for delivery via alternative routes of administration, thereby favouring patient compliance and reducing side effects.

2.1.4 From 2016 to the present day: state of the art and future prospects of nanosponges

The main field of application for nanosponges has been pharmaceutics, as evidenced by the research areas in which CD NSs are involved (Figure 3).
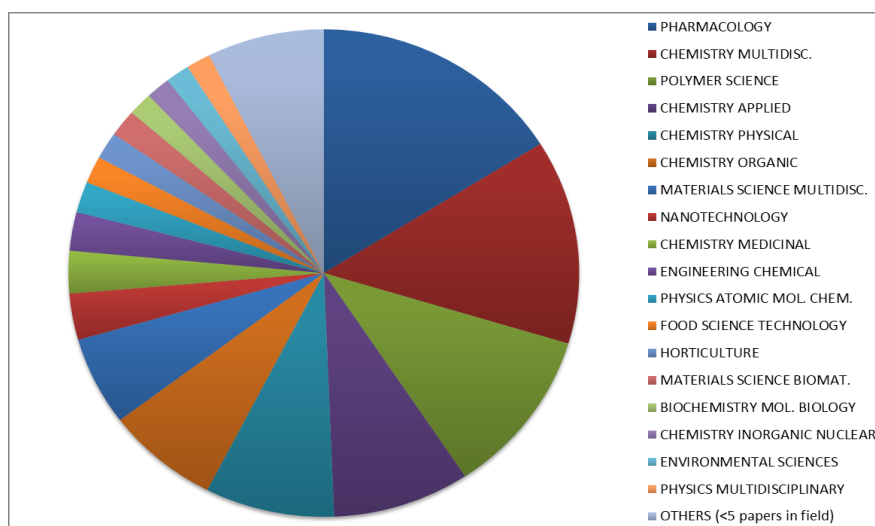
Figure 3. Research areas in which CD NSs are involved[26].

Nanosponges are widely studied in anti-cancer therapy[51–53].

In 2017 β-CD/CDI NSs loaded with anti-cancer drugs, such as erlotinib (an epidermal growth-factor receptor tyrosine kinase inhibitor) and camptothecin (a DNA Topoisomerase-I inhibitor), increased their oral bioavailability, solubility and dissolution, minimizing the dose-related adverse effects[51–53].

Curcumin and resveratrol and a combination of the two were loaded in β-CD NSs and tested[54–56]. Curcumin and resveratrol were combined by Pushpalatha et al. (2019) in order to exploit their synergistic effect against breast cancer through transdermal delivery[54]. The nanosponges not only enhanced the *in-vitro* release of both curcumin and resveratrol 10 and 2.5 times, respectively, but also the combination showed a synergistic cytotoxic effect on the breast cancer cell line selected.

In this field, nanosponges have evolved to meet the need to limit the side effects of anti-cancer therapies by becoming smart delivery systems capable of controlled release triggered by stimulating signals (i.e. pH and GSH) and the most recent ones having natural ligands grafted on the surface able to perform active targeting[26].

One example is the glutathione-responsive NS (GSH-NS) developed by Trotta et al. (2016) capable of releasing entrapped anticancer drugs in response to intracellular stimuli, such as intracellular glutathione, which is high in tumour cells[57]. The synthesis consisted of a single-step reaction between β-CD and 2-hydroxyethyl disulfide in the presence of pyromellitic dianhydride as a crosslinker[58]. GSH-NS was loaded with doxorubicin and showed remarkably higher effectiveness than free drug in cancer cells both *in vitro* and *in vivo*.

Glutathione-responsive NS was also used in 2017 for the delivery of erlotinib hydrochloride, which was associated with severe toxicity when administered in a systemic and uncontrolled way[59]. Biodistribution and *in-vivo* tumour growth inhibition studies revealed drug release to the cancer cell, thus preventing unnecessary drug exposure and exhibited extended drug release proportional to the external GSH concentration.

In 2018, plant hormones (strigolactones) were loaded into GSH/pH-sensitive NSs in order to investigate whether this stimulus-responsive nanocarrier reduced the viability of prostate cancer cells *in vitro* and positive results were achieved[60].

With regard to pH-sensitive NSs, in 2019, cyclodextrins and calixarenes were combined to develop a DDS the release of which was dependent on pH and was used to release tetracycline antibiotics[61]. Interesting improvements of the biocidal activity were achieved. These improvements may be attributable to the presence of particularly favourable Coulomb interactions occurring between the NS carrier and the bacterial cell wall. Further studies are ongoing in order to better

understand the possible mechanisms implicated in CyCaNS-bioactive molecule-bacterial cell interaction.

In 2018, attempts were made to overcome the inherent lack of cellular binding ability of NSs, which has limited their application in drug delivery. In fact, medical research has recently invested heavily on drug delivery systems capable of reaching the target site (cell/tissue/organ) in order to improve the efficacy of the drug and limit its adverse effects. This therapeutic approach called "Targeted drug delivery" has been experimented especially on anticancer drugs to limit their toxicity. Various approaches have been proposed, including the functionalization of nanoparticles with natural ligands, which bind to specific receptors on the surface of the target cells, thus increasing cellular drug uptake [8]. CD based NSs, even if still at an early stage, have been studied in this field of application as they can be easily functionalized with ligands as mentioned in paragraph 2. A method explored successfully by Singh P. et al. (2018) was the functionalization of the surface of CD based NSs with cholesterol, which is an ubiquitous endogenous molecule, responsible for cell interactions and protein binding[62]. Doxorubicin was selected as a model drug and its cellular uptake revealed an enhanced effect of doxorubicin when loaded in this innovative carrier.

This approach was also used for theranostic nanomedicines[63], which have attracted huge interest for imaging-guided drug/gene delivery in cancer treatment because of the combination of diagnostic and therapeutic functions. For example, folic acid was used as a targeting agent in a novel theranostic system based on a CD NS polymer anchored to the surface of magnetite nanoparticles, which was then decorated with folic acid[64].

In addition to the anti-cancer field, a large number of drugs have been tested, as shown by the studies mentioned below.

For example, Celecoxib, which possesses analgesic and anti-inflammatory actions, was loaded in β-CD/NN-methylene bisacrylamide nanosponge, which was incorporated in a hydrogel for topical application. The drug solubility and bioavailability were therefore enhanced[65].

Encapsulation studies of both hydrophilic and lipophilic drugs have continued in the last few years as evidenced by Patel et al. (2016) study[66]. More in detail, they investigated the ability of β-CD/DPC NSs to host both hydrophilic drugs, such as gemcitabine, and lipophilic drugs, such as bicalutamide, paclitaxel and letrozole. Lipophilic drugs had a higher drug loading capacity than hydrophilic drugs because of their large number of lipophilic sites available for drug complexation.

In the same year, β-CD/PMDA was used to encapsulate lansoprazole. The positive results obtained made this kind of NS promising for the treatment of gastric ulcer[67].

NSs were also used as multifunctional direct compression excipients for tablet design without adding any binder, lubricant or disintegrant. This kind of NS was synthesized by crosslinking β-CD with citric acid[68].

β-CD/DPC NS was used for the delivery of drugs, such as efavirenz and rilpivirine, for the treatment of HIV in order to enhance their solubility and bioavailability[69,70]. An improvement in the aqueous solubility was again achieved by using the same kind of NS (β-CD/DPC) for the delivery of chrysin, which has antioxidant and anti-tumorous properties[71].

The year before, Pushpalatha et al. explored the effect of different kinds of crosslinked cyclodextrins (β-CD, DPC and β-CD, PMDA) for the delivery of resveratrol. Having selected the best crosslinker ratio the NSs were compared in terms of physicochemical characterization together with photodegradation, *in-vitro* drug release, *in-vitro* cytotoxicity and *in-vivo* tests in order to find the most suitable choice for the selected drug[72]. Resveratrol and oxyresveratrol were also loaded in carbonate CD NSs to improve their solubility, release profile, photostability, antioxidant and cytotoxicity activity [73].

Alongside resveratrol, other natural antioxidants, such as ellagic and ferulic acids were studied[74]. When loaded in NSs, their solubility was enhanced, making low solubility no longer a limit for their application in the food and pharmaceutical industries. Dhakar and et al. (2019) studied the enhancement in aqueous solubility, antioxidant activity and *in-vitro* cell toxicity of kynurenic acid (KYNA) loaded in β-CD/CDI NS. As a high solubilisation and drug loading of KYNA were obtained, CD NSs proved to be suitable for biological applications[75].

Another recent innovation is the Molecularly Imprinted Polymer (MIPs), which belongs to the fourth generation of nanosponges obtained via interaction between template molecules and polymers by covalent, semi-covalent or non-covalent bonding[29]. They have a heteropolymer matrix with specific recognition elements for the template molecule even though it has been removed. Trotta et al. (2016) synthesized new MIP-NSs for the treatment of Parkinson's disease by crosslinking β-CD with CDI in DMF in the presence of L-DOPA as a template molecule. It has been confirmed that MIP-NSs showed a slower and more prolonged release profile making them a promising alternative for storage and controlled delivery of L-DOPA[76]. MIPs find also application in several fields alongside drug delivery, such as separation sciences and purification, biological antibodies receptor systems and catalysis.

The drug delivery studies are indicated in the summary table (Table 1) as examples.

Thus, considering the great variety of applications, researchers are increasingly aware of NS potential and need to fully characterize them in order to understand their structure and mechanism of action[77].

Knowledge of the analytical tools can significantly improve the assessment of the quality parameters of NSs, i.e. their safety, negligible toxicity, superior inclusion capability, marked swelling behaviour and biodegradability, which are fundamental for their use in drug delivery, drug targeting, tissue engineering and regenerative medicine. Therefore, in the scenario of growing importance of CD NSs, a long list of characterization techniques have been used. Fourier transform infrared spectroscopy in attenuated total reflectance geometry (FTIR-ATR), CHNS/O analysis, scanning electron microscopy (SEM), energy dispersive X-ray spectroscopy (EDX) analysis, light scattering analysis[78], low-frequency Raman scattering[79], high resolution magic angle spinning (HRMAS) NMR spectroscopy, carbon-13 nuclear magnetic resonance (^{13}C NMR), proton nuclear magnetic resonance (^{1}H NMR), thermogravimetric analysis (TGA), potentiometric titration, Brunauer–Emmett–Teller (BET) analysis, transmission electron microscopy (TEM), differential scanning calorimetry (DSC) and X-ray diffraction (XRD) have been extensively employed in the studies over the years[26]. In addition the nano-formulations developed need to be evaluated as far as encapsulation efficiency and loading capacity, stability, *in-vitro* drug release, *in-vivo* pharmacokinetic release, efficacy and toxicity are concerned in order to ensure quality and efficacy[39,44,84–91,46,56,71,76,80–83].

Table 1. Studies conducted on CD NSs in drug delivery field over the years.

Year	NS/crosslinker	Drug	Therapeutic indication	Reference
2010-2015	β-CD/DPC	Camptothecin	Cancer	38,92
	β-CD /CDI	Resveratrol	Cancer	40
	Fluorescent NS	Paclitaxel	Cancer	37
	Carboxylated nanosponges	Acyclovir	Herpes virus	48
	β-CD /CDI	Rutin, phloridzin and chlorogenic acid	Cancer, diabetes, obesity	39
2016	β-CD/PMDA	Lansoprazole	Gastric ulcers	67
	β-CD/DPC	Quercetin	Cancer	85
	β-CD /CDI	Erlotinib hydrochloride	Cancer	51
	GSH – NS (β-CD/PMDA)	Doxorubicin	Cancer	57
2017	β-CD/EDTA	Ibuprofen	Inflammation	89
	β-CD/DPC	Chrysin	Cancer	71
	β-CD/DPC	Nifedipine	Angina pectoris and hypertension	93
	β-CD/CDI	Camptothecin (CPT)	Cancer	52,53
	β-CD/DPC	Cefadroxil (CFD)	Gram-positive and Gram-negative bacteria	94
	β-CD/DPC	Efavirenz and Rilpivirine HCl	HIV	70,95
	β-CD/PMDA	Erlotinib glutathione	Cancer	59
2018	β-CD / DMC	Ellagic acid	Cancer	74
	β-CD/DPC	Mebendazole	Lymphatic worm infestations	96
	β-CD/TDI	Naproxen	Inflammation	97
	β-CD/CDI; PMDA	Rilpivrine	HIV	98
	β-CD/CDI	Atorvastatin calcium	Dyslipidemia	99
	β-CD/DPC	Norfloxacin	Urinary tract infections	100
	β-CD/CDI	Doxorubicin	Cancer	62

Table 1. Studies conducted on CD NSs in drug delivery field over the years (*continued*).

Year	NS/crosslinker	Drug	Therapeutic indication	Reference
2019-2021	β-CD/NDCA	Sage essential oil	Diabetes	101
	β-CD/DPC; PMDA	Curcumin and Resveratrol	Cancer	54,55,72
	β-CD / DPC	Ferulic acid and Imatinib Mesylate	Cancer	102,103
	β-CD/EPI	Curcumin	Cancer	56,64
	β-CD/CDI	Kynurenic acid and Paliperidone	Neurological disorders and Schizophrenia	75,104
	β-CD/PMDA	Imiquimod	Topical diseases	105
	β-CD/DPC	Curcumin	Cancer	106
	β-CD/DPC	Azelaic acid	Acne	107
	β-CD/DPC	5-Fluorouracil	Gastric cancer	108
	β-CD; HPβ-CD/ DPC	Ibuprofen	Inflammation	109
	β-CD/CDI	Flutamide	Cancer	110
	β-CD/DPC	Clobetasol propionate	Psoriasis	111
	β-CD/PMDA	Piroxicam	Inflammation	112
	β-CD/PMDA	Resveratrol	Cancer	113
	β-CD/DMC	Curcumin and caffeine	Psoriasis	114
	β-CD/PMDA	Insulin	Diabetes	115

Recently, special attention has been given also to the optimization of the formulations in order to find the best solution for the active molecule to be delivered, also by means of mathematical tools, such as a design approach.

Experimental design helps to minimize the number of experiments, develop the process and improve the product quality. It consists in exploring the behaviour of NSs in various experimental conditions in a limited number of tests and straightforward identification of the variables that affect the system the most, taking into account the synthesis[116] or the formulation process[54,96,117]. For example, this approach was adopted by Kamble et al. (2019) to synthesize NSs considering the effect that various levels of crosslinking agents and β-CD concentrations had on porosity, drug encapsulation, zeta potential and drug release[102]. Furthermore, Pushpalatha et al. (2019) optimized the curcumin-resveratrol loaded NS hydrogel formulation using a factor 3-level Box-Behnken design[54]. The concentrations of the two ingredients used for the hydrogel, together with the pH, were selected as independent variables at three levels. Transdermal flux of curcumin, transdermal flux of resveratrol and spreadability of gel were the dependent variables evaluated for optimization. Singireddy et al. (2019) optimized the synthesis of CD NSs to avoid low yields, and batch to batch variations due to differences in experimental conditions (reaction temperature in

°C, reaction time in minutes and stirring speed in rpm). The reaction conditions for the synthesis of NSs were optimized by using central composite design and response surface methodology[116].

Pushpalatha et al. (2018) also used the hierarchy analysis approach to choose the best crosslinker among various kinds for obtaining NSs for drug delivery[117]. The most common crosslinkers were investigated. The selection was made on the basis of the process, materials, and physicochemical characteristics of the output. From this study, it emerged that this kind of analysis helped to reduce the number of experiments, shorten the development process, and improve product quality.

Over the past few years, alongside the pharmaceutical field, the great versatility of NSs has been confirmed by studies conducted in the food industry identifying new applications, such as active/intelligent packaging. Other applications have been found in the environmental field, the textile industry, solid-phase extraction and catalysis[26].

To conclude, the development of nanosponges was slow at the start but rapidly gained momentum through a major increase in the number of studies, which undoubtedly reflects the scientific community's awareness of their potential.

Their success is certainly due to their ability to keep up with the times while retaining their initial features, i.e. low cost, environmental compatibility, non-toxicity and the ability to host various kinds of molecules. In addition, their synthesis has evolved in the direction of greener processes culminating in the most recent solvent-free synthesis[118]. All of these advantages would make NSs suitable for future industrial scale-up.

For the reasons discussed above, NS research has not yet reached its conclusion. On the contrary, the potential advantages that could be obtained from their use certainly justify further studies aimed, on the one hand, at investigating in greater depth their existing fields of application in which appropriately optimized NSs are useful as carriers and, on the other, at exploring new fields in which their potential could be exploited to the full as a promising, safe innovation for human health and activities.

3. Protein delivery

Peptides and proteins have been found to have great potential as therapeutic agents in numerous fields, such as oncology, immunology, infectious diseases and endocrinology[119].

In recent years, the focus has shifted from small molecule therapeutics (<900 Daltons) to peptides and proteins, with a rapid growth of the market, which is estimated to be around 10% of the total pharmaceutical market and will continue to grow in the future[120]. This is due to recent advances in recombinant DNA technology and solid-phase peptide and protein synthesis, which have allowed for large-scale production of therapeutic peptides and proteins[121]. Not to mention the advantages of peptides and proteins over small molecule drugs, such as the fact that they are more specific to their target sites, thus limiting side effects, and that they are less immunogenic because they are produced naturally in the body.

Since the introduction of the first recombinant protein, human insulin, proteins have emerged as a major new class of therapeutics and they provided life-saving medicines (insulin and ACTH) in the first half of the 20th century[120]. Indeed the US FDA has approved 239 therapeutic proteins and peptides for clinical use[122].

Therapeutic proteins can be classified in the following major categories, monoclonal antibodies (i.e. bevacizumab, panitumumab, rituximab and adalimumab[123]), fusion proteins (i.e. etanercept, alefacept and abatecept[124]) or native biologics (i.e. erythropoietins, interferons, insulins, clotting factors, growth hormones and interleukins) [125].

The first attempts with monoclonal antibodies in the clinical field involved the use of murine antibodies, but as the human anti-mouse antibody response occurred, they were gradually substituted by chimeric, humanized and fully human monoclonal antibodies.

Fusion proteins are indicated for the treatment of chronic inflammatory diseases such as rheumatoid arthritis, plaque psoriasis, ankylosing spondylitis and multiple sclerosis.

Native biologics belong to a class of drugs that are also referred to as secreted proteins or replacement therapies and represent the earliest category of biotherapeutic drugs approved by the US FDA.

Despite the immense therapeutic potential of proteins and peptides, their use is limited due to sensitivity to chemical and enzymatic degradation as well as poor cellular uptake, thus resulting in low bioavailability[13].

To date the most common method of administration is via the parenteral route, which unfortunately results in poor patient compliance due to the frequent injections, especially in life-long therapies[126].

Hence the urgent need for suitable delivery strategies to enable the administration of proteins and peptides via alternative routes[127].

Other routes for example, such as nasal and pulmonary routes, have received considerable attention because of their low proteolytic activity and their highly vascularized and large absorptive surfaces especially in the lungs, which result in improved absorption. However, high molecular weight, proteolytic instability and physiological barriers, e.g. mucociliary clearance, are the main limitations that can affect protein absorption via these routes. Similarly, hydrophilicity and large molecular size also limit transdermal protein delivery[128].

Among all routes, the oral one is certainly the most appealing as it would dramatically improve the quality of life of patients who rely on chronic, injectable doses of therapeutic peptides and proteins. In addition, it is cheap, simple, requires fewer sterility restrictions and offers more possibilities in the design of the formulation (including sustained and controlled delivery)[129,126,130].

Even though oral administration is the most desired, a number of concerns need to be kept in mind to achieve a successful therapeutic outcome.

For example, the gastrointestinal tract (GI) presents multiple levels of barriers thus making the absorption mechanism complex[130]. There is a long list of variables that influence the GI absorption of drugs, especially proteins and peptides, which are grouped in technical challenges, physicochemical properties of the drug and environmental factors[131].

The technical challenges concern the pharmaceutical form, and care must be taken when including proteins in a pharmaceutical formulation due to sensitivity to light, heat, moisture, pH, intermolecular interactions following co-precipitation or gelling, self-aggregation, adsorption, and interaction with excipients[132].

The physicochemical properties of the drug include its molecular weight, lipophilicity, pKa, metabolism due to the activity of bacterial flora and intestinal mucosa.

The environmental factors that influence drug integrity and absorption consist of pH and enzymes, stomach emptying, intestinal transit time, the bloodstream and surface area of absorption.

In the stomach, the secretion of gastric acid by oxyntic cells make the pH highly acidic (pH=1.5–3.5), which may alter the ionization of amino acids affecting the bonds that hold together the secondary and tertiary structure of proteins, thus destabilizing protein structure and making it susceptible to enzymatic degradation by pepsin.

Small peptides have been shown to have higher stability in gastric fluids and mucosa compared to larger ones. Gastric protection is therefore necessary for large peptides administered orally in order to avoid acid denaturation and pepsin digestion.

Proteins and peptides are massively degraded in the small intestine due to the action of enzymes[129]. These proteolytic enzymes produced by the pancreas and by the mucosal cells that line the gut (pepsin, trypsin, chymotrypsin, and elastase) promote the breakdown of peptides and proteins into their constituent amino acids.

The aforementioned physicochemical properties (molecular weight, hydrophilicity, the potential for ionic or hydrogen bond formation, the number of enzyme-susceptible groups present, and low structural flexibility) make proteins more or less susceptible to proteolysis.
For example, peptides that lack a cyclic structure and small peptides fewer than 12 amino acids in length (desmopressin, oxytocin, Arg-vasopressin octreotide, and cyclosporin) are less readily digested by proteases than proteins or larger peptides containing more than 12 amino acids (somatostatin, calcitonin, glucagon, secretin, and insulin) and having more complex structures[121].

The low bioavailability of orally administered therapeutic proteins and peptides is also linked to their reduced ability to cross the epithelial lining in the small intestine and its protective mucus layer.

On the contrary, the large intestine, due to the neutral to slightly alkaline pH (pH range 6–8), the absence of proteolytic enzymes, and the extended residence time make it an exciting target for the delivery of peptides and proteins.

Last but not least, the first-pass effect should be borne in mind when dealing with the oral route as it is certainly a limiting factor. It refers to the metabolism (mainly in the liver) of the drug before it reaches the systemic circulation, which may lead to a drop in bioavailability[133].
Figure 4 depicts all chemical and enzymatic barriers in the gastrointestinal tract.
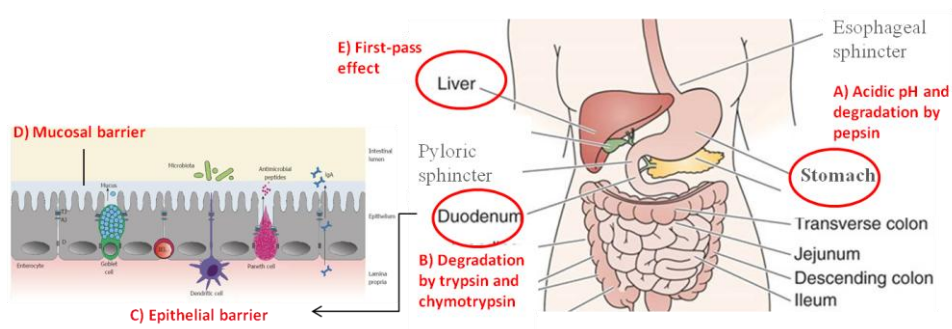
Figure 4. Gastrointestinal barriers for protein oral delivery.

4. Aim of the PhD

Finding adequate carriers for oral protein and peptide delivery has become an urgent need, due to the growing number of macromolecules identified as having therapeutic potential. Nano-DDSs have been considered as particularly promising for peptides and proteins[134] with polysaccharide-based nanocarriers in particular at the forefront of the challenge.

This class includes cyclodextrin-based nanosponges, which have proven to have excellent properties as drug delivery systems due to their unique nanoporous structure, as discussed extensively in the introduction. Many studies have demonstrated their versatility in that they can deliver a wide range of drugs, but only a limited number of studies have focused on their potential to deliver macromolecules such as proteins[90,92,135].

Thus, the aim of this PhD project is to investigate and improve the knowledge of starch NSs in protein delivery, by developing NS-based formulations for the oral delivery of proteins. Different kinds of NSs were included, that is, a well-known β cyclodextrin-based nanosponge, an innovative linecaps-based NS and an industrial prototype, the composition of which is confidential.

Insulin was selected as a case study due to its importance for diabetes treatment and the extremely positive impact on patients if administered orally rather than subcutaneously, which is currently the most common route.

The approach herein developed is intended to overcome the challenges related to the delivery of insulin, such as high molecular weight, amphiphilic properties, susceptibility to degradation and aggregation with consequent loss in activity.

The project has included the optimization of the preparation method in order to make the formulation suitable for oral delivery, selection of the techniques for a full physicochemical characterization of the formulation, *in-vitro* tests to understand the drug release kinetics and absorption at the intestinal level and *in-vivo* studies to check the actual absorption of insulin in blood and the lowering of blood sugar levels in diabetic mice.

The idea behind this research project was to create an innovative drug delivery system that could also be used in the future for other proteins for pharmaceutical use.

5. Case study: nanosponges as carriers for insulin

Insulin is a polypeptide hormone secreted by pancreatic β cells and involved in the regulation of glucose homeostasis.

It is made up of 51 amino acid residues and has a molecular weight of 5808 Da. It comprises two peptide chains (A and B) connected by two disulfide bonds, with an additional disulfide formed within the A chain (Figure 5).
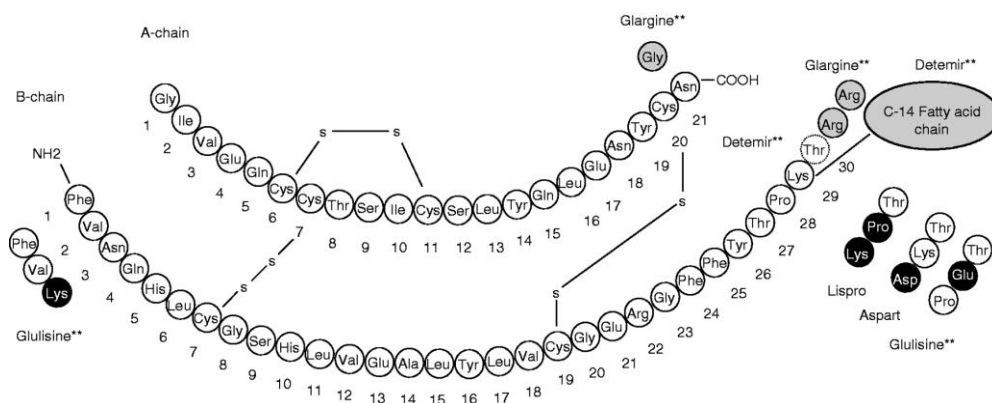
Figure 5. Structure of insulin taken from a review by Varewijck et al.[136].

Insulin has saved millions of lives since its introduction in the treatment of diabetes, the complications of which and the proportion of the population affected have made this disease one of the most complicated health problems of the twenty-first century[127].

According to the International Diabetes Federation, 382 million people in 2013 had diabetes, and this number is expected to increase to 592 million by 2035[137]. China has the world's largest diabetic population, with an approximated 35 million people accounting for 10% of the adult population, followed by India and the United States.

Factors contributing to the rising incidence of diabetes include population growth, aging, urbanization, an increase in obesity and physical inactivity, as well as unhealthy diets and sedentary lifestyles[127].

Diabetes mellitus is a chronic metabolic condition characterized by progressive cell destruction and loss of function, or by a loss of tissues' ability to respond to insulin in diabetes types 1 and 2, respectively.

The alteration of blood glucose homoeostasis caused by the absence or shortage of endogenous insulin results in hyperglycaemia, which causes long-term complications, such as heart disease, stroke, kidney disease, retinopathy, peripheral neuropathy, and lower limb amputation.

Patients handle diabetes mellitus type 1 by injecting insulin subcutaneously every day. In fact, the primary therapeutic strategy is to control postprandial blood sugar levels, which is accomplished by administering exogenous insulin to mimic pancreatic insulin secretion.

Subcutaneous injection is currently the most common method of administering insulin, but it has a number of drawbacks that have a significant impact on the patient's quality of life[138].

Multiple daily injections, for example, which are required to keep blood sugar levels stable, cause pain and hypertrophy at the injection site due to insulin accumulation. In addition, if the injection is not performed correctly, self-administration may result in infection.

Furthermore, as the hepatic metabolism is bypassed when insulin is administered this way, insulin enters the peripheral circulation at high concentrations, which may cause overstimulation of cell growth and, in the long run, diabetic complications.

This path differs from that of endogenous insulin, which is secreted by pancreas in blood vessels and reaches the hepatic portal circulation where it undergoes a large first-pass metabolism before entering the general circulation. As a result, the amount of insulin is regulated by the liver.

A delivery strategy that exploits a path that more closely mimics endogenous insulin would be more suitable and, for this reason, intense research has focused on the development of new strategies for insulin administration via alternative routes of administration[139].

The oral route has been studied in depth as over 7400[140] papers have been published in the last 10 years due to its advantages, as it is non-invasive, painless and preferred by patients.

Insulin alone, like other proteins, is not suitable for oral intake as it is susceptible to the harsh conditions in the stomach, it is degraded in the intestine by proteolytic enzymes and it has poor permeability across the intestinal epithelium.

To improve the oral administration of insulin, antiproteolytic agents have been used to avoid its enzymatic degradation, penetration enhancers to promote its gastrointestinal absorption, bioadhesive delivery systems to prolong its residence time at the intestinal absorption level, modified insulin to improve its stability and nanoparticle delivery systems to increase insulin bioavailability by overcoming GI barriers[127].

Polysaccharides, such as alginate, chitosan, starch, pectin and gelatin, have been studied as nanoparticle-based oral insulin delivery systems. Indeed, as discussed previously, the intrinsic properties of natural polymers that make them particularly suitable for drug delivery have piqued researchers' interest. These include gel-forming properties, which allow for the gradual release of encapsulated drugs while avoiding a burst effect, as well as the ability to modify their structure, thereby modulating their drug delivery properties. As examples, Table 2 contains a collection of studies on insulin oral delivery.

Table 2. Natural polymers used in oral insulin delivery.

Polymer	Dose (IU/kg)	Animal model	Purpose	Ref.
Alginate crosslinked dextran sulphate poloxamer coated albumin	50	Diabetic male Wistar rats	Evaluation of the hypoglicemic effect	[141]
Alginate dextran-chitosan	50	Diabetic male Wistar rats	Evaluation of the hypoglicemic effect	[142]
Chitosan-TBA (Tert-Butyl Alcohol)	11	Diabetic male Wistar rats	Evaluation of the hypoglicemic effect	[143]
Chitosan-polyglutamic acid	30	Diabetic male Wistar rats	Evaluation of the hypoglicemic effect	[144]
Chitosan polymethylmethacrylate	100	Non-diabetic Sprague-Dawley rats	Evaluation of the hypoglicemic effect	[145]
Laurylsuccinylchitosan	60	Diabetic male Wistar rats	Evaluation of the hypoglicemic effect	[146]
Dextran sulphate-chitosan	100	Diabetic female Wistar rats	Evaluation of the hypoglicemic effect	[147]
Vitamin B12 dextran sulphate-chitosan	20	Diabetic rats	Evaluation of the hypoglicemic effect	[148]

Natural polymers include the starch nanosponges investigated in this PhD project.

Pyromellitic NS (PMDA-βCD-1:4), a nanosponge made of β-CDs crosslinked with pyromellitic dianhydride, was selected for this purpose due to its remarkable properties, which have been demonstrated in various studies, such as biocompatibility and biodegradability, safety, storage, physiological stability, low cost, and ability to host and release in a sustained manner a variety of drugs[54,67,149]. It was thus hypothesized that this type of nanosponge could be suitable for loading insulin, protecting it from degradation in the stomach and promoting its intestinal absorption due to the controlled release properties given by the crosslinker to the CD NS.

Along with this nanosponge, two others were investigated: Linecaps citric NS (CTR-LC-1:8) made of linecaps crosslinked with citric acid[150] provided by the University of Turin's Chemical and Material Science Research Group (Prof. Trotta et al.) and an industrial NS synthesized by Roquette Frères, the company that funded this PhD, the composition of which is confidential.

Linecaps are spray-dried high amylose pea maltodextrins with a molecular weight of 12000 Da derived from partial hydrolyses of pea starch (about 40% amylose). Glucose, oligosaccharides, and polysaccharides make up the remaining 60% of its composition[151].

In water, the amylose linear molecule easily forms helical structures[152] with an inner hydrophobic cavity, which have been studied for drug encapsulation for masking flavour to improve patient compliance, particularly in paediatrics and geriatrics[151].

This flexible, helical structure, which was included in a crosslinked network by adding citric acid to form a hyper-crosslinked polymer, was thought to be promising for insulin delivery and was thus investigated and compared with cyclodextrin-based nanosponges in this project.

The formulation of PMDA-βCD-1:4 NS, CTR-LC-1:8 NS and industrial NS was fine-tuned by adopting a top-down approach in order to obtain stable blank nanosuspensions, which involved the use of a high shear homogenizer followed by a high pressure homogenizer (HPH).

The nanosuspensions were then loaded with bovine insulin by adding insulin solution drop by drop under stirring at room temperature. Insulin-loaded NSs were collected through centrifugation and freeze-dried overnight.

The formulations obtained were characterized from a physicochemical point of view (e.g. size, zeta potential, pH) and their loading capacity and encapsulation efficiency were determined to understand whether the nano-carriers and the formulation protocol selected were suitable for protein delivery.

The ability of the NSs to release the drug and drug release kinetics were investigated at different pH values to mimic the gastrointestinal environment in order to assess the pH-dependent behaviour of NSs, which is especially useful in oral delivery.

The studies conducted on cells, that is, the cytotoxicity test and intestinal permeability test, were fundamental to assess the safety of the nano-carriers and their ability to promote insulin absorption at the intestinal level.

The *in-vivo* pharmacokinetic study was performed on healthy rats. They underwent surgery for duodenal cannula installation and were treated with insulin-loaded NSs via the duodenal route as the objective was to investigate into the absorption of insulin at the intestinal level.

The efficacy study included two animal models, i.e. streptozotocin-induced diabetic mice (STZ mice) and non-obese diabetic mice (NOD mice) to test the hypoglycaemic effect after oral administration of insulin-loaded NSs. The efficacy study included a large number of mice due to inter and intra-variability of response to treatment.

6. Materials and methods

6.1 Materials

Roquette Frères (Lestrem, France) provided β-CD and Linecaps, which were dried in an oven at 80°C overnight before use., Ethanol, acetone, triethylamine, pyromellitic dianhydride, citric acid, insulin from bovine pancreas and ELISA kit were purchased from Sigma-Aldrich (Munich, Germany). Deionized and milliQ® water were obtained using a Millipore Direct-QTM 5 production system. The cell culture reagent was purchased from Gibco/Invitrogen Life Technologies (Paisley, UK). All other chemicals used were commercially available analytical grade products.

Wistar male rats and female NOD mice, were provided by Charles River (Charles River Laboratories Italia s.r.l, Lecco, Italy).

6.2 NS syntheses

6.2.1 Synthesis of the PMDA-βCD-1:4 nanosponge

A volume of 16.6 ml of dimethyl sulfoxide (DMSO) was poured into a dry, clean, round-bottom flask. Then 14.10 g of dehydrated β-CD was dissolved in DMSO and stirred until a colourless homogeneous solution was obtained. Subsequently, 4.17 ml of triethylamine (TEA) was pipetted into the solution followed by addition of 3.13 g of pyromellitic dianhydride (PMDA). The nanosponge appeared like a dark amorphous solid-like gel and was left over night to solidify. After grinding with a pestle and mortar, it was washed in a Buchner flask with 500 ml of distilled water and 500 ml of acetone. Once dry, the nanosponge underwent Soxhlet extraction with acetone at 60-70°C for 48 hours. Finally, the coarse powder was stored in a clean container in a cool, dry place.

6.2.2 Synthesis of the CTR-LC-1:8 nanosponge

A quantity of 4.4 g of anhydrous LC was dissolved in 15 ml of distilled water followed by the addition of 0.80 g of catalyst, i.e. sodium hypophosphite monohydrate (SHP) and 5.96 g of crosslinker, i.e. citric acid (CA). The reaction was carried out in the vacuum oven at 140°C for 1h, and 100°C for 15 hours. After grinding with a pestle and mortar, it was washed in a Buchner flask with 500 ml of distilled water and 500 ml of acetone. Once dry, the nanosponge underwent Soxhlet extraction with acetone at 60-70°C for 48 hours. Finally, the coarse powder was stored in a clean container in a cool, dry place.

6.3 Preparation of blank NS nanosuspensions

Blank nanoformulations were prepared using a top-down method. The synthesized NS were weighed and suspended in distilled water at a concentration of 10 mg/ml at room temperature.

Then the suspensions were dispersed using a high-shear homogenizer (Ultraturrax®, IKA, Konigswinter, Germany) for 10 minutes at 24000 rpm. The suspensions were also subjected to high-pressure homogenization at a back-pressure of 500 bars for 90 minutes, using an EmulsiFlex C5 instrument (Avastin, USA), in order to further reduce the particle size and therefore obtain stable nanosuspensions. They were then purified by dialysis (Spectrapore, cellulose membrane, cut-off 12000 Da) to eliminate any residues of synthesis and stored at 4°C in closed glass containers. The average size of blank NS nanosuspensions was determined by Laser Light Scattering using a 90plus Instrument (Brookhaven) and Nanoparticle Tracking Analysis. The pH was measured at room temperature using a pH meter (Orion model 420 A).

6.4 Preparation of insulin-loaded nanosponges

Insulin was incorporated in each nanosponge nanosuspension by adding an acidic aqueous solution (pH=2.3) of insulin (2 mg/ml) at a ratio of 1:5 (mg insulin/mg NS). The mixtures were stirred at room temperature for 30 minutes, and centrifuged at 22000 rpm for 20 minutes, at the end the sediments were collected and freeze-dried overnight. The lyophilized insulin-loaded NSs were stored at 4°C in a closed glass container.

In order to perform the physicochemical characterizations, *in-vitro* release studies and *in-vivo* tests, the lyophilized insulin-loaded nanoformulations were reconstituted by adding saline solution to an appropriate amount of powder.

The preparation method was also modified in order to investigate into the mechanism behind the loading process by changing the pH of the insulin solution (from acidic to neutral) and omitting stirring and precipitation steps. The following batches were therefore investigated:

- 2 mg/ml insulin acidic solution (pH=2.3) mixed with blank industrial NS nanosuspension at a ratio of 1:5 (mg insulin/mg NS), left stirring, centrifuged and freeze-dried.
- 2 mg/ml insulin neutral solution (pH=7) mixed with blank industrial NS nanosuspension at a ratio of 1:5 (mg insulin/mg NS) left stirring, centrifuged and freeze-dried.
- 2 mg/ml insulin acidic solution (pH=2.3) mixed with blank industrial NS nanosuspension at a ratio of 1:5 (mg insulin/mg NS) left stirring and directly freeze-dried.
- 2 mg/ml insulin acidic solution (pH=2.3) mixed with blank industrial NS nanosuspension at a ratio of 1:5 (mg insulin/mg NS), directly centrifuged and then freeze-dried.

6.5 Physicochemical Characterization

6.5.1 Dynamic Light Scattering (DLS) and Nanoparticle Tracking Analysis (NTA)

Photon correlation spectroscopy (PCS) using a 90 Plus particle sizer (Brookhaven Instruments Corporation, USA) equipped with Mas option particle sizing software, was used to measure the average diameter and polydispersity index of the blank and insulin-loaded nanosuspension. The measurements were performed setting a fixed scattering angle of 90 and at 25°C. The samples were diluted with distilled water before each measurement. Zeta potential determination was carried out using an additional electrode in the same instrument. The NS formulations were diluted with distilled water (200 µl of NS in 3 ml of water) and placed in the electrophoretic cell, to which an electric field of approximately 15 V/cm was applied. A few drops of 0.1 mM KCl were added to adjust the conductance when needed.

The Nanoparticle Tracking Analysis (NTA) model NS300 was used to determine the nanoparticle size of both blank and insulin-loaded nanosuspensions in greater depth. The samples were diluted to 1:10000 with milliQ water and injected in the instrument for analysis. This technique is based on the refractive index of the nanoparticles and combines laser light scattering microscopy with a charge-coupled device (CCD) camera, which enabled the nanoparticles in solution to be visualized and recorded. The NTA software identified and tracked individual nanoparticles moving under Brownian motion and related the movement to a particle size.

6.5.2 Fourier-Transform Infrared Spectroscopy

Fourier-transform infrared (FTIR) spectra of free insulin, blank and insulin-loaded NSs were collected using a Perkin Elmer Spectrum 100 FTIR in the region of 4000-650 cm^{-1} in the attenuated total reflectance ATR mode with a diamond crystal, using 32 scans for each spectrum and a resolution of 4 cm^{-1}. The spectrum software version 10.03.05 Perkin Elmer Corporation was used for data acquisition.

6.5.3 Differential Scanning Calorimetry

Differential Scanning Calorimetry (DSC) was carried out using a Perkin Elmer DSC/7 differential scanning calorimeter (Perkin-Elmer, CT-USA) equipped with a TAC 7/DX instrument controller. The instrument was calibrated with indium for the melting point and heat of fusion. A heating rate of 1 °C/min was applied in the 25-90°C temperature range. Standard aluminium sample pans (Perkin-Elmer) were filled with 0.25 ml of sample. The analyses were performed in triplicate under a nitrogen stream.

6.5.4 Transmission Electron Microscopy

Transmission electron microscopy (TEM) analysis was performed to evaluate particle shape and morphology. A Philips CM 10 transmission electron microscope was used and the particle size was measured using the NIH image software. The NS nanosuspensions were sprayed on a Formwar-coated copper grid and air-dried before observation.

6.5.5 *In-vitro* mucoadhesion capability evaluation

In-vitro evaluation of the mucoadhesive properties of NSs was performed by studying the interaction between mucin and the NS before and after loading with insulin through turbidimetric measurements. One ml of mucin solution (from porcine stomach) was mixed with 0.5 ml of NS nanosuspension, stirred for 30 min and centrifuged for 5 min at 10000 rpm. The concentration of mucin bound to the NSs was determined using an external standard calibration. The transmittance of the supernatant (measured at 500 nm) allowed the amount of free mucin to be detected and therefore the amount of bound mucin to be calculated by subtraction from the concentration of the mucin solution (2 mg/ml).

6.5.6 Swelling degree evaluation

Fixed amounts of dry NSs were stirred overnight in excess of deionized water at room temperature. The swollen NSs were immediately weighed after decanting the excess of water and put into comparison with the dry weight. The swelling degree (SD) was then calculated using the following equation:

$SD = (W_{swollen} - W_{dry})/W_{dry} \times 100$

$W_{swollen}$: weight of swollen NS after 24 hours

W_{dry}: weight of dry NS

The swelling degree evaluation also included a swelling test in buffer solutions, which had different pH values (pH=1.2 and pH=6.8) in order to mimic the gastric and intestinal environments. The evaluation was performed at scheduled times up to 24 hours.

6.5.7 High Performance Liquid Chromatography

High Performance Liquid Chromatography (HPLC) was used to detect and quantify insulin. An HPLC pump (Perkin Elmer 250B, Waltham, MA) equipped with a spectrophotometer detector (Flexar UV/Vis LC, Perkin Elmer, Waltham, MA) and an analytical column C18 (150 mm × 4.6 mm, ODS ultrasphere 5 μm; Beckman Instruments, USA) were used. The mobile phase consisted of a mixture of 0.1 M sodium sulphate in distilled water and acetonitrile (72:28 v/v) adjusted with phosphoric acid to reach a pH value of 2.3, filtered through a 0.45 μm nylon membrane and ultrasonically degassed before use. The ultraviolet wavelength was fixed at 214 nm and the flow

rate was 1 ml/min. An external standard method was used to construct standard calibration curves to calculate insulin concentration. Linear calibration curves were obtained over the concentration range of 2−20 µg/ml, linear plotted with a regression coefficient of 0.99.

6.5.8 Encapsulation efficiency and loading capacity

Drug loading and encapsulation efficiency were determined by sonicating in an ultrasonic bath a proper amount of freeze-dried NS formulations suspended in a suitable extraction solvent (i.e. mobile phase) in order to disrupt the insulin-NS interaction and dissolve insulin in the extraction solvent. The supernatant was filtered and injected in HPLC coupled with UV for quantification. Drug loading and encapsulation efficiency were calculated using the applicable formulas[153].

6.5.9 *In-vitro* release of insulin from the loaded NS formulations

The *in-vitro* release was carried out using multi-compartment rotating cells with a dialysis membrane (Sartorius, cut off 100000 Da). The donor phase consisted of freeze-dried insulin-loaded formulations suspended in 1ml of distilled water. In the receiving compartment phosphate buffer solutions with fixed pH values, one simulating gastric fluid (pH=1.2) and another intestinal fluid (pH=6.8) maintaining sink conditions. The receiving phase was completely withdrawn and replaced with fresh medium at fixed time intervals. The collected samples were diluted and analyzed using HPLC-UV. The concentration of insulin released was calculated and plotted on a graph showing the percentage of insulin release as a function of time.

6.5.10 Stability study in simulated gastric and intestinal fluids

A dialysis bag (Spectrapore, cellulose membrane, cut-off 12000 Da), containing blank industrial NS nanosuspension, was immersed in 50 ml of simulated gastric and intestinal fluids and stirred at 37°C for up to 6 hours. Size and zeta potential of the nanosuspension were determined after 30 minutes and 2 hours in SGF and 30 minutes and 6 hours in SIF to assess the stability of the formulation.

6.5.11 Aggregation state evaluation of insulin

The HPLC pump (Perkin Elmer 250B, Waltham, MA) equipped with the spectrophotometer detector (Flexar UV/Vis LC, Perkin Elmer, Waltham, MA) and an analytical column Agilent AdvanceBio SEC (130 Å, 7.8 . 300 mm, 2.7 µm) were used. The mobile phase consisted of a mixture of 200 ml of anhydrous acetic acid, 300 ml of acetonitrile, 400 ml of distilled water adjusted to pH 3.0 with concentrated ammonia, and diluted to 1000 ml with distilled water. It was filtered through a 0.45 µm nylon membrane and ultrasonically degassed before use. The ultraviolet wavelength was fixed at 276 nm and the flow rate was 0.5 ml/min with isocratic elution mode. An external standard

method was used to construct standard calibration curves to calculate insulin concentration. Linear calibration curves were obtained over the concentration range of 10-60 µg/ml, linear plotted with a regression coefficient of 0.99.

Once the analytical procedure was established, an *in-vitro* release study by means of multi-compartment rotating cell was performed to assess the state of insulin released from the nanosponges in the receiving phase. For this purpose, a suitable dialysis membrane (Sartorius, cut off 100000 Da) was used to separate donor and receiving compartments. The donor phase consisted of freeze-dried insulin-loaded industrial formulation suspended in 1ml of distilled water. In the receiving compartment a phosphate buffer solution at pH=6.8 prepared as indicated in USP was put to simulate the intestinal environment. The receiving phase was completely withdrawn and replaced with fresh medium at fixed time intervals, i.e. 15,30,45,60,120,180 and 360 minutes, the same used in the previous pharmacokinetic study on rats. The collected samples were diluted and analyzed using HPLC-UV. The concentration of insulin released was calculated and plotted on a graph showing the percentage of insulin release as a function of time.

6.6 *In-vitro* studies

6.6.1 Cytotoxicity test

Cytotoxicity was assessed through the MTT test: cell survival assay using human umbilical vein endothelial cells (HUVECs).

Insulin solution, blank NSs and insulin-loaded NSs were prepared bearing in mind that they were going to be used for *in-vitro* testing: all of the instruments were washed previously with ethanol and distilled filtered water to prevent contamination, the samples were suspended in autoclaved Eppendorf tubes with autoclaved saline solutions and their pH was adjusted to a value within the range 5-7.4.

6.6.2 *In-vitro* intestinal permeation test

A Caco-2 cell line (ATCC HTB-37™), after 3 weeks of incubation in Transwell support in order to obtain cell differentiation, was used to evaluate the intestinal absorption of insulin in the loaded NS formulations. Trans Epithelial Electrical Resistance (TEER) was checked to ensure integrity of the tight junctions and monolayer integrity.

Insulin solution, blank NSs and insulin-loaded NSs were prepared as indicated in the previous section. In addition, fluorescently labelled nanosuspensions were prepared for this test following the method described in the literature[45]. In detail, an excess of 6-coumarin was added to fresh nanosponge nanosuspensions (10 mg/ml) and stirred at room temperature for 3 days.

Centrifugation was used to separate fluorescent nanosponges from free 6-coumarin. To determine the amount of 6-coumarin complexed to NSs, the fluorescent nanosponges were sonicated after dilution in the extraction solvent (ethanol), and the supernatants, which were collected after centrifugation, were analyzed with the EnSight fluorometer.

The *in-vitro* intestinal permeation test was conducted on insulin solution, blank NSs, insulin-loaded NSs and blank fluorescently labelled NSs, which were diluted in the cell medium and pipetted in the Transwell donor compartments.

At scheduled times (15, 30, 45, 60, 90, 120, 180 and 240 minutes) the receiving phase was withdrawn and replaced with fresh medium. At the end of the experiment the cells were washed with a washing solution and disrupted with TRITON X. Both solutions were collected.

The receiving phases, cell washing solutions, and cell lysate solutions were analyzed with the EnSight fluorometer to trace fluorescently labelled NSs.

6.7 *In-vivo* pharmacokinetic study

To evaluate intestinal absorption, insulin-loaded industrial NS and CTR-LC-1:8 NS formulations were administered directly into the duodenal lumen of rats.

The experiment was conducted on 14 male Wistar rats (Charles River Laboratories Italia s.r.l, Lecco, Italy), weighing about 250 g, which were housed in standard facilities, and maintained according to the ethical regulations of Italian Institutional Animal Care and Use Committee. The rats were kept under controlled environmental conditions (24 ±1 °C, 50-60% humidity, 12 hours light and dark cycles, lights on at 7:00 a.m.) and given ad-libitum access to food and water.

The day before the pharmacokinetic study, the rats underwent surgery in order to insert cannulas in the duodenum for sample administration and inside the right jugular vein for blood withdrawal.

Free insulin solution, used as a control, and insulin-loaded industrial NS and CTR-LC-1:8 NS were administered via the duodenal cannula to non-fasted rats.

Blood was withdrawn through the cannula inserted in the jugular vein at fixed times (0, 15, 30, 45, 60, 120, 180 and 360 minutes) after administration and put into heparinized tubes.

The dose of insulin (60 IU/kg) was adjusted on the basis of the weight of the rats.

After one week, a number of rats underwent a second operation for the installation of the cannula in the left jugular vein and their response to treatment was investigated a second time.

The samples, route of administration, dose, rat code and purpose are listed in Table 3.

Table 3. List of experiments carried out on healthy rats.

Sample	No. of animals	Route of administration	Dose (IU/kg)	Rat code	Purpose
Bovine insulin solution	5		60	Rat 1,2,3,5,6	control
Saline solution	1		---	Rat 4	
Insulin-loaded industrial NS	10	Duodenal	60	Rats 7-16	Evaluation of insulin
Insulin-loaded CTR-LC-1:8 NS	4		60	Rats 17-20	intestinal absorption

All animals were treated as established by the Bioethics Committee for Animal Experimentation of the University of Turin and the Ministry of Health in Rome (no. 678/2018-PR).

6.7.1 Detection of bovine insulin in rat plasma

Heparinized rat blood withdrawals were centrifuged in order to collect the supernatant, that is, plasma. The plasma samples were analysed through an immunological assay (ELISA test) to detect insulin.

The assay consisted in filling the wells of the ELISA plate with 100 µl of a dilution buffer as controls (blank), bovine insulin standards within a concentration range from 4.69 to 300.16 µIU/ml and plasma samples diluted 1:1 with a dilution buffer.

All samples were analysed in duplicate and the concentration of insulin was determined using a standard calibration curve.

The ELISA plate was then incubated at room temperature for 2.5 hours with gentle shaking in order to promote interaction between the bovine insulin and the immobilized antibody already present in the wells.

After incubation, the wells were washed 4 times with 300 µl of wash buffer, and 100 µl of biotinylated detection antibody specific for insulin was added and left to shake for 1 hour.

After washing away unbound biotinylated antibody (4 times with 300 µl of wash buffer), 100 µl of HRP-conjugated streptavidin was pipetted into the wells to enable interaction between biotin and streptavidin and left to shake for 45 minutes.

The wells were washed again (4 times with 300 µl of wash buffer), 100 µl of a Tetramethylbenzidine (TMB) substrate solution was added to the wells and the action of the enzyme HRP on the TMB substrate caused chemiluminescence with the development of colour in proportion to the amount of insulin bound. After 30 minutes, 50 µl of stop solution was added, changing the colour from blue to yellow, and the intensity of the colour was measured at 450 nm with a Victor plate reader.

6.8 Efficacy study on diabetic mice

6.8.1 NOD mice

To evaluate the hypoglycaemic effect, insulin-loaded NS formulations were administered to NOD mice via oral gavage.

The experiment was conducted on female NOD mice (Charles River Laboratories Italia s.r.l, Lecco, Italy), weighing about 25 g, which were housed in standard facilities, and maintained according to the ethical regulations of Italian Institutional Animal Care and Use Committee. The mice were kept under controlled environmental conditions (24 ±1 °C, 50-60% humidity, 12 hours light and dark cycles, lights on at 7:00 a.m.) and given ad-libitum access to food and water.

Three groups of this animal model were included in the efficacy study:

- Group no.1: 24 female NOD mice 63/69 days old.
- Group no.2: 25 female NOD mice 84 days old, the age of which was selected in order to speed up the monitoring process of the development of diabetes.
- Group no.3: 25 female NOD mice 84 days old.

Their weight and baseline blood sugar levels (BSL) were checked weekly in order to monitor the development of diabetes.

To assess the suitability of the mice for the efficacy study, the response to treatment (oral administration of insulin-loaded industrial NS) in comparison with the control (saline solution) was investigated on NOD mice having high (over 200 mg/dl) and low (around 100 mg/dl) baseline blood sugar levels. On the basis of the outcome of this preliminary test, only the mice having baseline sugar levels of over 200 mg/dl were selected for the efficacy study.

The NOD mice included in the efficacy experiment were fasted overnight. At the beginning of the test, blood collected from the tail was used to assess baseline blood sugar levels with an ACCU-CHEK glucometer. Then a 5% glucose solution was injected intraperitoneally (IP) in order to increase the blood sugar level and, after 10 minutes, the samples were administered according to their group via oral gavage.

The blood glucose level was determined at scheduled times, that is, at 0, 15, 30, 45, 60, 90 and 120 minutes.

Group no.1 was treated with insulin-loaded industrial NS at 2 doses, i.e. 60 and 90 IU/kg administered via oral gavage. Saline solution was given orally as a control. Insulin-loaded CTR-LC-1:8 NS was also administered orally to 3 mice at a dose of 60 IU/kg.

Group no.2 was treated with saline solution and insulin-loaded industrial NS at a dose of 60 IU/kg orally and free insulin solution and insulin-loaded industrial NS subcutaneously at 1.5 IU/kg.

Group no.3 was treated with saline solution, free insulin solution and insulin-loaded industrial NS at a dose of 60 IU/kg orally and free insulin solution and insulin-loaded industrial NS subcutaneously at 1.5 IU/kg.

The summary table below shows the total number of animals selected per treatment belonging to the three groups of NOD mice.

Table 4. Number of mice, treatment, route of administration and purpose of the experiments in all NOD mice groups.

Mouse health status	No. mice	Sample	Route of administration	Dose (IU/kg)	Purpose
Diabetic	16	Saline solution	Oral gavage	---	Control
Healthy	4	Saline solution	Oral gavage	---	Control
Diabetic	22	Insulin solution	Oral gavage	---	Control
Healthy	11	Insulin solution	Oral gavage	---	Control
Diabetic	10	Insulin solution	Subcutaneous injection	1.5	Control
Healthy	11	Insulin solution	Subcutaneous injection	1.5	Control
Diabetic	43	Industrial NS insulin-loaded	Oral gavage	60	Evaluation of efficacy
Healthy	18	Industrial NS insulin-loaded	Oral gavage	60	Evaluation of efficacy
Diabetic	8	Industrial NS insulin-loaded	Oral gavage	90	Evaluation of efficacy
Diabetic	3	CTR-LC-1:8 NS insulin-loaded	Oral gavage	60	Evaluation of efficacy
Diabetic	12	Industrial NS insulin-loaded	Subcutaneous injection	1.5	Evaluation of efficacy
Healthy	12	Industrial NS insulin-loaded	Subcutaneous injection	1.5	Evaluation of efficacy

The specific mice codes and the experiments conducted on NOD mice groups 1, 2 and 3 are present in Tables A1, A2 and A3 in the Annexe.

The mice were sacrificed upon completion of all the experiments.

The animals were treated as established by the Bioethics Committee for Animal Experimentation of the University of Turin and the Ministry of Health in Rome (no. 678/2018-PR).

6.8.2 Efficacy study on STZ-induced diabetic mice

The C57BL6J animal model was selected and 35 mice (C57BL6J) were included in the efficacy study.

Thirty mice were treated with multiple doses of streptozotocyn (STZ) to induce diabetes. The efficacy experiment was scheduled for the fourth week. Their weight and blood sugar levels were monitored periodically, mice were considered diabetic when the BSL was over 250 mg/dl.

Five mice were not given STZ and thus formed the healthy mice group, which was used as a control.

The other mice were divided into groups on the basis of the sample administered, the dose and the route of administration. The insulin-loaded industrial NS was investigated at 2 doses, i.e. 90 and 120 IU/kg and administered via oral gavage. It was also administered by subcutaneous injection at a dose of 1.5 IU/kg. Free insulin solution was administered orally at a dose of 90 IU/kg and subcutaneously at 1.5 IU/kg. Saline solution was given orally to both diabetic and healthy mice. All treatments are shown in Table 5.

Table 5. Design of the efficacy experiment on STZ mice with the insulin-loaded industrial NS and CTR-LC-1:8 NS.

Mouse health status	No. mice	Sample	Route of administration	Dose (IU/kg)	Purpose
Diabetic	10	Saline solution	Oral gavage	-	control
Healthy	10	Saline solution	Oral gavage	-	control
Diabetic	19	Industrial NS insulin-loaded	Oral gavage	90	Evaluation of efficacy
Diabetic	6	Industrial NS insulin-loaded	Oral gavage	120	Evaluation of efficacy
Diabetic	2	Insulin solution	Oral gavage	90	control
Diabetic	7	Insulin solution	Subcutaneous injection	1.5	control
Diabetic	3	Industrial NS insulin-loaded	Subcutaneous injection	1.5	Evaluation of efficacy
Diabetic	10	CTR-LC-1:8 NS insulin-loaded	Oral gavage	90	Evaluation of efficacy
Diabetic	3	CTR-LC-1:8 NS insulin-loaded	Subcutaneous injection	1.5	control

The mice were fasted on the day of the experiment.

Firstly, blood collected from the tail was used to assess baseline blood sugar levels with a glucometer. Then a 5% glucose solution was injected intraperitoneally in order to increase the blood sugar and after 10 minutes the formulation or saline solution were administered via the administration route selected. The blood glucose was determined at scheduled times, i.e. 0, 15, 30, 60, 90 and 120 minutes. The mice were sacrificed upon completion of all the experiments.

6.8.3 Statistical analysis

The *in-vivo* response to treatment of diabetic mice was analysed using the GraphPad Prism 5 software. A two-tailed unpaired Student's t-test was selected for analysing blood sugar levels of controls and treated STZ mice having previously verified that the data were normally distributed using the D'Agostino-Pearson normality test.

The two-tailed unpaired Student's t-test was also used to analyse the blood sugar levels of controls and treated NOD mice when the data passed the D'Agostino-Pearson normality test. If this was not the case, the Mann-Whitney U Test was selected. The outcome of the Student's t-test performed on controls vs. oral treatments and between the two oral treatments was confirmed also with a one-way non-parametric ANOVA (Kruskal-Wallis test followed by Dunn's post test).

The results were expressed as mean ± SD. If $p < 0.05$, a significant difference was considered to exist.

7. Results and Discussion

The aim of this PhD project was to investigate the use of starch nanosponges for the oral delivery of proteins, using insulin as a case study.

Three prototypes, that is, an industrial NS, the composition of which is confidential, and another two synthesized by the Chemical and Material Science Research Group (Prof. Trotta et al.) at the University of Turin were investigated.

The latter two include a nanosponge obtained by crosslinking β-cyclodextrins with pyromellitic dianhydride at a 1:4 ratio (PMDA-βCD-1:4) and a nanosponge made up of linecaps with citric acid at a 1:8 ratio (CTR-LC-1:8) (Figure 6).

The use of pyromellitic dianhydride and citric acid as crosslinkers leads to the formation of polymers that contain, in their network, free ionisable carboxylic groups sensitive to the pH of the external medium. In fact, carboxylic derivatives being weak acids, they are undissociated in a highly acid medium, whereas a gradual deprotonation occurs when the pH of the medium increases. Deprotonation leads to a modification of the polymer structure, which causes the nanosponge to start swelling and release the drug loaded by diffusion[154].

This property may be particularly useful if the NSs are intended for oral administration, as the release of the drug is influenced by the pH of the GI tract. In fact, the nanosponge would retain the drug in the stomach where the pH is very low (pH=1.2) and the presence of agents like enzymes risks causing degradation of the drug, on the contrary, at the intestinal level (pH=6.8), which is the site of systemic absorption, it would release the drug slowly.

In addition, as cyclodextrin (CD) and linecaps (LC)-based nanosponges are starch derivatives, they are natural biodegradable compounds, due to their ester bonds susceptible to hydrolysis and have proven to be safe in previous studies both *in vitro* and *in vivo* [92,155].

All the features discussed above made us hypothesize PMDA-βCD-1:4 and CTR-LC-1:8 NSs as promising candidates for oral insulin delivery as well as the industrial NS proposed by the company Roquette Frères.
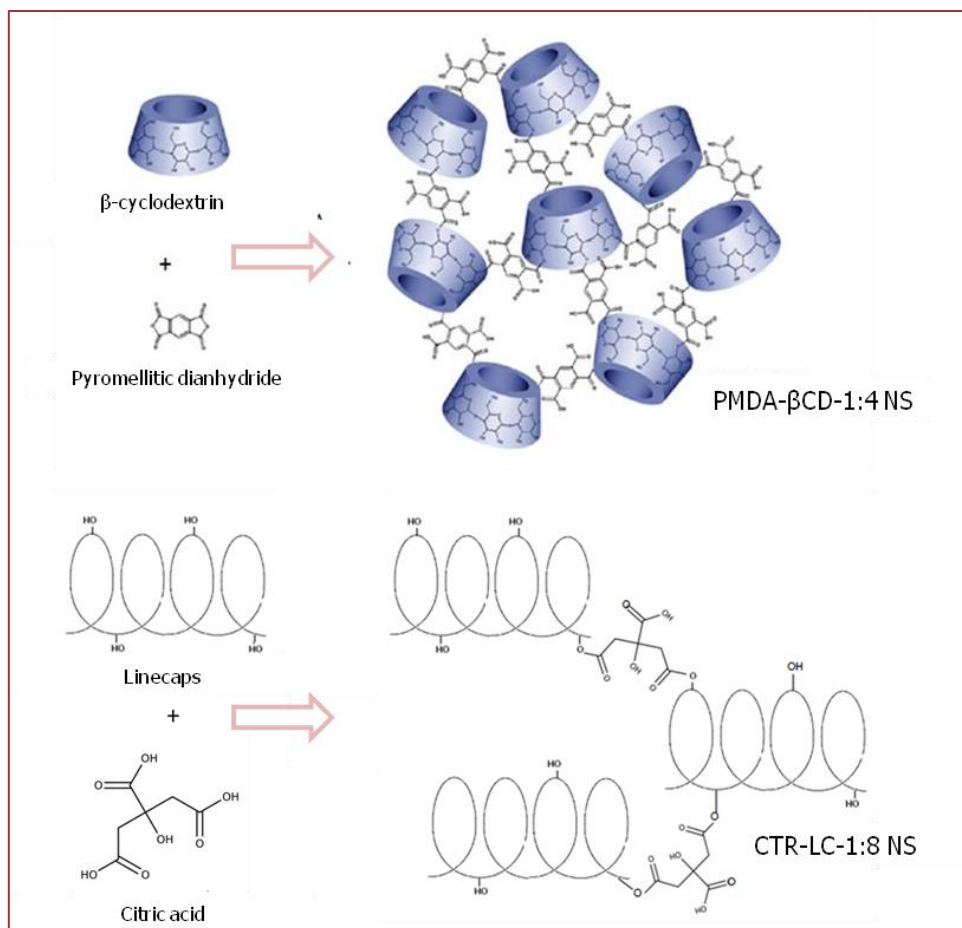
Figure 6. Schematic representation of the nanosponges synthesized at the University of Turin, with PMDA-βCD-1:4 at the top[115] and CTR-LC-1:8 at the bottom.

7.1 Physicochemical characterization

After synthesis, the NSs were formulated in order to obtain stable aqueous nanosuspensions.

To assess the success of the HPH homogenization step, the average size of the nanoparticles and the zeta potential were measured, as nanosized particles and a highly negative zeta potential are required for a physically stable nanosuspension. In addition, these two parameters were put into comparison between blank and insulin-loaded nanosponges to understand if any changes occurred.

The average particle size of blank NSs measured with DLS was approximately 240 nm, it increased when loaded with insulin, particularly in the industrial and CTR-LC-1:8 NSs (Table 6).

The pH of the NS aqueous suspensions ranged from acidic to neutral, while the average pH after insulin encapsulation was 4 in all formulations.

Table 6. Average size measured with DLS and pH of blank and insulin-loaded NSs.

Nanosponge code	Average diameter (nm)	Polydispersity index	pH
Blank PMDA-βCD-1:4	240.9±1.0	0.237±0.009	4.72
Insulin-loaded PMDA-βCD-1:4	285.7±8.8	0.221±0.030	4.20
Blank CTR-LC-1:8	255.7±3.1	0.366±0.017	3.41
Insulin-loaded CTR-LC-1:8	379.5±3.8	0.365±0.045	3.97
Blank industrial NS	225.9±1.9	0.276±0.004	7.08
Insulin-loaded industrial NS	361.0±5.7	0.296±0.014	4.44

Alongside DLS, NTA was used to study nanoparticle size in depth. This innovative technique is indicated for sizing nanoparticles from about 30 to 1000 nm[156]. Unlike in DLS analysis, large particles, such as dust particles or small amounts of large aggregates, have negligible interference with the analysis, thus enabling an accurate particle size distribution analysis to be conducted[156]. Average diameter and D10, D50, D90 values, representing the percentage of the particles, which have a size equivalent to or less than the value indicated are listed in Table 7.

Table 7. Average size, particles per ml and D10, D50, D90 values of blank and insulin-loaded NSs, measured by NTA.

Nanosponge code	Particles per ml	Average diameter (nm)	D10	D50	D90
Blank CTR-LC-1:8	$(2.2±0.1)*10^{13}$	145±3.1	98	132	206
Insulin-loaded CTR-LC-1:8	$(3.62±2.1)*10^{12}$	183.7±4.5	127	165	264
Blank PMDA-βCD-1:4	$(1.2±0.1)*10^{12}$	155±5.3	106	135	230
Insulin-loaded PMDA-βCD-1:4	$(3.98±7.7)*10^{12}$	177.8±2.1	121	166	243
Blank industrial NS	$(4.9±0.1)*10^{13}$	133±2.3	88	125	182
Insulin-loaded industrial NS	$(1.3±0.1)*10^{13}$	177±5.3	104	156	306

Figure 7 shows the particle size distribution of blank and insulin-loaded NSs measured with NTA.
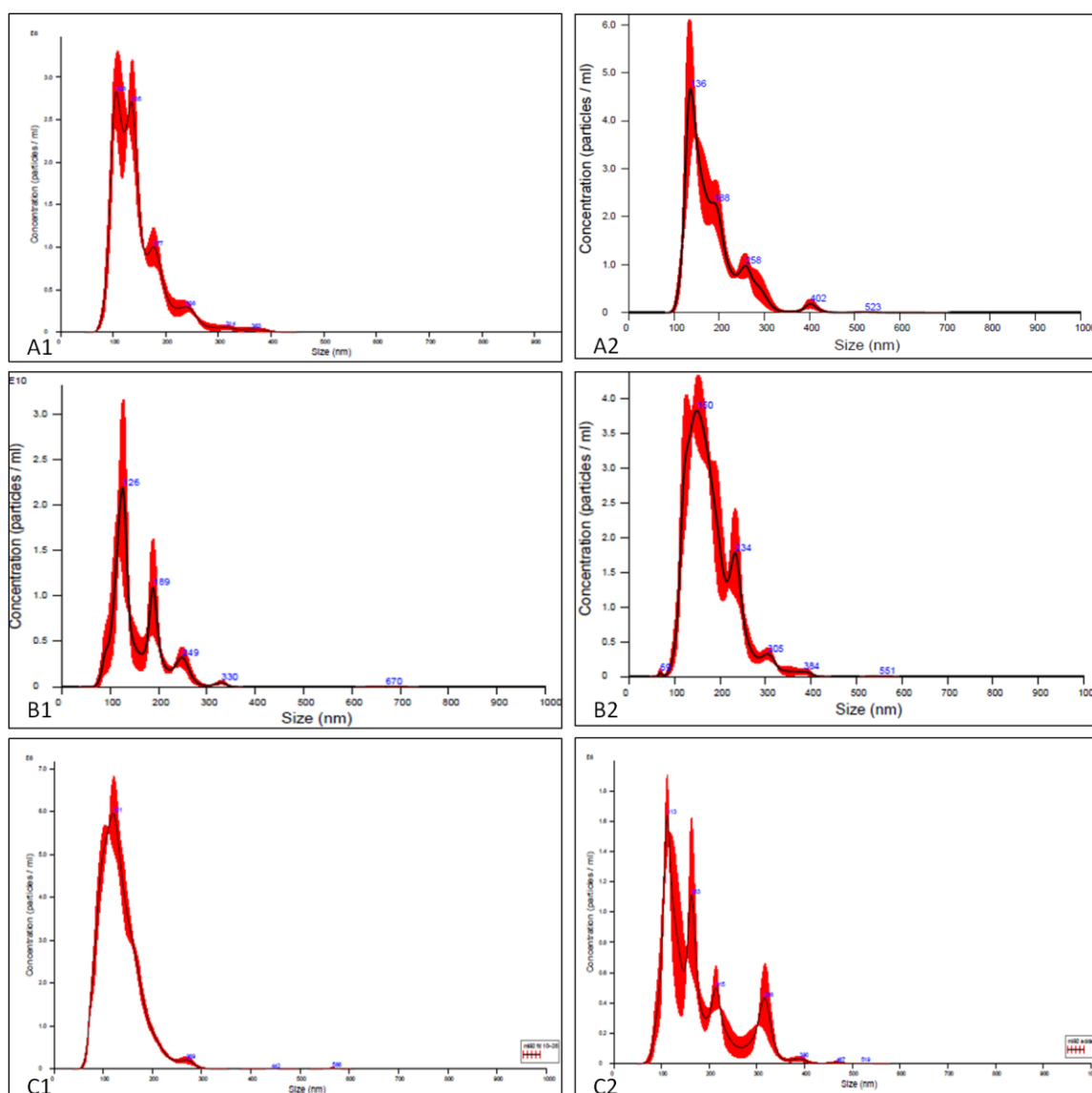
Figure 7. Size distribution measured with NTA of blank CTR-LC-1:8 (A1) and insulin-loaded CTR-LC-1:8 (A2), blank PMDA-βCD-1:4 (B1) and insulin-loaded PMDA-βCD-1:4 (B2), blank industrial NS (C1) and insulin-loaded industrial NS (C2).

Even in this more detailed particle size analysis, there is a general increase in particle size after insulin incorporation, which is more pronounced in CTR-LC-1:8 and the industrial NS, and consistent with DLS results.

PMDA-βCD-1:4 nanoscale size was also confirmed through TEM analysis, which also revealed the spherical shape of the nanoparticles (Figure 8)[115].
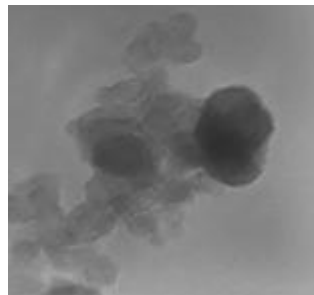
Figure 8. TEM image of insulin-loaded PMDA-βCD-1:4 (105,000X magnification)

The zeta potential of blank NSs was strongly negative (around -30 mV), enough to ensure physical stability and avoid aggregation (Table 8). Interestingly, this value did not change after loading with insulin, thus suggesting that insulin was incorporated inside the nanosponges.

Table 8. Zeta potential measurements of blank and insulin-loaded NSs.

Nanosponge code	Zeta potential
Blank CTR-LC-1:8	-29.54±7.92
Insulin-loaded CTR-LC-1:8	-28.45±5.29
Blank PMDA-βCD-1:4	-26.65±1.79
Insulin-loaded PMDA-βCD-1:4	-26.75±1.01
Blank industrial NS	-33.99±2.01
Insulin-loaded industrial NS	-30.24±2.62

During the tuning preparation process, quantitative analyses were also conducted to assess the production yield (w/w)[157] of NS formulations.

The quantitative analysis consisted in determining the amount of freeze dried nanosponges in the main steps of NS nanosuspension preparation, that is:

- before and after HPH treatment followed by dialysis on the blank suspensions
- after the loading process, on the precipitated amount of insulin-loaded NSs

The following figure shows the process steps and the red stars indicate the stages in which the quantitative analysis was performed.
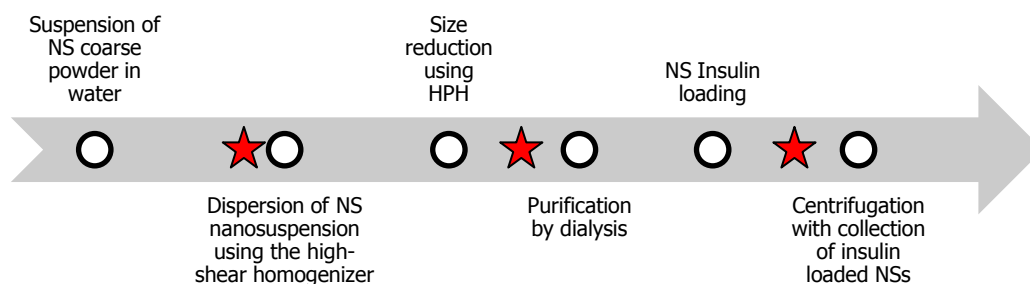
Figure 9. NS formulation steps and stages of the quantitative analysis.

The data collected in this test are presented in Table 9.

Table 9. Recovery of nanosponge powder after freeze-drying of 1ml of suspension in critical formulation steps.

NS code	Amount of freeze-dried nanosponge (mg)		
	Before HPH	After HPH and dialysis	After insulin loading
CTR-LC-1:8	9.9	9.1	5.2
PMDA-βCD-1:4	10.1	9.5	5.3
Industrial NS	12.2	9.3	5.4

In comparison with the theoretical value, i.e. 6 mg comprehensive of $mg_{insulin}$ and mg_{NS} in 1 ml of suspension, the production yield of insulin-loaded CTR-LC-1:8, PMDA-βCD-1:4, and the industrial NS was 87%, 88%, and 90%, respectively. When the actual amount of blank NS recovered after the destructive process performed by HPH was considered, these values increased to 94%, 92%, and 96%, respectively.

As mentioned previously, we hypothesized that PMDA-βCD-1:4 and CTR-LC-1:8 nanosponges could incorporate a large, charged molecule like insulin due to their nanoporous structure consisting of CD and linecaps internal cavities, respectively, and the interstitial pores between them and crosslinker units and swelling ability. This was confirmed by high loading capacity (over 14 %) and encapsulation efficiency (over 86 %) as shown in the table below.

Table 10. Loading capacity and encapsulation efficacy.

NS code	Loading capacity (%)	Encapsulation efficiency (%)
Insulin-loaded CTR-LC-1:8	14.4±0.7	86.2±4.3
Insulin-loaded PMDA-βCD-1:4	14.4±0.9	86.6±5.2
Insulin-loaded industrial NS	15.3±1.3	91.6±7.6

Alongside the loading capacity and encapsulation efficiency determination, two analytical methods were selected, i.e. Fourier-Transform Infrared (FTIR) Spectroscopy and Differential Scanning Calorimetry (DSC), to investigate insulin incorporation inside the nanosponges.

ATR-FTIR was used to analyse bovine insulin, blank nanosponges and insulin-loaded nanosponges in order to detect the structural features of both bovine insulin and nanosponges and check whether any change in the spectra occurred when insulin was encapsulated inside the polymer. Special attention was therefore paid to the characteristic absorption peaks of insulin, i.e. those corresponding to amide I and II. These features were searched for in insulin-loaded nanosponge spectra to understand if any physical interactions occurred between insulin and the polymer.

ATR-FTIR spectra of PMDA-βCD-1:4 (Figure 10) revealed structural features of insulin, such as α-helix and β-sheet represented by amide I and amide II bands in the region of 1700−1600 and 1600−1500 cm^{-1}, respectively, at 1650.81 cm^{-1} (80% C=O stretching vibration, 20% in plane C-N stretching) and 1535.13 cm^{-1} (40% C-N stretching, 60% N-H bending). The absorption band of the carbonyl groups (C=O stretching) of pyromellitic dianhydride was present at 1721.34 cm^{-1} in the NS spectrum. The O–H stretching band at 3319.33 cm^{-1} can be attributed to both primary and secondary hydroxyl groups and to carboxylic OH stretching deriving from the opening of the cyclic dianhydride. At 1300–1440 cm^{-1} combinations of bands were visible due to OH bending and C–O stretching of unreacted carboxyl groups. FTIR spectra of insulin-loaded NS showed mainly the peaks of the NS overlapping and shifting the characteristic peaks of insulin.

Figures 11 and 12 show the ATR-FTIR spectra of the industrial NS and CTR-LC-1:8, respectively.
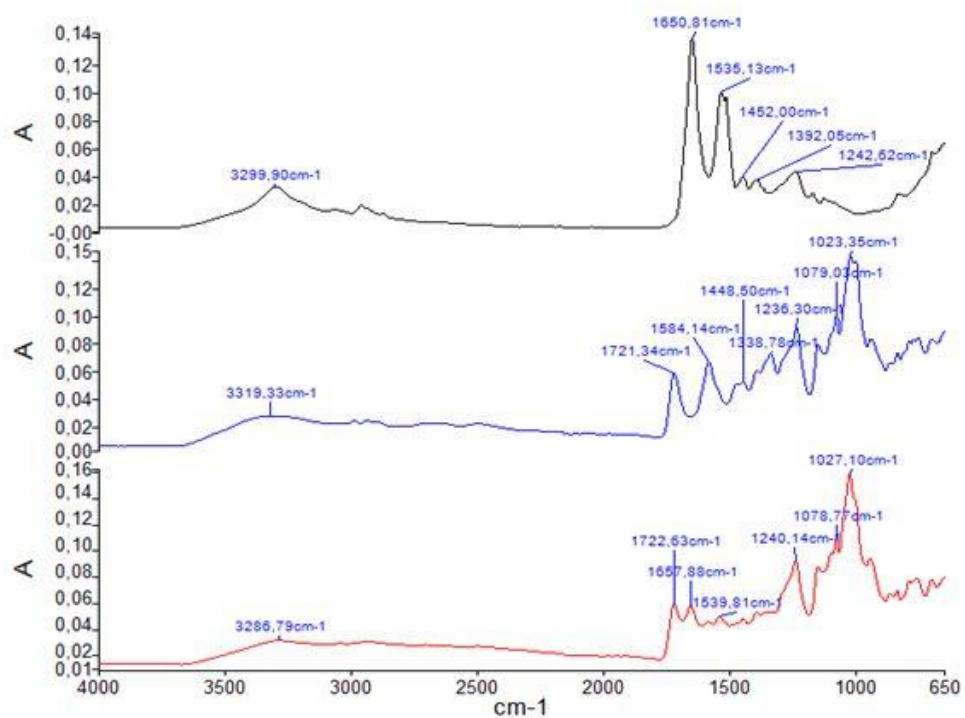
Figure 10. ATR-FTIR spectra of Insulin (black), blank PMDA-βCD-1:4 (blue) and the insulin-loaded PMDA-βCD-1:4 (red)[115].
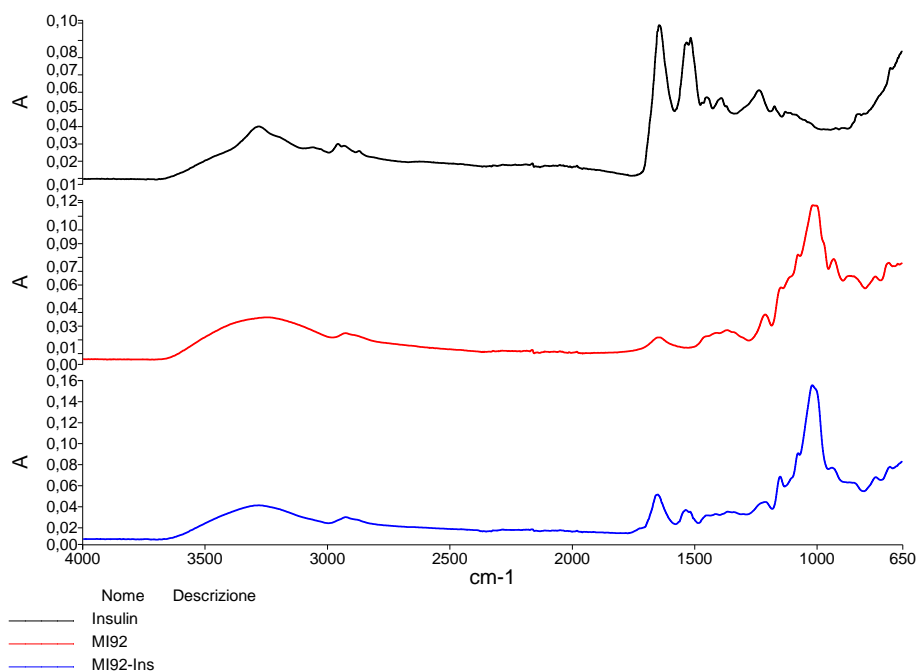
Figure 11. ATR-FTIR spectra of Insulin (black), blank industrial NS (red) and insulin-loaded industrial NS (blue).
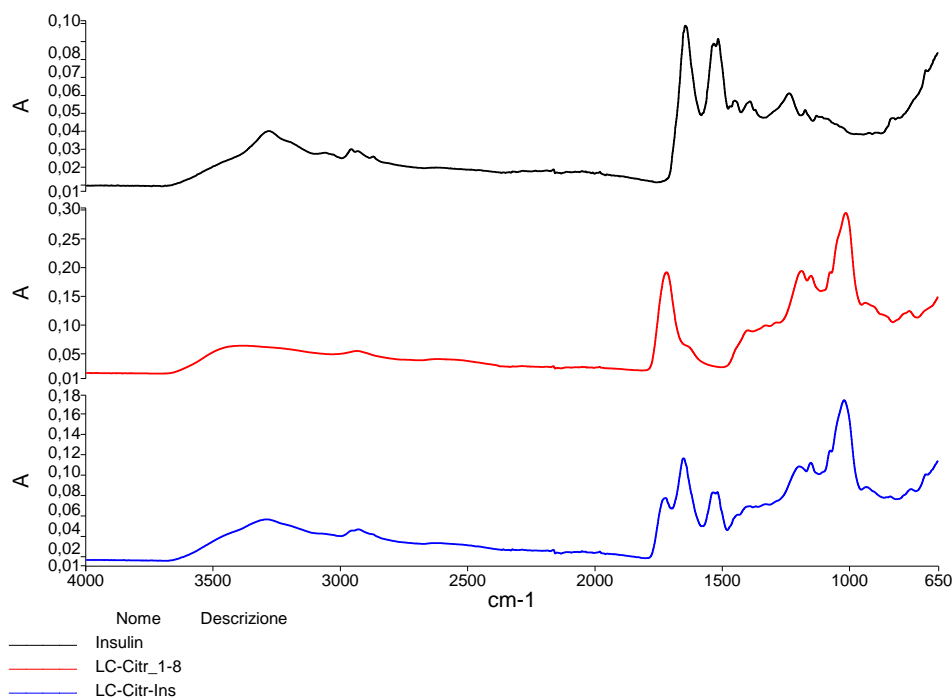
Figure 12. ATR-FTIR spectra of Insulin (black), blank CTR-LC-1:8 (red) and insulin-loaded CTR-LC-1:8 (blue).

DSC experiments were carried out on insulin-loaded nanosponge as the DSC technique can reveal structural changes of proteins when incorporated in delivery systems[158] and may give valuable information on the encapsulation of insulin inside the polymer matrix.

Both insulin solution and insulin-loaded nanosuspensions were analysed (Figure 13). The DSC curve of insulin was in line with previous studies[158,159] and was used for comparison purposes. No endothermic peak related to the denaturing point of insulin (around 75 °C) was observed in insulin-loaded NS curves, thus indicating the molecular dispersion of insulin inside the polymer matrices. The amorphous nature of the freeze-dried NSs was also confirmed using the same instrument. No peaks correlated with temperature changes were observed up to 250 °C.
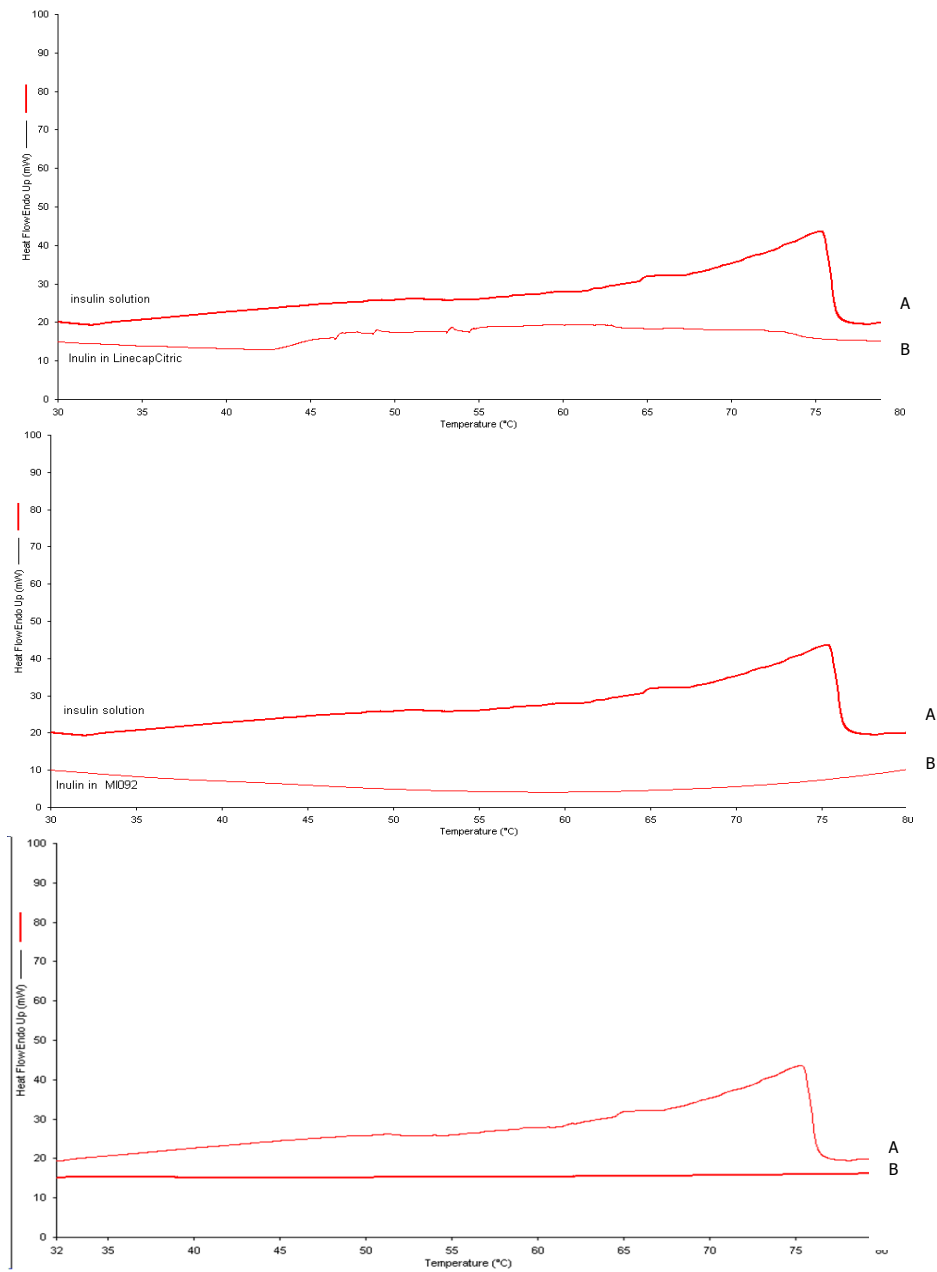
Figure 13. From top: DSC analysis of insulin-loaded CTR-LC-1:8, industrial NS and PMDA-βCD-1:4. Curve A represents insulin solution and curve B insulin-loaded NS nanosuspension.

Mucoadhesion and swelling capacity results revealed other useful properties for oral drug delivery. Mucoadhesion is a desirable property in drug delivery as it contributes to prolong the residence time of drugs in the mucosal layer of intestinal epithelial cells, favouring their absorption[160,161]. Mucoadhesive polymers are generally hydrophilic and carry a high density of functional groups, such as carboxyl (COOH), hydroxyl (OH) and amine groups (NH3), just like PMDA-βCD-1:4 and CTR-LC-1:8 NSs.

Mucoadhesion was tested on blank and insulin-loaded nanosponges and was over 80% in all prototypes (Table 11). This result indicates the interaction between NS and mucin, possibly consisting of hydrogen bonds and hydrophobic interactions[162].

Interestingly, there is a negligible difference before and after insulin loading, thus suggesting successful incorporation of insulin inside the polymeric structure without affecting the superficial mucoadhesive interactions.

Table 11. Mucoadhesion before and after insulin loading.

NS code	Mucoadhesion (%)	
	Before loading	After loading
Industrial NS	83.0±3.8	96.2±1.2
PMDA-βCD-1:4	93.1±1.2	95.2±1.5
CTR-LC-1:8	89.5±0.9	88.2±0.4

Swelling is a particularly interesting property of drug delivery systems as there is evidence that swelling enables the gradual release of drugs encapsulated within the carrier[154,163,164].

The swelling test was performed at first in distilled water (Table 12).

Table 12. Swelling degree of the NSs in water.

NS code	Swelling degree (%)	
	Powder	Freeze-dried NS nanosuspensions
Blank industrial NS	898.9±7.7	1738.2±19.8
Blank PMDA-βCD-1:4	823.7±11.8	1189.1±4.8
Blank CTR-LC-1:8	299.8±9.8	355.6±13.6

The coarse powders of the industrial NS and PMDA-βCD-1:4 absorbed a large amount of water, which increased even more in lyophilized NS nanosuspensions. This could be due to the homogenization step, which resulted in a significant reduction in nanoparticle size with an increased surface area. CTR-LC-1:8 exhibited a different behaviour, with a swelling degree of less

than 300% in water, which increased slightly in the swollen freeze-dried NS nanosuspension for the reason stated above.

The NS prototypes were also put in contact with simulated gastric and intestinal fluids to study their swelling in order to make preliminary predictions about their behaviour in the gastrointestinal tract.

The monitoring of the swelling degree of PMDA-βCD-1:4 NS over time at gastric and intestinal pH values, 1.2 and 6.8, is shown in the figure below.
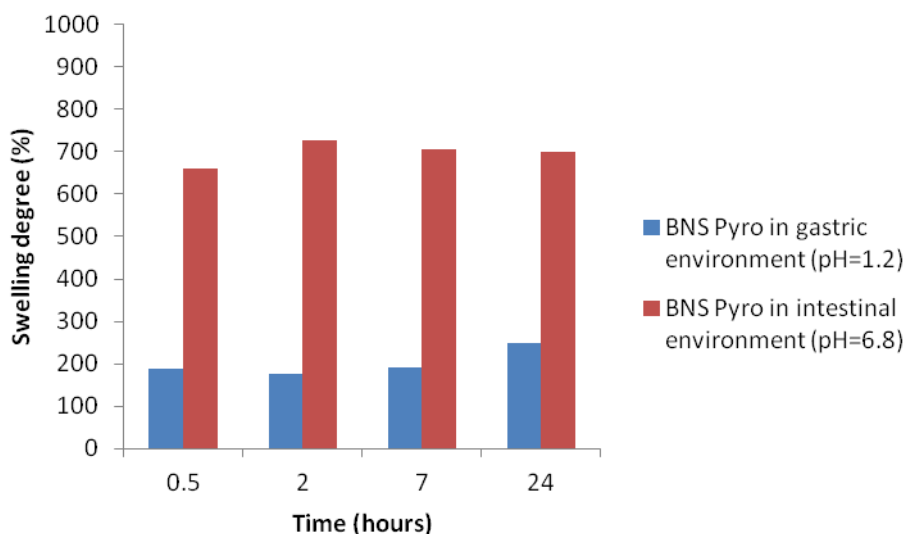
Figure 14. Swelling test of PMDA-βCD-1:4 NS at pH=1.2 (blue) and pH=6.8 (red). The bars represent the swelling degree of the nanosponge as a function of time up to 24 hours.

The mean swelling degree of PMDA-βCD-1:4 at pH= 6.8 was 3.5 times as high as that of PMDA-βCD-1:4 at pH=1.2. PMDA-βCD-1:4 at pH= 6.8, formed a gel only after 30 minutes unlike at the acidic pH.

As this test showed almost unchanged behaviour over time, it was conducted on all three prototypes directly at 24 h and compared (Table 13).

Table 13. Swelling behaviour in simulated gastric fluid (SGF) and simulated intestinal fluid (SIF) after 24 hours.

NS code	Blank industrial NS	Blank CTR-LC-1:8	Blank PMDA-βCD-1:4
Weight (mg) NS before swelling test in SGF	49.8	50.7	53.6
Weight (mg) NS before swelling test in SIF	50.2	50.3	52.8
Weight (mg) swollen NS in SGF	413.5	195.0	171.6
Weight (mg) swollen NS in SIF	442.9	267.3	469.4
% swelling degree SGF	**730.3**	**284.6**	**220.1**
% swelling degree SIF	**782.3**	**431.4**	**789.0**

The results show a general increase in swelling in the intestinal fluid compared to the gastric fluid. Barely noticeable in the case of the industrial NS, while marked in CTR-LC-1:8 and PMDA-βCD-1:4 with 3.6-fold and 1.5-fold increases, respectively. CTR-LC-1:8 swelled less than the other two prototypes at the intestinal pH, as it did in the previous swelling test in distilled water. CTR-LC-1:8 is characterised by a very acidic pH when suspended in water (Table 6) and so it was checked that the pH of the nanosponge itself had not varied the pH of the intestinal fluid. As the pH at the end of the swelling test was 4.5, the pH was increased by adding 1M NaOH to reach the correct pH of 6.8 and the test was carried out again.

A similar approach was adopted for the industrial NS, which apparently showed no appreciable difference in swelling between the gastric and intestinal media. In fact, the pH of the NS (pH=7) affected the pH of SGF raising it to 2.90, so it was reduced to pH 1.2 with 1M HCl and the test was repeated. The updated results of the swelling test are as follows:

Table 14. Updated swelling behaviour in simulated gastric fluid (SGF) and simulated intestinal fluid (SIF) after 24 hours.

NS code	Blank industrial NS	Blank CTR-LC-1:8	Blank PMDA-βCD-1:4
% swelling degree in SGF	**603.6**	**284.6**	**220.1**
% swelling degree in SIF	**782.3**	**646.0**	**789.0**

The data shown in Table 14 demonstrate that NS swelling is pH dependent, which confirmed our initial hypothesis, whereby the carboxylic groups within the polymer structure, being sensitive to the pH of the medium, gradually undergo deprotonation due to the increase of the pH, thus resulting in a modification of the polymer structure, which causes swelling.

These findings are encouraging because the NSs should be able to limit insulin release at the gastric pH and release it in a sustained manner via diffusion through the polymer matrix at the intestinal pH, as investigated in the *in-vitro* release kinetics study described below.

The *in-vitro* release kinetics test carried out using multi-compartment rotating cells revealed a pH-dependent release of insulin from PMDA-βCD-1:4 NS (figure 15). The bars represent the amount of insulin found in the receiving compartments at scheduled times and more specifically, the ones coloured blue represent the amount of insulin (%) found in the pH=1.2 buffer solution, whereas the red ones represent the amount of insulin (%) found in the pH=6.8 buffer solution. The release of insulin was remarkably low at the acidic pH (pH=1.2), but gradual at pH= 6.8 and at 2 hours the total amount of insulin released was 10 times as high.
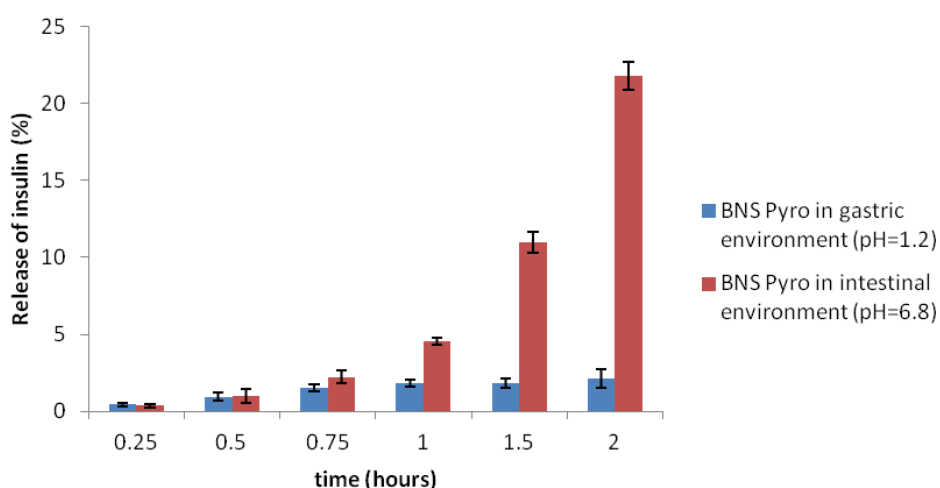
Figure 15 *In-vitro* release kinetics of PMDA-βCD-1:4 NS at gastric and intestinal pH using multi-compartment rotating cells.

This is certainly attributable to the pH-dependent swelling behaviour discussed previously: the NS swells at pH=6.8 enabling the drug to diffuse gradually in the environment, whereas at pH=1.2 swelling is limited as is the release of the encapsulated drug.

The test was also performed on the other two prototypes and the total amount of insulin released in the receiving phases at pH=1.2 and 6.8 at 2 hours was put into comparison (Table 15).

Table 15. Insulin released from CTR-LC-1:8, PMDA-βCD-1:4 and the industrial NS after 2 hours in gastric and intestinal pH values.

NS code	Total amount of insulin released (%)	
	SGF	SIF
CTR-LC-1:8	11.29±1.25	22.81±9.27
PMDA-βCD-1:4	2.32±0.26	21.80±0.93
Industrial NS	0.93±0.19	24.34±1.14

The release at the intestinal pH was investigated up to 24 hours (Table 17) (Figure 16) with a release of insulin of over 90%. It was gradual and prolonged with no initial burst and constant release kinetics (zero−order) rate up to 7 hours (Figure 17).
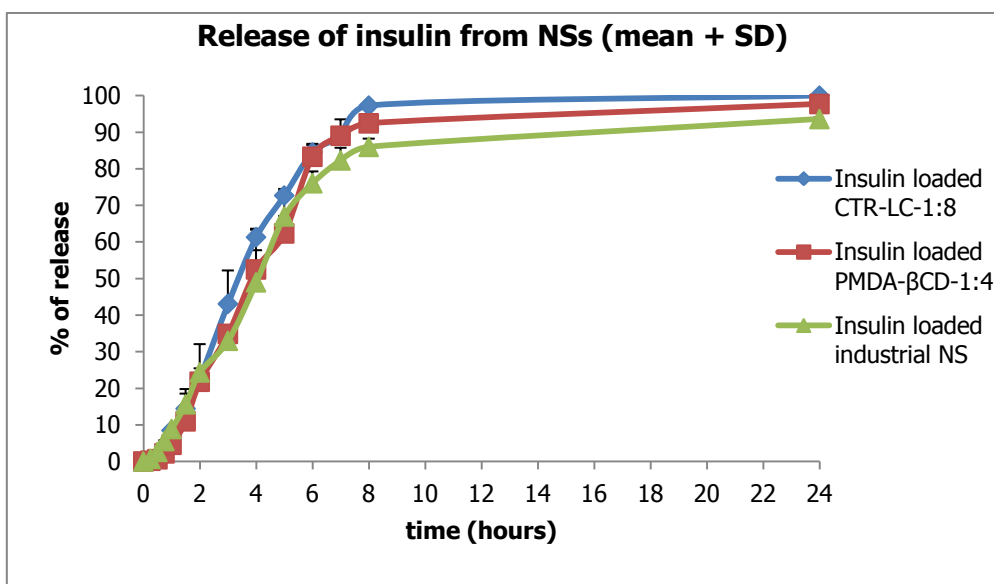
Figure 16. Drug release kinetics of insulin-loaded NS formulations in SIF up to 24 hours (% of release).
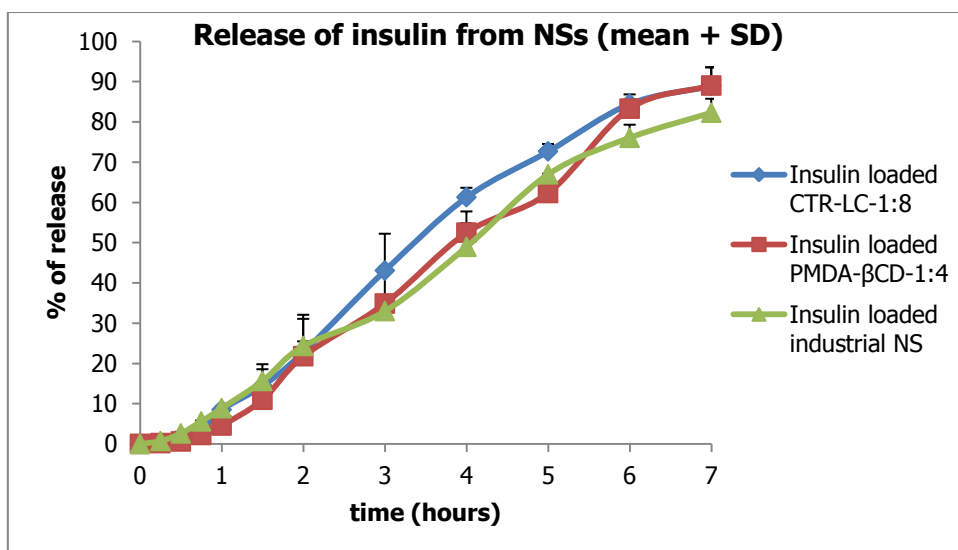
Figure 17. Drug release kinetics of insulin-loaded NS formulations in SIF up to 7 hours (% of release).

The data regarding the release *in vitro* in SGF and SIF are present in the tables below.

Table 16. Results of the *in-vitro* release study in SGF with insulin concentration and insulin cumulative release expressed as µg/ml and %.

Sample		CTR-LC-1:8			PMDA-βCD-1:4			Industrial NS		
	Time (hours)	Insulin concentration (µg/ml)	Insulin release (µg/ml)	% of release	Insulin concentration (µg/ml)	Insulin release (µg/ml)	% of release	Insulin concentration (µg/ml)	Insulin release (µg/ml)	% of release
Receiving phase (SGF)	0.25	1.52	1.52	0.15	1.33	1.33	0.43	0.96	0.96	0.14
	0.5	7.73	9.25	0.92	1.58	2.91	0.95	0.84	1.80	0.27
	0.75	10.97	20.22	2.01	1.78	4.68	1.53	1.01	2.81	0.43
	1	20.10	40.32	4.01	0.93	5.59	1.83	---*	2.81	0.47
	1.5	31.97	72.29	7.18	---*	5.59	1.83	2.15	5.26	0.80
	2	50.19	122.49	12.17	0.92	6.52	2.13	1.69	6.95	1.06
Donor	2	883.98			298.88			643.01		
Total		1006.47			305.40			649.96		

*not detected

Table 17. Results of the *in-vitro* release study in SIF with insulin concentration and insulin cumulative release expressed as µg/ml and %.

Sample	Time (hours)	CTR-LC-1:8			PMDA-βCD-1:4			Industrial NS		
		Insulin concentration (µg/ml)	Insulin release (µg/ml)	% of release	Insulin concentration (µg/ml)	Insulin release (µg/ml)	% of release	Insulin concentration (µg/ml)	Insulin release (µg/ml)	% of release
Receiving phase (SIF)	0.25	2.02	2.02	0.29	0.60	0.60	0.11	1.81	1.81	0.60
	0.5	2.88	4.90	0.70	1.62	1.62	0.31	5.34	7.15	2.35
	0.75	9.60	14.50	2.06	11.44	13.06	2.51	10.45	17.60	5.79
	1	49.61	64.11	9.11	11.59	24.65	4.73	10.70	28.30	9.32
	1.5	57.99	122.10	17.34	29.96	54.61	10.48	28.49	56.79	18.69
	2	84.66	206.76	29.36	55.30	109.91	21.08	15.15	71.94	23.68
	3	142.10	348.86	49.55	72.63	182.54	35.02	31.89	103.83	34.18

Table 17. Results of the *in-vitro* release study in SIF (*continued*).

Sample	Time (hours)	CTR-LC-1:8			PMDA-βCD-1:4			Industrial NS		
		Insulin concentration (µg/ml)	Insulin release (µg/ml)	% of release	Insulin concentration (µg/ml)	Insulin release (µg/ml)	% of release	Insulin concentration (µg/ml)	Insulin release (µg/ml)	% of release
Receiving phase (SIF)	4	94.35	443.21	62.95	130.43	312.97	60.04	64.87	168.70	55.53
	5	77.67	520.88	73.98	54.14	367.11	70.42	35.79	204.49	67.31
	6	85.71	606.59	86.15	54.26	421.37	80.83	35.04	239.53	78.84
	7	42.53	649.12	92.19	42.88	464.25	89.06	19.52	259.05	85.27
	8	37.20	686.32	97.47	27.95	492.20	94.42	8.73	267.78	88.14
	24	2.88	689.20	97.88	27.81	520.01	99.76	17.54	285.32	93.91
Donor	24	14.91			1.20			18.49		
Total		704.11			521.21			303.81		

Having verified that NSs have a pH-dependent release, it was decided to exploit this property to investigate the mechanism behind the loading process, i.e. to check whether the electrostatic interaction between NS and insulin influences drug encapsulation.

The rationale consisted in varying the pH of the insulin solution to be encapsulated in the NS to a pH higher than the isoelectric point of insulin (pI=5.3) and then checking whether the nanosponge was able to retain the insulin inside the polymer in an acidic environment or whether it released it, suggesting that it is free insulin.

The two solutions of insulin, below and above the isoelectric point had different solubility: at pH=2.3 a clear solution was obtained, whereas at pH 7 an opalescent colour developed after stirring. These solutions were loaded inside blank industrial NS nanosuspensions to prepare batches 1a and 1b (Table 18).

Table 18. Batches prepared by loading insulin solution above and below its pI in the industrial NS nanosuspensions.

Batch	Kind of NS	pH of blank NS nanosuspension	pH of insulin solution	Preparation method
Batch 1a	Industrial NS	7	< pI	✅stirring ✅centrifugation
Batch 1b			> pI	✅stirring ✅centrifugation

The visual inspection revealed some differences: in batch 1a the insulin-loaded sediment obtained through centrifugation looked like a gel with a homogeneous colour, unlike batch 1b, in which a white portion on the bottom of the test tube could be clearly observed. This white portion is attributable to the precipitation of bovine insulin, which is insoluble at a pH> pI, with no incorporation inside the swollen polymer matrix.

Alongside the visual inspection, *in-vitro* drug release experiments with multi-compartment rotating cell equipment were carried out in simulated gastric and intestinal environments to test the release ability of the NS batches. This kind of experiment was selected as it highlights the pH-dependent behaviour of the polymer. This property is not only necessary *in vivo* to protect insulin from the gastric environment, it is also a useful tool for understanding *in vitro* whether insulin has been encapsulated efficiently inside the polymer matrix. In fact, if insulin is not incorporated, a burst effect should be observed in the release kinetics study.

Batches 1a and 1b were put in contact with SGF (Figure 18).
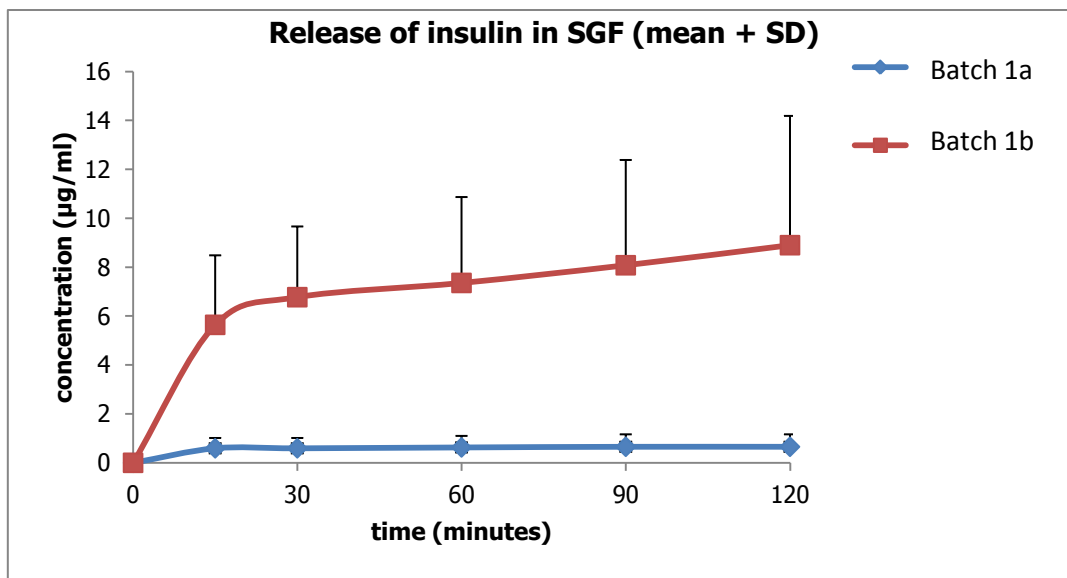
Figure 18. Cumulative release from batches 1a (in blue) and 1b (in red) in SGF.

Table 19. Cumulative release data from batches 1a and 1b in SGF.

Time (minutes)	Cumulative release of bovine insulin (µg/ml) in SGF	
	Batch 1a	Batch 1b
15	0.59	5.64
30	0.59	6.78
60	0.63	7.36
90	0.66	8.08
120	0.66	8.90

These results show a negligible release of bovine insulin at a gastric pH over time in batch 1a, in which insulin was loaded at pH< pI, thus demonstrating that insulin has been loaded successfully inside the polymer matrix.

On the contrary, the amount of bovine insulin released from batch 1b in SGF was 13.6 times as high as that of batch 1a with a clear burst effect at 15 minutes. This behaviour could be attributable to the presence of non-encapsulated insulin.

The following figure and table show the comparison between the release profiles of bovine insulin from batches 1a and 1b in SGF and SIF.
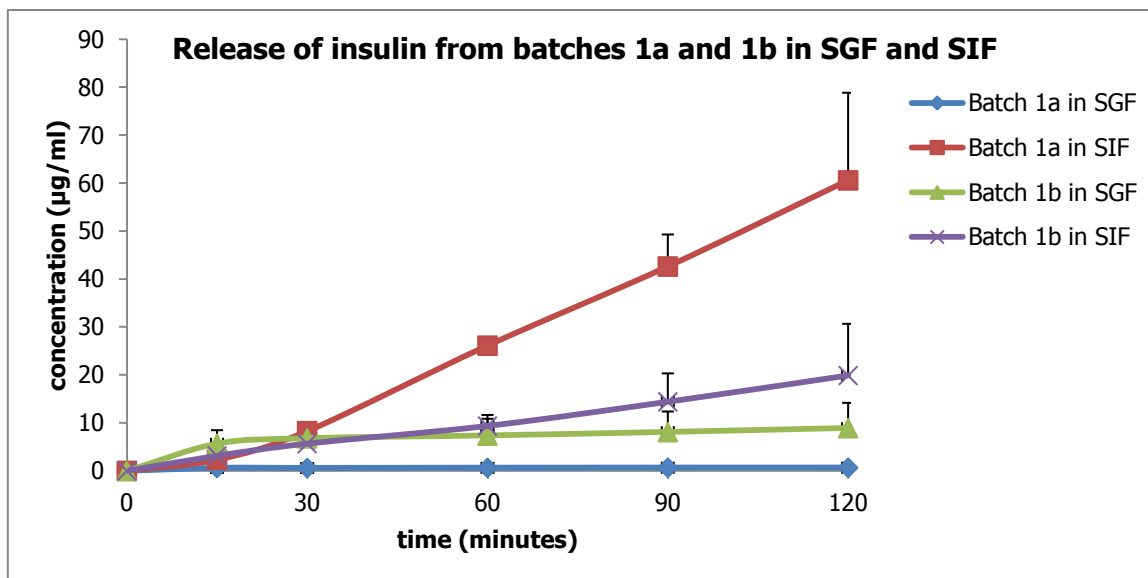
Figure 19. Release kinetics profiles of batches 1a and 1b in SGF and SIF put into comparison.

Table 20. Cumulative release data from batches 1a and 1b in SGF and SIF.

Time (minutes)	Cumulative release of bovine insulin (µg/ml) in SGF		Cumulative release of bovine insulin (µg/ml) in SIF	
	Batch 1a	Batch 1b	Batch 1a	Batch 1b
15	0.59	5.64	2.34	3.14
30	0.59	6.78	8.28	5.67
60	0.63	7.36	26.11	9.36
90	0.66	8.08	42.61	14.40
120	0.66	8.90	60.58	19.87

The best profile was achieved by loading bovine insulin in the industrial NS at pH<pI as insulin was retained at gastric pH and released gradually at intestinal pH. In the other loading condition, that is at pH>pI there was a negligible distinction between the release in gastric and intestinal media, which is negative *in vivo* because an early release of insulin in the stomach would cause its rapid degradation without reaching the absorption level in the intestine. In addition, the overall amount of insulin released in two hours at intestinal pH was 3 times smaller. It could be attributable to the aggregation state of insulin during the loading step at pH>pI which interfered with the diffusion of insulin through the polymer matrix and/or the diffusion across the dialysis membrane placed between donor and receiving compartments. Worthy of note is that insulin, *in vivo,* is active only as a monomer, not in its aggregated form.

Alongside the pH, also the influence of stirring and centrifugation steps on the encapsulation of insulin inside nanosponges was investigated. For this purpose 2 batches were prepared skipping stirring or centrifugation (batches 2 and 3) and put into comparison with batch 1a (Table 21).

Table 21. Batch codes, pH of insulin solution and preparation method of the samples included in this investigation.

Batch	Kind of NS	pH of insulin solution	Preparation method
Batch 1a	Industrial NS	< pI	✓ stirring ✓ centrifugation
Batch 2		< pI	✓ stirring ✗ centrifugation
Batch 3		< pI	✗ stirring ✓ centrifugation

In-vitro drug release experiments with multi-compartment rotating cell equipment were again carried out in simulated gastric and intestinal environments to test the release ability of the NS batches.
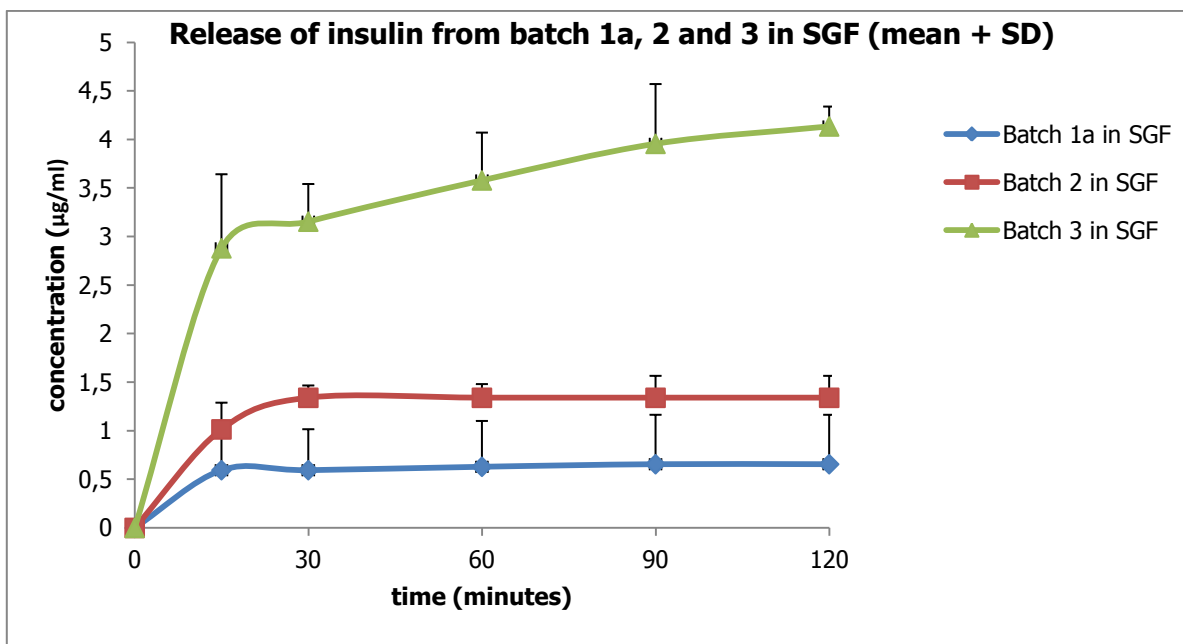
Figure 20. Cumulative release of insulin from batches 1a (in blue), 2 (in green) and 3 (in red) in SGF.

Table 22. Cumulative release data from batches 1a, 2 and 3 and in SGF.

Time (minutes)	Cumulative release of bovine insulin (µg/ml) in SGF		
	Batch 1a	Batch 2	Batch 3
15	0.59	1.01	2.88
30	0.59	1.34	3.15
60	0.63	1.34	3.58
90	0.66	1.34	3.96
120	0.66	1.34	4.13

In batch 3 there was a burst effect with a 5 fold release of insulin in 15 minutes compared to batch 1a. As stirring was skipped in batch 3, insulin-nanosponge complexation was neglected. The best profile is the one obtained following the established method (batch 1a) in which both stirring and precipitation steps are present with a negligible release of insulin in SGF.
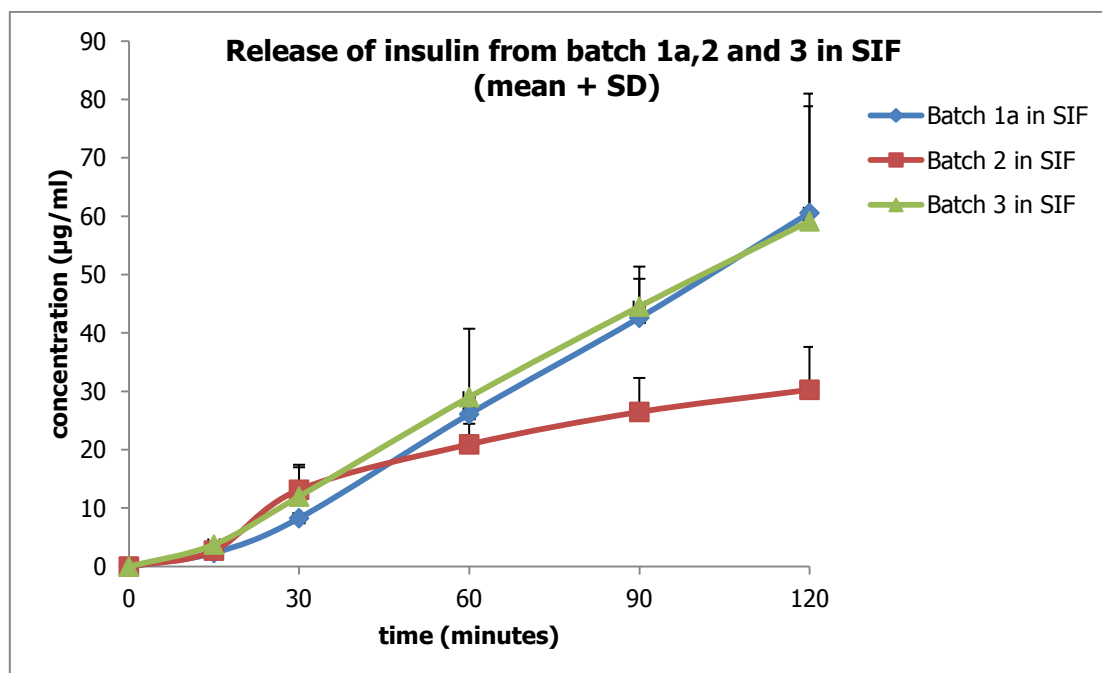
Figure 21. Cumulative release of insulin from batches 1a (in blue), 2 (in red) and 3 (in green) in SIF.

Table 23. Cumulative release data from batches 1a, 2 and 3 and in SIF.

Time (minutes)	Cumulative release of bovine insulin (µg/ml) in SIF		
	Batch 1a	Batch 2	Batch 3
15	2.34	2.74	3.77
30	8.28	13.15	12.00
60	26.11	20.94	29.02
90	42.61	26.49	44.52
120	60.58	30.28	59.14

In SIF the pharmacokinetic profiles of batches 1a, 2 and 3 were not so different, in all cases the release was gradual.

In the figure below, the cumulative release of all batches at acidic pH can be observed.
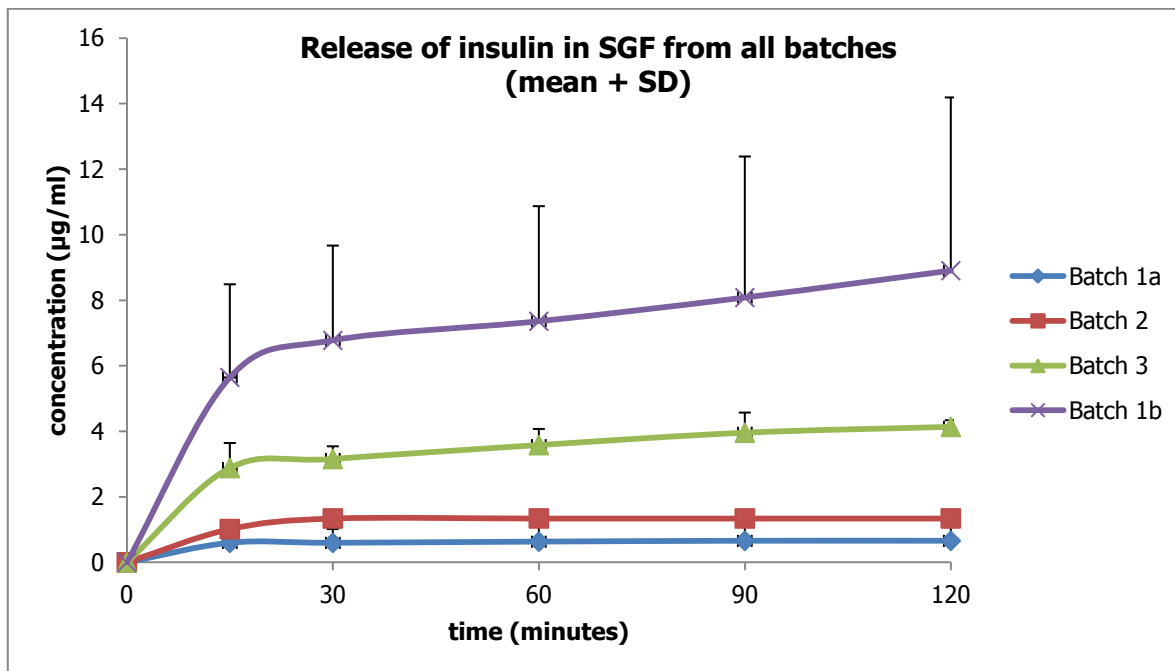
Figure 22. Cumulative release of insulin from batches 1a (in blue), 1b (in violet), 2 (in red) and 3 (in green) in SGF.

Table 24. Cumulative release of insulin from batches 1a, 1b, 2 and 3 in SGF.

Time (minutes)	Cumulative release of bovine insulin (µg/ml) in SGF			
	Batch 1a	Batch 2	Batch 3	Batch 1b
15	0.59	1.01	2.88	5.64
30	0.59	1.34	3.15	6.78
60	0.63	1.34	3.58	7.36
90	0.66	1.34	3.96	8.08
120	0.66	1.34	4.13	8.90

To conclude, in order to understand what affected the encapsulation of bovine insulin in nanosponges the most, *in-vitro* release studies were carried out. They highlighted the behaviour of the polymer in different media and therefore helped us to identify what parameters affected the system, i.e. pH of the insulin solution in the loading step (above or below the pI of insulin), stirring and centrifugation. From the results herein collected, we deduced that pH and therefore complexation are fundamentally important to achieve successful formulations.

The colloidal stability study, which was conducted on the industrial NS formulation, showed that the particle size and polydispersity index (PDI) remained unchanged after 2 hours and 6 hours at

37°C in both gastric and intestinal fluids (Table 25), which are comparable to the size and PDI of NS nanosuspension in water (Table 6).

The zeta potential remained stable at intestinal pH (strongly negative) comparable to that of the NS nanosuspension in water (Table 8) but probably rose at gastric pH due to the pH change.

The lack of precipitation of the suspension observed during the visual inspection after 24 hours with no change in size or PDI in the gastric environment leads us to hypothesize that the zeta potential was sufficient to ensure the stability of the suspension by preventing NS aggregation.

To ensure stability over time, the formulation process of all three insulin-loaded nanosponges also included the freeze-drying step, which is a convenient and effective method of storing the drug and could be exploited in an industrial setting.

Table 25. Colloidal stability data in gastric and intestinal fluids.

Medium	Time (hours)	Size (nm)	PDI	Zeta potential (mV)
SGF (pH=1.2)	0.5	254.1	0.304	-7.03
	2	233.8	0.397	-5.55
SIF (pH=6.8)	0.5	238.3	0.319	-29.1
	6	273.4	0.379	-25.3

The investigation of the aggregation state of bovine insulin, which was used for nanosponge loading, was conducted to confirm that insulin is released in its active form.

In fact, attention must be paid when handling proteins during the formulation process as they are susceptible to degradation and aggregation, thus compromising the safety and efficacy of pharmaceuticals[165]. These concerns have led to routine analysis and quantitation of dimers, trimers, and higher order aggregates for a wide variety of biological therapies, including insulin. Insulin is present in hexameric, dimeric and monomeric states, but there is evidence that only monomeric insulin binds to its receptor and therefore enables insulin action[166].

Size exclusion chromatography (SEC) was selected for this purpose as it is the method of choice for purity analysis, and for detecting aggregates of drug products[167]. The analytical protocol followed was that of Agilent, which was used as a reference[168]. The following figure shows the insulin standard peak, the retention time of which is around 14 minutes and was put into comparison with that of monomer insulin in the Agilent report.
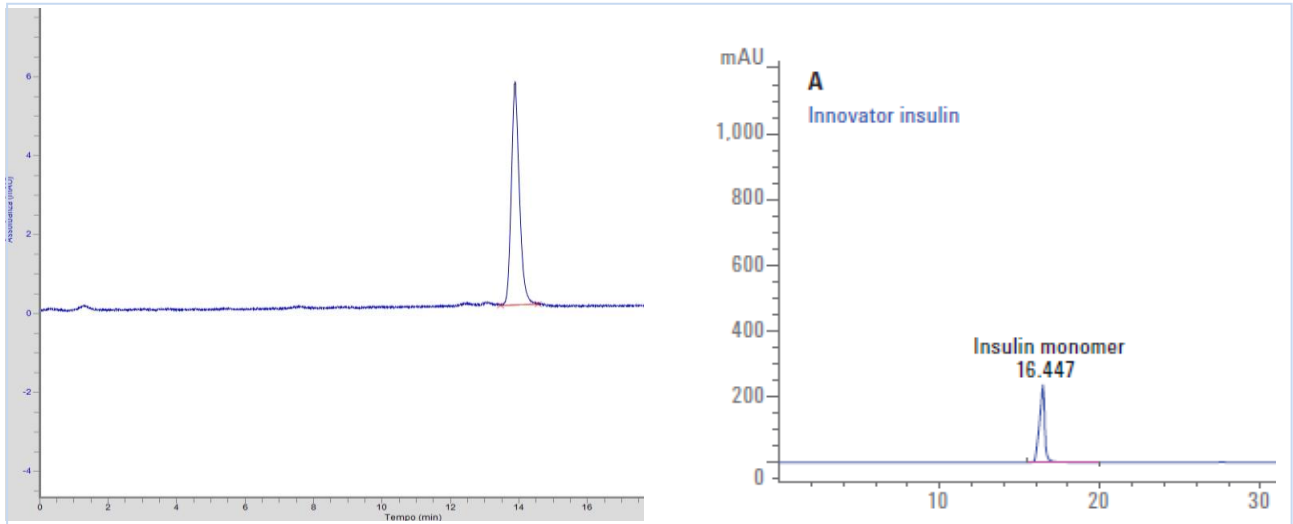
Figure 23. Comparison of SEC profiles of bovine insulin (SIGMA ALDRICH) on the left and monomeric insulin in the Agilent protocol, in which a commercial insulin product purchased from a local pharmacy was used, on the right.

The difference in retention time is attributable to the insulin product, as bovine insulin provided by SIGMA-ALDRICH was analysed here whereas Agilent used a commercial insulin. In addition to this, the analytical systems were different (different HPLC-UV equipment). We therefore hypothesized that the SIGMA-ALDRICH insulin peak found at 13.7 minutes was insulin in its monomeric form.

To further confirm this result, insulin was subjected to heat stress to promote the formation of aggregates and distinguish them from the monomer. In detail, a solution of bovine insulin (3.4 mg/ml) was left for 6 hours at 60°C to induce aggregation. At the end of the experiment, the sample was cooled to room temperature, diluted in the mobile phase and injected in an HPLC-UV apparatus (Figure 24).
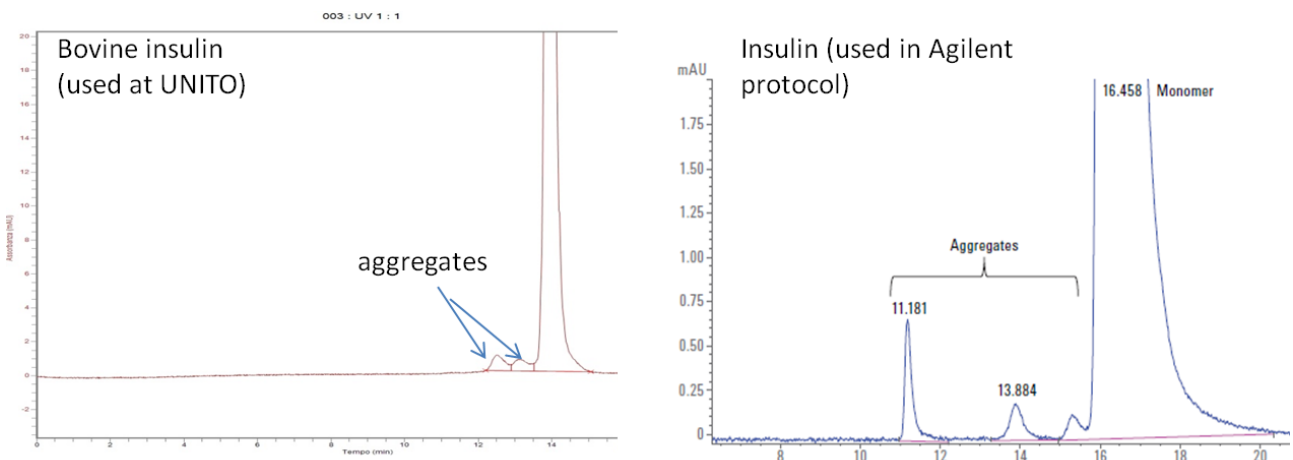
Figure 24. SEC profile of heat stressed insulin showing the baseline separation of insulin aggregates obtained in this study versus that of the Agilent protocol.

The comparison between the results obtained in this study and in the Agilent protocol seems to confirm that the highest peak corresponds to the monomer while the others are aggregates. It may therefore be deduced that the insulin standard (SIGMA-ALDRICH) used for calibration is in its monomeric state.

In addition, a solution of insulin (2 mg/ml) was left stirring for 30 minutes at ambient temperature to mimic the conditions of loading insulin in the nanosponge nanosuspension and determine whether stirring induces aggregation. The chromatogram obtained showed only one peak as in Figure 23 thus demonstrating that the formulation protocol herein developed did not affect insulin.

Then the *in-vitro* release study by means of multi-compartment rotating cells was conducted to understand in what state insulin was released from the industrial NS in intestinal fluid. Interference after 17 minutes attributable to the nanosponge carrier, as it was found in the receiving phase collected after 1 hour from blank nanosponge (Figure 25), did not affect insulin analysis.
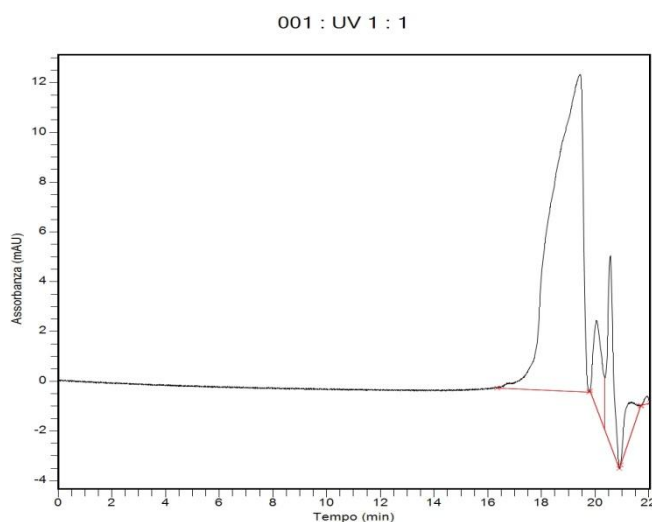
Figure 25. Chromatographic interference attributable to the NS carrier.

The receiving phases were analysed by HPLC-UV using both SEC and C18 columns for comparison as shown in Table 26 and Figure 26 and the results were comparable.

Table 26. Cumulative insulin release at pH=6.8 from the industrial NS using SEC and C18 column for insulin HPLC-UV analysis.

Time (min)	SEC column		C18 column	
	Insulin cumulative release (µg/ml)	Insulin cumulative release (%)	Insulin cumulative release (µg/ml)	Insulin cumulative release (%)
15	11.54	1.01	9.31	0.88
30	34.44	3.02	26.15	2.48
45	52.27	4.58	40.31	3.83
60	66.62	5.84	52.05	4.94
120	97.86	8.57	75.04	7.13
180	127.78	11.19	95.60	9.08
360	174.48	15.28	127.62	12.12
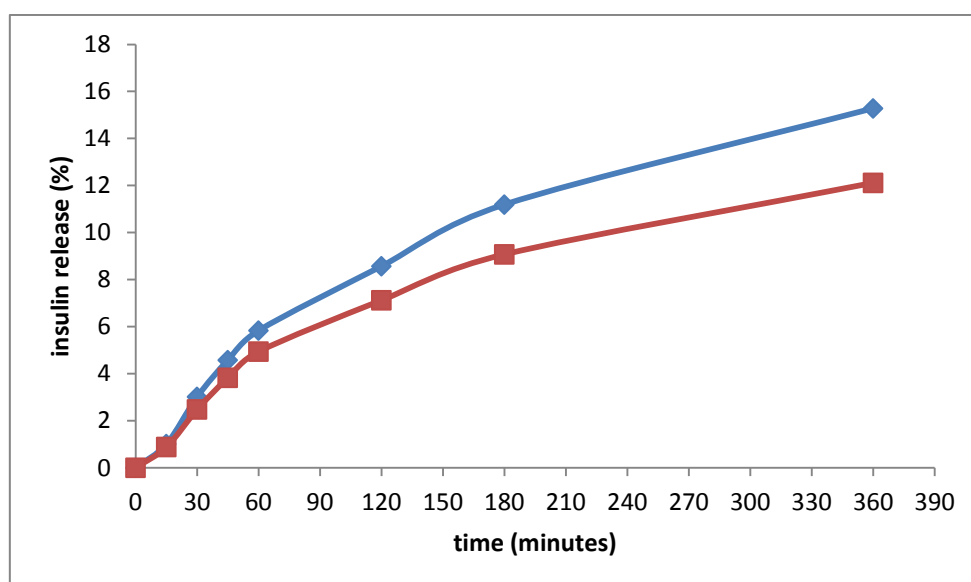
Figure 26. Cumulative insulin release at pH=6.8 analysed using SEC (blue curve) and C18 column (red curve) for insulin HPLC-UV analysis.

The insulin retention time found in the receiving phases corresponds to that of the monomeric peak of standard insulin as shown in Figure 27 and so it may be concluded that insulin was released from the nanosponge as a monomer. This result suggests that the loading process of insulin inside the polymer matrix did not affect the insulin state.
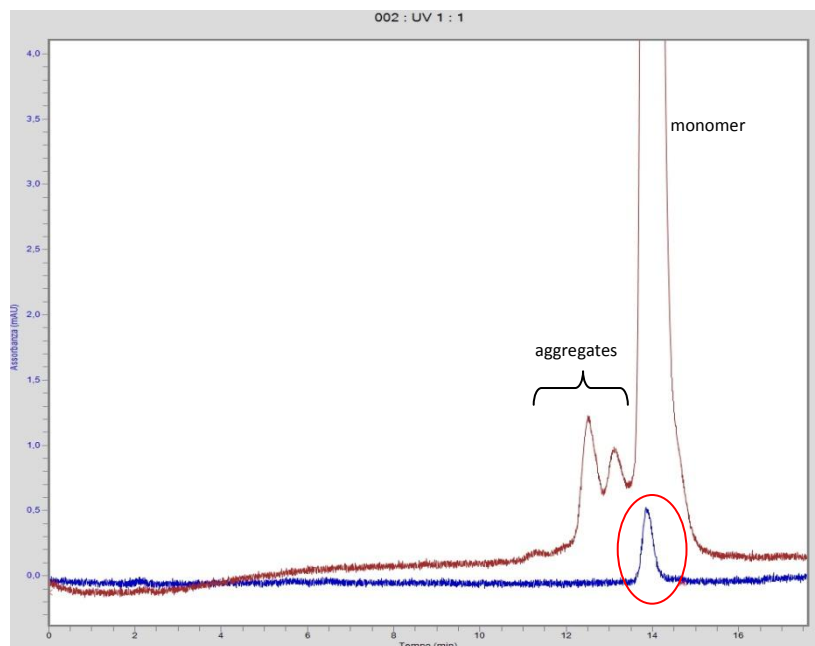
Figure 27. Overlay of the chromatographic profiles of the receiving phase collected at 60 minutes (in blue) reported as an example and that of the heat-stress experiment with insulin as a monomer and aggregates (in red).

To conclude, the results collected demonstrate that neither the stirring used for the loading process nor the encapsulation affected insulin and that the nanosponge preserved the insulin in time without damaging it and releases it in its monomeric form.

7.2 *In-vitro* experiments on cells

The cytotoxicity test consists of a simple, accurate and reproducible colorimetric assay, the key reagent of which is MTT (3-[4,5-dimethylthiazol-2-yl]-2,5-diphenyl tetrazolium bromide). The enzyme able to cleave the tetrazolium ring, leading to the development of purple formazan crystals, is active only in viable cells. Cytotoxicity is therefore evaluated on the basis of the amount of formazan formed, which is analyzed spectrophotometrically.

The results of the MTT test are shown in the figure below. Cell medium (in black) was used as a control. Various dilutions of blank and insulin-loaded NSs (shades of red, the darker the red the higher the sample concentration) did not affect the amount of formazan produced (indicated by the absorbance at 570 nm), thus demonstrating no cell injury, except for CTR-LC-1:8 (especially the 100µl/400 µl dilution) which increased the signal. This result could be attributable to an absorbance interference of the nanosponge.
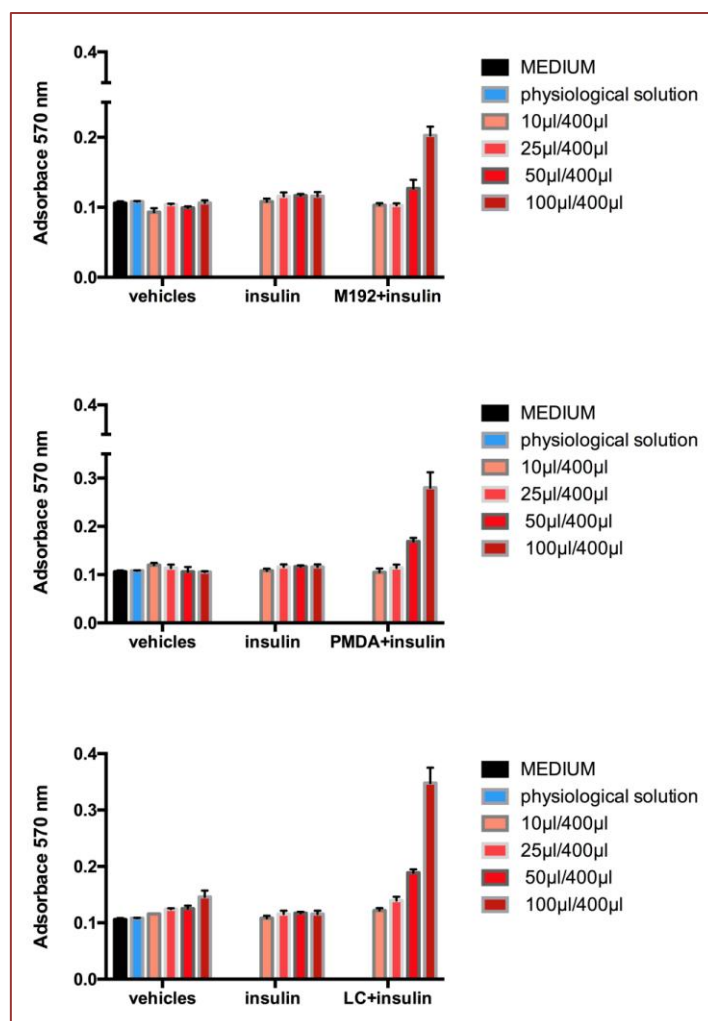
Figure 28. Results of the MTT assay conducted using cell medium (black), saline solution (light blue), NS nanosuspensions (shades of red on the left), insulin solution (shades of red at the centre) and insulin-loaded NSs (shades of red on the right) from the top industrial NS, PMDA-βCD-1:4 and CTR-LC-1:8, respectively.

Moreover, unlike free insulin, insulin-loaded NSs interestingly increased the formazan signal because of insulin activity as a growth factor, thus meaning that it may be due to an enhanced internalization in cells of insulin as it is carried by nanosponges.

For a better understanding of the role of NSs in the intestinal absorption of insulin, *in-vitro* intestinal permeation tests were carried out on a human epithelial cell line (Caco-2 cells). The Caco-2 cell line derives from a colon carcinoma and has the ability to spontaneously differentiate into a monolayer of cells, which mimics absorptive enterocytes. Caco-2 cells were chosen as they have been widely used as an *in-vitro* static transwell cell model of the intestinal epithelial barrier[169]. Such a cell culture model is commonly used in order to have an idea or even possibly predict the drug absorption *in vivo*.

The objective was to understand the role of the nanosponges in the delivery of insulin and its permeation at the intestinal level. In the donor compartments, insulin and insulin-loaded NSs were

diluted with a cell medium to reach a concentration of 262 µg/ml of insulin. Figure 29 and Table 27 show an enhanced intestinal absorption of insulin when loaded inside the NSs compared to free insulin. The permeation kinetics was sustained and prolonged and a remarkable amount of insulin could be found in the receiving compartments already after 15 minutes.
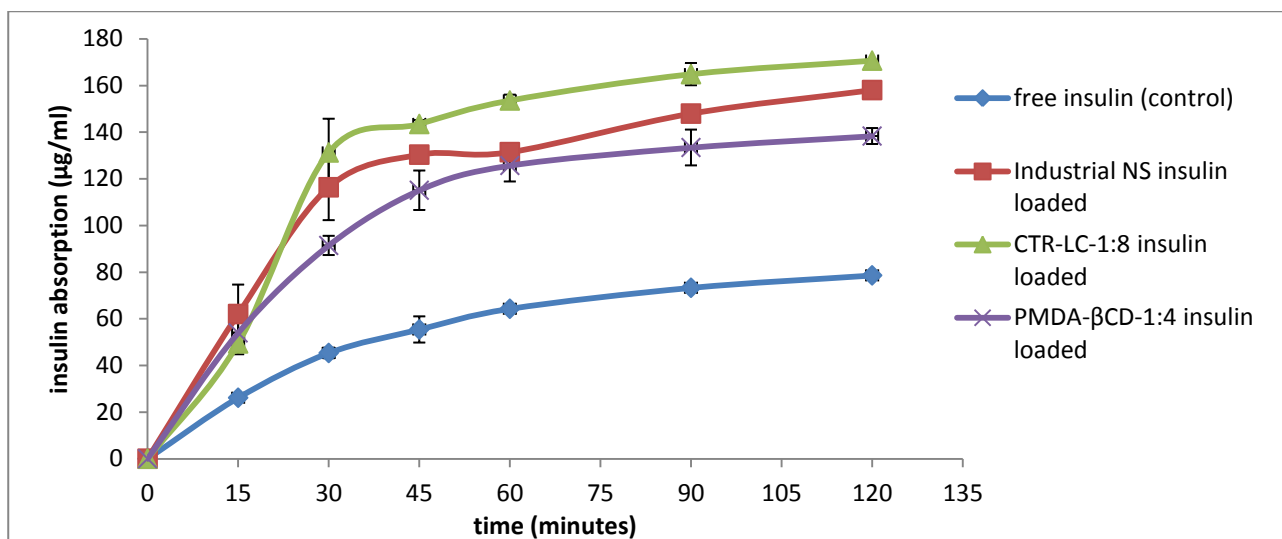
Figure 29. Cumulative absorption of insulin across the Caco2 cell barrier coming from the industrial NS (red), CTR-LC-1:8 (green), PMDA-βCD-1:4 (violet) and free insulin (blue).

Table 27. Cumulative absorption of insulin across the Caco2 cell barrier.

Time (min)	Mean cumulative absorption (µg/ml) of insulin			
	Free insulin	Industrial NS insulin-loaded	CTR-LC-1:8 insulin-loaded	PMDA-βCD-1:4 insulin-loaded
15	26.13	62.00	49.41	53.93
30	45.32	116.33	131.25	91.41
45	55.39	130.33	143.47	115.05
60	64.27	131.39	153.54	125.67
90	73.26	147.91	164.82	133.38
120	78.57	158.00	170.61	138.30

Alongside the study of the contribution made by the nanosponge to promote the intestinal absorption of insulin, the nanosponges were made fluorescent so that they could be traced in order to understand whether they cross the intestinal barrier made up of a Caco-2 cell monolayer or remain strongly adhered to it.

Table 28 shows that a negligible amount of fluorescent NSs crossed the intestinal barrier while the rest was still inside the donor, cell washing solution and cell lysate (Table 29).

Table 28. Caco2 permeability test on fluorescent industrial NS, CTR-LC-1:8 and PMDA-βCD-1:4.

Time (min)	Industrial NS			CTR-LC-1:8			PMDA-βCD-1:4		
	6-coumarin mean concentration (μg/ml)	SD	Cumulative release of 6-coumarin (%)	6-coumarin mean concentration (μg/ml)	SD	Cumulative release of 6-coumarin (%)	6-coumarin mean concentration (μg/ml)	SD	Cumulative release of 6-coumarin (%)
15	0.03	0.008	0.03	0.14	0.109	2.82	0.12	0.089	1.93
30	0.26	0.103	0.34	0.04	0.037	2.82	0.11	0.108	2.80
45	0.41	0.207	0.69	0.04	0.035	3.38	0.20	0.247	5.17
60	0.44	0.334	1.01	0.03	0.045	3.65	0.05	0.046	5.17
90	0.25	0.049	1.07	0.06	0.041	4.46	0.02	0.024	5.19
120	0.22	0.092	1.08	0.00	0.006	4.53	0.05	0.074	6.13
180	0.42	0.221	1.48	0.01	0.015	4.95	0.05	0.082	7.15

Table 29. Mean concentration of 6-coumarin in cell washing solutions and cell lysate.

Sample	Industrial NS			CTR-LC-1:8			PMDA-βCD-1:4		
	Mean concentration of 6-coumarin (μg/ml)	SD	Mean concentration of 6-coumarin (%)	Mean concentration of 6-coumarin (μg/ml)	SD	Mean concentration of 6-coumarin (%)	Mean concentration of 6-coumarin (μg/ml)	SD	Mean concentration of 6-coumarin (%)
Cell washing solution	10.84	3.12	13.2	1.24	0.379	24.21	0.88	0.464	13.13
Cell lysate	1.95	0.696	2.4	0.42	0.090	8.20	0.28	0.111	4.17

These findings are consistent with our hypothesis on the role of the NS in oral drug delivery: it adheres to the intestinal barrier due to its mucoadhesive properties and releases insulin slowly due to its swelling state. This behaviour, which is in common with other mucoahesive polymers discussed in the literature[170], is desirable as it can dramatically change the pharmacokinetics, including the prolongation of their residence time at the administration site via non-parenteral routes.

On the basis of the results obtained from the physico-chemical characterization and *in-vitro* cell tests, we moved on to the *in-vivo* evaluation of insulin-loaded industrial NS and CTR-LC-1:8.

7.3 Pharmacokinetic study on rats

The first step of the *in-vivo* study consisted in administering the formulation to rats via the duodenal route, thus bypassing the obstacles related to the stomach (acidic pH and presence of degrading enzymes). We adopted a protocol optimized over the years for the study of oral delivery of drugs encapsulated in nanocarriers[171–173]. The main goal of the experiment on rats was to evaluate whether the nanosponges were able to release insulin at the intestinal level and promote its absorption *in vivo*, as previously shown in the Caco-2 cell test.

Insulin was determined through an ELISA assay, which was able to detect not only bovine insulin but also native insulin. The amount of insulin found in blood in controls and treatments was therefore put into comparison as shown in the following tables.

Table 30. Endogenous insulin concentration in rat plasma at different times. Rats 1, 2, 3, 4, 5 and 6 were used for control purposes and therefore were treated via duodenal route with bovine insulin solution at a dose of 60 IU/kg except for rat 4, which was treated with saline solution.

Insulin concentration (µIU/ml)								
Time (min)	RAT 1	RAT 2	RAT 3*[1]	Rat 4	Rat 5	Rat 6	Mean concentration (µIU/ml)	SD
0	3.42	n.i.*[2]	22.65	11.60	9.63	17.26	12.91	7.36
15	29.52	23.1	1.07	8.12	8.32	7.15	12.87	10.94
30	80.09	20.28	2.75	8.11	5.85	5.94	20.50	29.82
45	8.58	53.01	5.44	5.52	11.41	6.73	15.11	18.71
60	10.92	13.08	0.07	10.40	8.79	6.33	8.26	4.61
120	16.88	12.55	2.47	10.30	4.71	5.78	8.78	5.43
180	15.76	19.89	3.42	10.29	8.77	9.10	11.21	5.79
360	16.28	23.7	1.13	7.79	9.71	8.52	11.19	7.80

*[1] rat 3 died due to post-surgery complications; *[2] not indicated due to analytical error

Table 31. Insulin concentration in rat plasma at different times after duodenal treatment with insulin-loaded industrial NS at a dose of 60 IU/kg.

Time (min)	Rat 7	Rat 8	Rat 9	Rat 10	Rat 11	Rat 12	Rat 13	Rat 14	Rat 15	Rat 16	Mean concentration (µIU/ml)	SD
0	2.82	215.88	19.47	136.40	8.13	69.48	21.91	1.48	80.64	5.42	29.18	44.61
15	146.29	198.87	52.22	317.50	16.82	1341.89	524.87	14.77	25.47	11.98	265.07	413.57
30	236.51	104.77	36.51	82.48	21.22	306.60	155.61	11.55	21.14	17.25	99.36	103.21
45	269.41	252.66	351.41	11.10	455.84	110.57	22.99	9.52	18.70	11.71	151.39	167.32
60	249.63	299.06	61.83	128.41	273.69	46.30	12.35	17.09	251.16	7.18	134.67	120.80
120	102.96	242.55	26.64	427.89	188.80	161.01	185.02	493.31	18.67	10.38	185.72	165.97
180	257.00	472.84	100.47	55.07	11.43	788.14	641.96	195.78	25.09	62.55	261.03	278.42
360	309.45	10.10	16.57	49.22	30.16	121.15	15.16	9.90	289.29	9.54	86.05	117.47

Table 32. Insulin concentration in rat plasma at different times after duodenal treatment with insulin-loaded CTR-LC-1:8 NS at a dose of 60 IU/kg.

	Insulin concentration (µIU/ml)					
Time (min)	Rat 17	Rat 18	Rat 19	Rat 20	mean concentration (µIU/ml)	SD
0	6.79	5.20	10.30	6.25	7.14	2.21
15	49.37	10.28	22.58	9.30	22.88	18.66
30	24.28	38.85	10.11	19.21	23.11	12.02
45	59.33	18.10	13.86	21.56	28.21	20.98
60	19.08	14.46	11.82	11.29	14.16	3.56
120	107.09	8.07	9.17	6.80	32.78	49.55
180	49.03	7.99	60.38	18.89	34.07	24.68
360	35.73	37.16	8.72	10.45	23.02	15.53
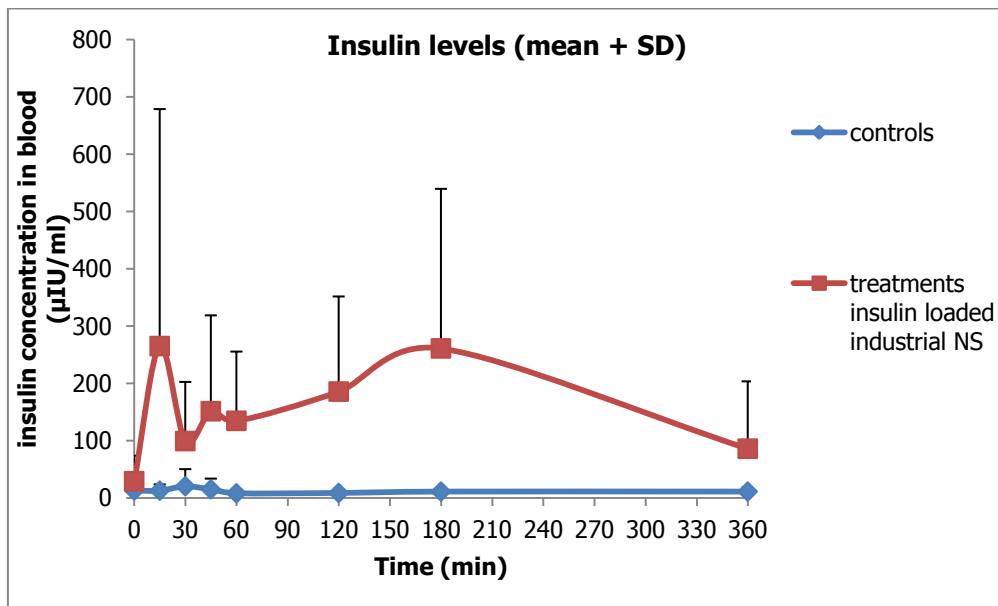
Figure 30. Insulin concentration in rat plasma at different times after duodenal treatment with insulin-loaded industrial NS at a dose of 60 IU/kg put into comparison with rats 1, 2, 3, 4, 5 and 6 used as controls.
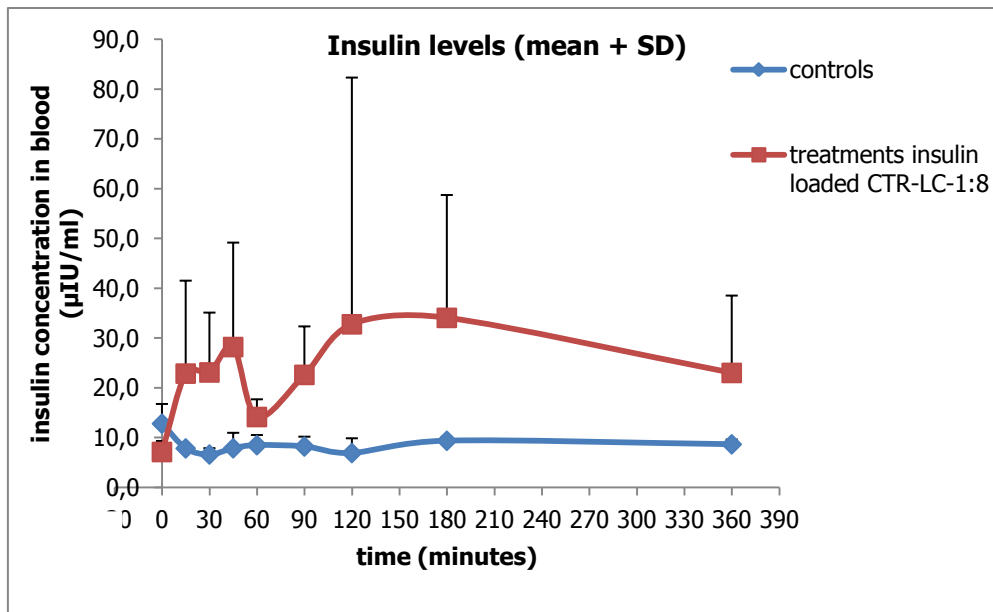
Figure 31. Insulin concentration in rat plasma at different times after duodenal treatment with insulin-loaded CTR-LC-1:8 NS at a dose of 60 IU/kg put into comparison with rats 1, 2, 3, 4, 5 and 6 used as controls.

The standard deviations were higher in the treated rats than in the controls, indicating that the intestinal administration of insulin-loaded NSs caused variability in insulin levels in the blood.

Nonetheless, apart from T0, the mean insulin concentration in plasma after intestinal administration of insulin-loaded formulations was higher than that of controls containing only endogenous insulin, implying that the increase in insulin levels was due to the insulin-loaded formulation administered.

Thus, the administration of these two prototypes to rats was used to understand the response to treatment, which demonstrated that NSs were effective, despite variations between animals and formulations. To conclude, they allowed insulin to cross the intestinal barrier *in vivo*.

7.4 Efficacy study on diabetic mice

The second step *in vivo* consisted in assessing the efficacy of the formulation in diabetic mice.

Animal models have a long history in diabetes research because they have helped to understand the pathophysiology of diabetes and are always used as the first step in investigating the efficacy of a promising new therapy[174]. A careful selection of the animal model is thus essential to assess the efficacy of a new formulation, in this case insulin-loaded nanosponges to treat type 1 diabetes orally. The oral administration was selected in order to test the ability of the nanosponge to protect insulin from the gastric environment without the use of an enteric coating and to deliver it to the absorption site.

For this purpose, two animal models of type 1 diabetes that have been extensively reviewed in the literature were chosen: non-obese diabetic mice (NOD mice) and streptozotocin-induced diabetic mice (STZ-induced diabetic mice). They both present β-cell ablation, which can be achieved via a spontaneous development of autoimmune diabetes, as in NOD mice, or through chemical depletion of β cells, as in STZ-induced diabetic mice[175].

The NOD mice model was chosen for the efficacy study as it has been widely studied over the years[176] and the progression of diabetes is similar to that in humans.
NOD mice, discovered in the 1970s in Japan, develop insulitis due to the infiltration of activated immune cells, including $CD4^+$ and $CD8^+$ lymphocytes, in the pancreatic islets, thus leading to the destruction of insulin producing β cells[177].
The symptoms appear around 10-14 weeks after a 90% reduction in pancreatic insulin. When NOD mice become overtly diabetic, they rapidly lose weight and require insulin treatment.
Females have a higher diabetes incidence, ranging from 60% to 90%, whereas males have a lower incidence, ranging from 10% to 30%. It appears to be linked to the composition of the gut microflora; in fact, specific microbial communities can alter testosterone levels while also promoting disease-protective commensal bacteria in the gut[178].
The development of diabetes is also influenced by the degree of cleanliness of the mouse facility and exposure to microbial and dietary factors.
This animal model was chosen for the efficacy study because it closely resembles the diabetic condition in humans as mentioned previously.

In the efficacy experiments, the weight and blood sugar levels of each group of mice were monitored periodically in order to check the development of diabetes. The data regarding groups 1, 2 and 3 are present in the Annexe in Tables A4, A5 and A6, respectively. The data highlighted in red represent the blood glucose values typical of diabetes.

Blood glucose monitoring of mice that developed diabetes are shown in the figure below (from top to bottom groups 1, 2 and 3) where a sudden rise in blood glucose from one week to the next can be observed.
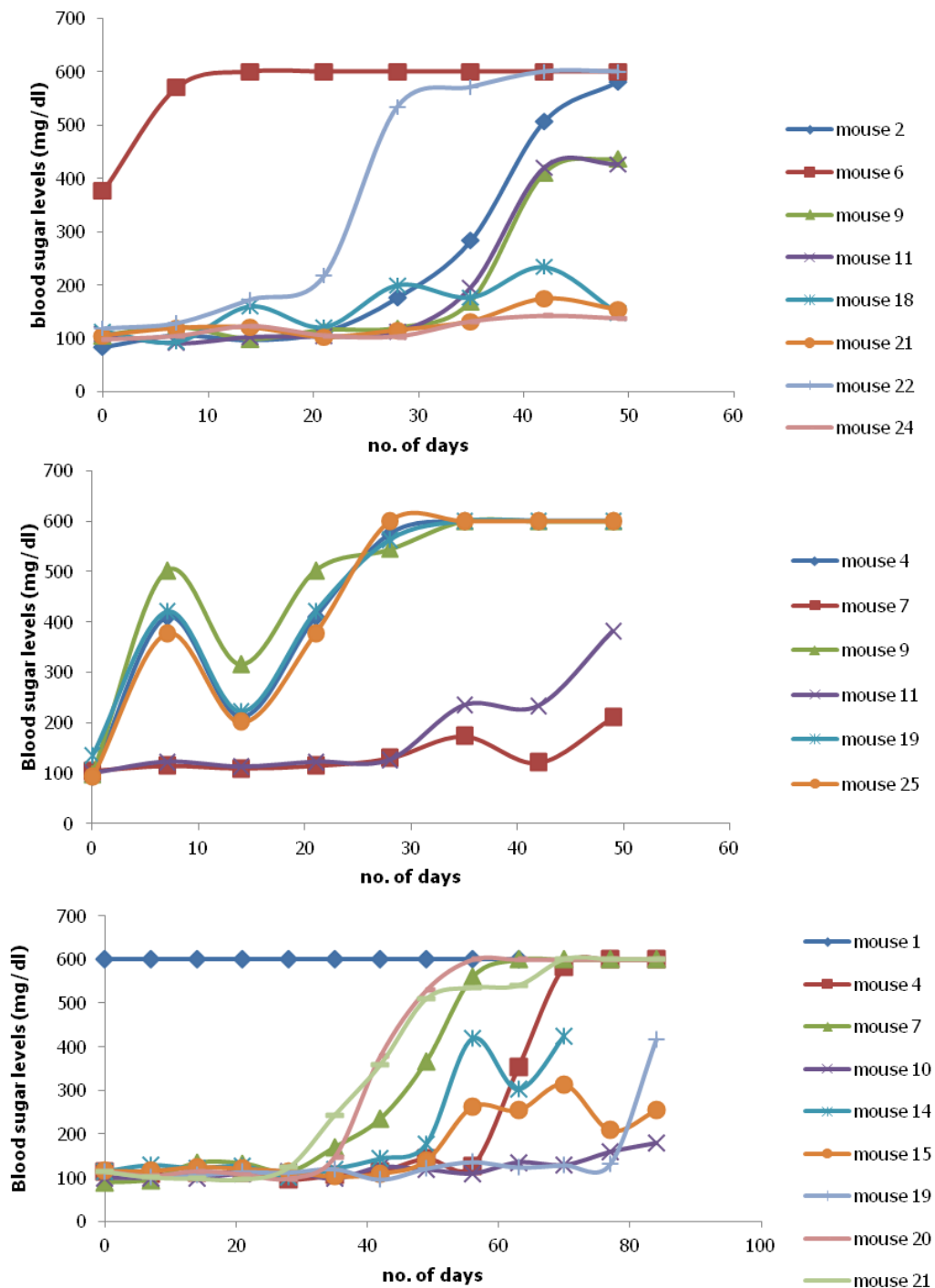
Figure 32. Monitoring of blood sugar levels in NOD mice that developed diabetes.

Tables A7-A19 in the Annexe contain all the results of the efficacy study carried out on the NOD mouse animal model.

Figure 33 shows the decrease of blood sugar levels over time in healthy and diabetic NOD mice after receiving an intraperitoneal injection of glucose solution to induce a glycaemic peak and being treated orally with insulin solution. Healthy mice, unlike diabetic mice, can overcome hyperglycaemia efficiently due to the presence of endogenous insulin. The blood sugar reduction at different time points can be observed in Table 33.
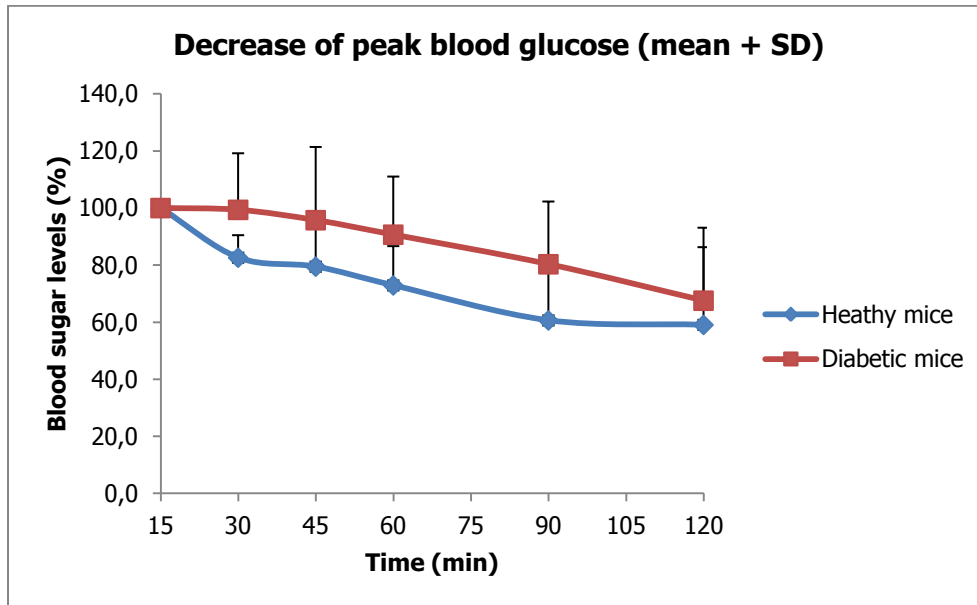
Figure 33. Percentage decrease of peak blood glucose in healthy and NOD diabetic mice treated orally with insulin solution.

Table 33. Blood sugar levels of healthy and diabetic NOD mice after oral administration of insulin solution (60 IU/kg). The glycaemic peak is in bold.

		0	15	30	45	60	90	120
Healthy mice	Mean glycaemia (mg/dl)	85	**139**	115	110	101	84	82
	% of maximum glycaemia		100	83	80	73	61	59
	% glycaemic decrease			17	21	27	39	41
Diabetic mice	Mean glycaemia (mg/dl)	198	**363**	361	348	329	292	245
	% of maximum glycaemia		100	99	96	91	80	68
	% glycaemic decrease			1	4	9	20	33

Insulin solution and saline solution were administered via oral gavage to diabetic NOD mice, which were used as controls, and the responses of the animals were compared. As expected, since insulin solution has no hypoglycaemic effect when taken orally, the Student's t-test showed no statistically significant difference in glucose levels.

Insulin-loaded industrial NS was administered to diabetic NOD mice via oral gavage at a dose of 60 IU/kg. The overall response to treatment of the 3 animal groups was analysed statistically to determine the hypoglycaemic effect of insulin-loaded NS compared to the controls (mice treated with saline solution). The Student's t-test, confirmed also by the one-way ANOVA, showed a statistically significant difference in glucose levels from 15 minutes onwards, thus confirming the effectiveness of the treatment (Figure 34).
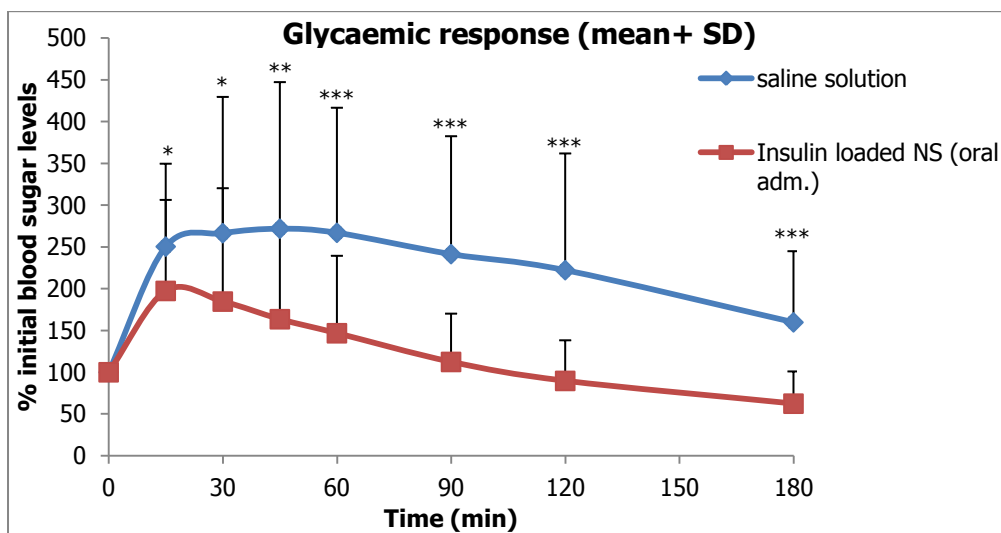
Figure 34. Percentage of the initial blood sugar levels following exposure to saline solution (n=16) and insulin-loaded industrial NS (n=43) in diabetic NOD mice at a dose of 60 IU/kg; p value vs. saline solution (*p< 0.05; **p< 0.01; ***p< 0.001).

The higher dose of insulin-loaded industrial NS (90 IU/kg) was statistically different from the controls but its effect was no better than that of 60 IU/kg (Figure 35) as confirmed by Student's t-test and one-way ANOVA with no statistical difference between the two doses.
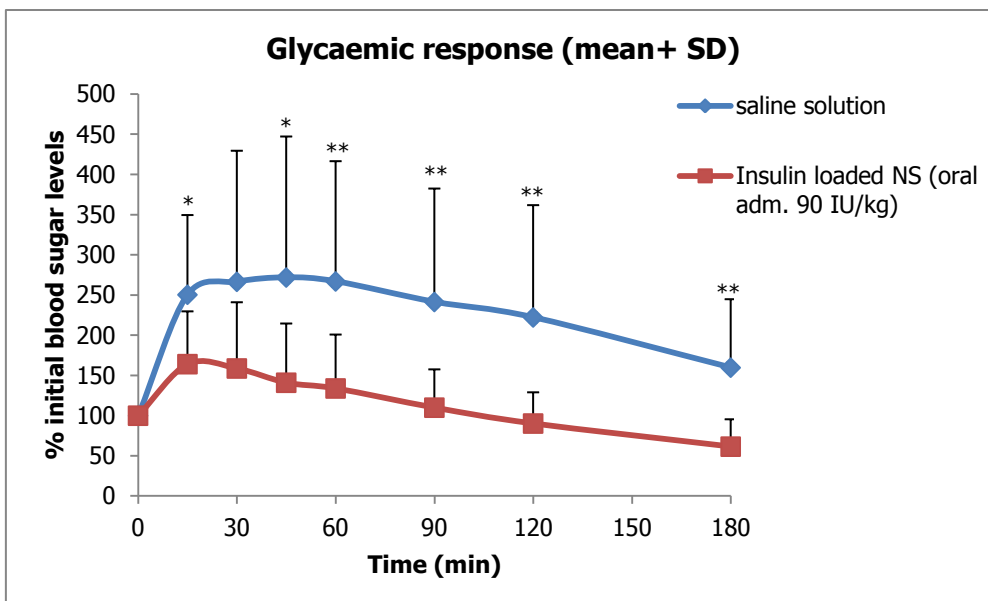
Figure 35. Percentage of the initial blood sugar levels following exposure to saline solution (n=16) and insulin-loaded industrial NS at 90 IU/kg (n=8) in diabetic NOD mice; p value vs. saline solution (*p< 0.05; **p< 0.01; ***p< 0.001).

The subcutaneous administration of insulin-loaded industrial NS at a dose of 1.5 IU/kg determined a marked hypoglycaemic effect with a final glycaemia level of 24 % compared to the initial blood sugar levels. The glycaemic profile was comparable to that of insulin solution administered via the same route as shown in Figure 36. This finding demonstrates that the formulation process did not affect the state of insulin as it was active *in vivo*.
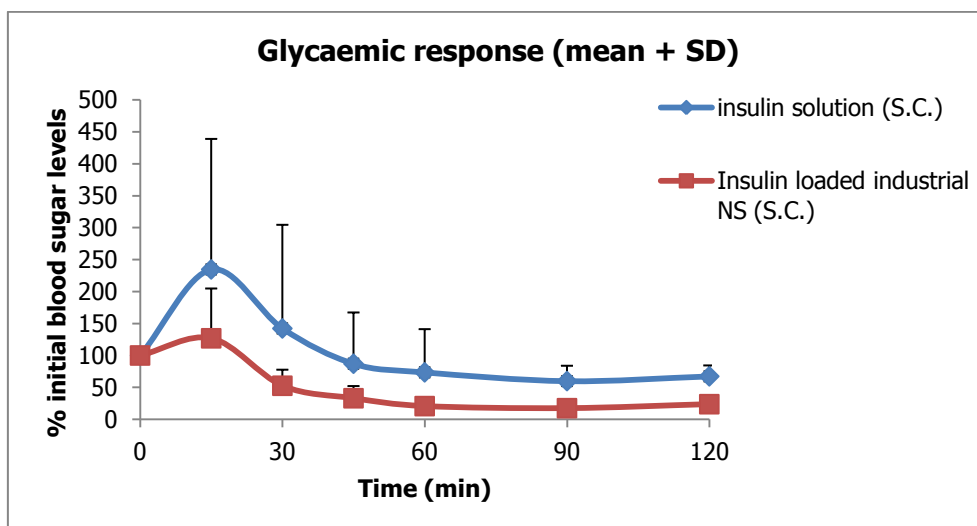
Figure 36. Glycaemic response to subcutaneous administration of insulin solution and insulin-loaded industrial NS at a dose of 1.5 IU/kg in diabetic NOD mice.

In the STZ-induced diabetic mice model, the antibiotic streptozotocin is used to induce pancreatic β-cell destruction and is widely used experimentally for assessing the pathological consequences of diabetes and for screening potential therapies for its treatment[179]. Its mechanism of action consists in accumulating pancreatic β cells through the GLUT2 glucose transporter receptor due to the similarity of its chemical structural with glucose. If a single high dose is administered, STZ targets β cells through its alkylating property, whereas at multiple low doses STZ prompts an immune and inflammatory reaction.

Table A20 in the Annexe contains all the results of the efficacy study carried out in this animal model.

Figure 37 shows how healthy and diabetic mice react to an intraperitoneal injection of glucose solution to induce a glycaemic peak. It is clear that healthy mice, unlike diabetic mice, can overcome hyperglycaemia with a progressive lowering of blood sugar levels due to endogenous insulin (≈45% and 9% decrease at 120 minutes, respectively).

Diabetic mice given saline solution orally were thus used as a control group to evaluate the efficacy of the insulin-loaded NS formulations.

Insulin-loaded industrial NS was administered to STZ-induced diabetic mice via oral gavage at a dose of 90 IU/kg. As mentioned previously and observed in Figure 38, saline solution did not induce a decrease in the blood sugar levels. In contrast, the oral administration of insulin-loaded industrial NS (90 I.U./kg) led to a progressive reduction of glucose levels (≈33% after 60 minutes with respect to the maximum glucose level induced by IP injection of glucose solution and the response remained stable up to 120 minutes. Student's t-test showed a statistically significant difference in glucose levels from 30 minutes onwards, thus highlighting the effectiveness of the treatment. The higher dose of insulin-loaded industrial NS (120 IU/kg) was not as effective as 90 IU/kg (Figure 39).

In comparison to the subcutaneous administration of free insulin solution, the subcutaneous administration of insulin-loaded industrial NS at a dose of 1.5 IU/kg achieved comparable overall glucose reduction (≈80%) as shown in Figure 40. These findings demonstrate that the formulation process did not affect the state of insulin as it was active *in vivo*.
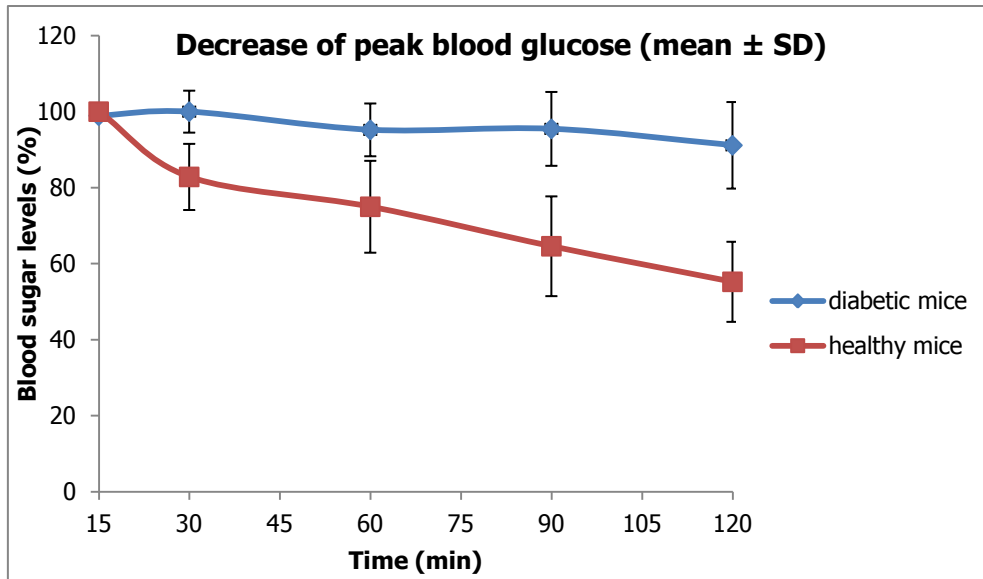
Figure 37. Percentage decrease of peak blood glucose in healthy and STZ-induced diabetic mice treated orally with saline solution.
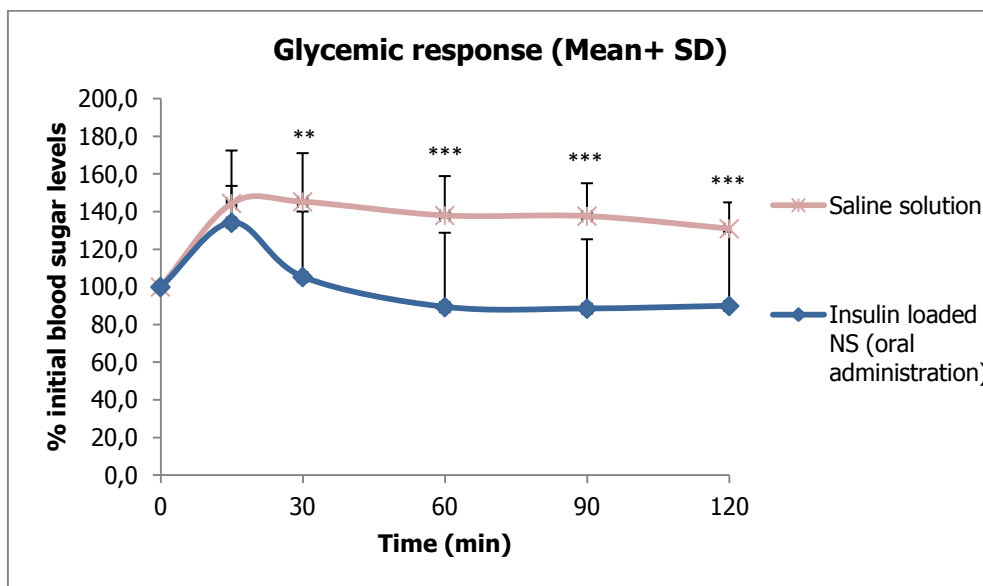
Figure 38. Percentage of the initial blood sugar levels following exposure to saline solution (n=10) and insulin loaded industrial NS (n=19) in STZ-induced diabetic mice; p value vs. saline solution (*p< 0.05; **p< 0.01; ***p< 0.001).
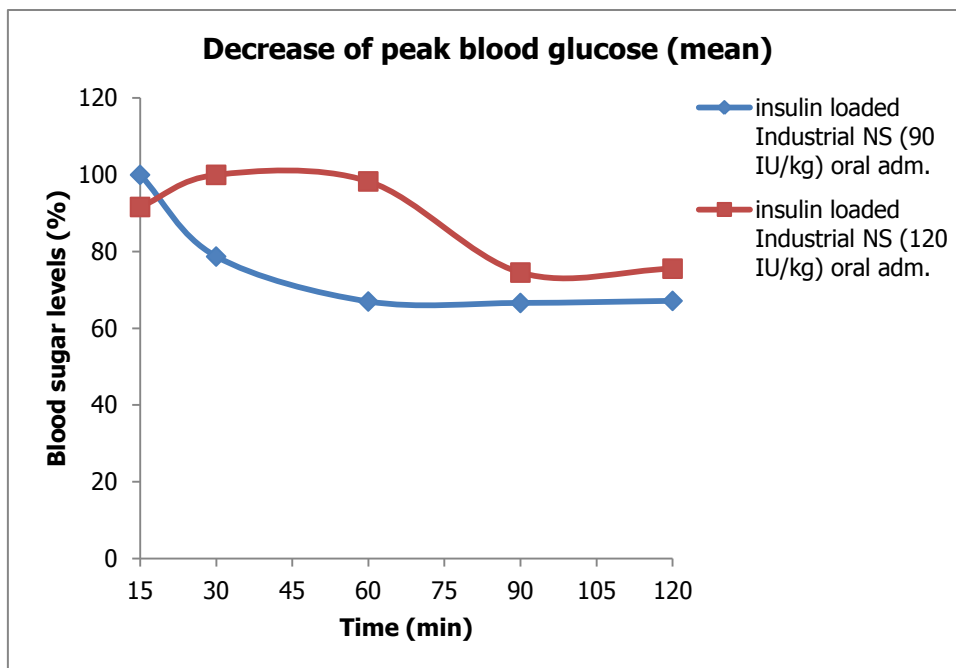
Figure 39. Percentage decrease of peak blood glucose in STZ-induced diabetic mice treated orally with insulin-loaded industrial NS at two different doses, 90 and 120 IU/kg.
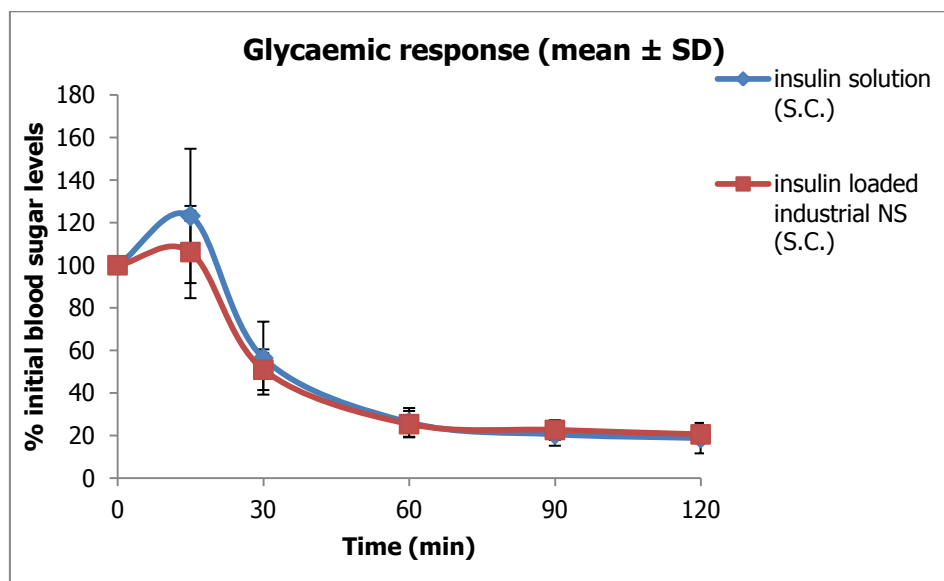
Figure 40. Glycaemic response to subcutaneous administration of insulin solution and insulin-loaded industrial NS at a dose of 1.5 IU/kg in STZ-induced diabetic mice.

Insulin-loaded CTR-LC-1:8 was also administered to STZ-induced diabetic mice via oral gavage at a dose of 90 IU/kg, which led to a progressive reduction of glucose levels (≈25% after 120 minutes with respect to the maximum glucose level induced by IP injection of glucose solution). Student's t-test showed a statistically significant difference in glucose levels from 90 minutes onwards, thus highlighting the effectiveness of the treatment (Figure 41).
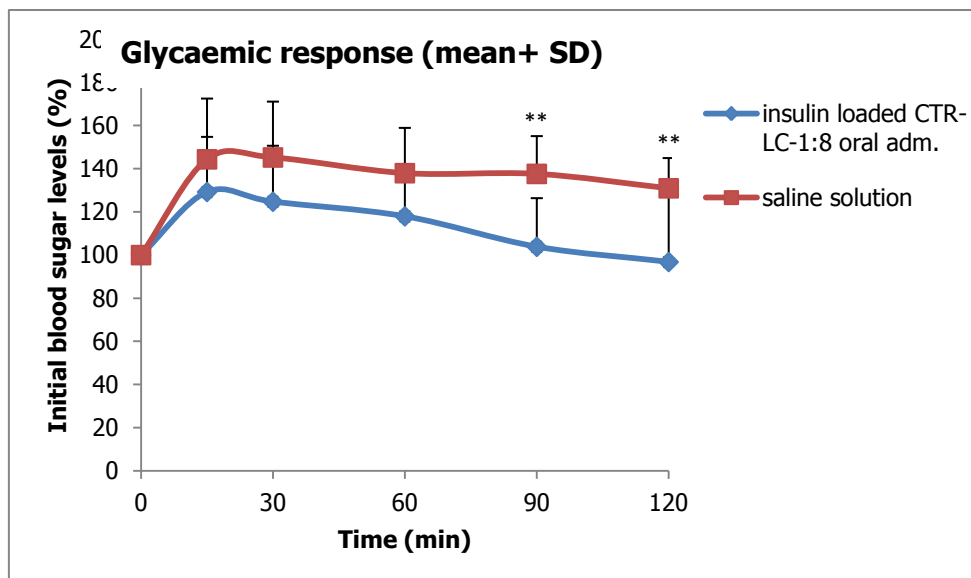
Figure 41. Percentage of the initial blood sugar levels following exposure to saline solution (n=10) and insulin loaded CTR-LC-1:8 (n=10) in STZ-induced diabetic mice; p value vs. saline solution (*p< 0.05; **p< 0.01; ***p< 0.001).

The subcutaneous administration of insulin-loaded CTR-LC-1:8 at a dose of 1.5 IU/kg achieved a comparable final glucose reduction to that of subcutaneous insulin solution as 25% of glycaemia was reached at 120 minutes in two mice out of three, the third mouse did not respond to the treatment.

This study demonstrated the efficacy of two different formulations of insulin-loaded NSs in the STZ-induced diabetic mice model since a statistically significant hypoglycaemic effect following oral administration of insulin-loaded industrial NS and CTR-LC-1:8, was found, respectively, as early as 30 minutes and 90 minutes and maintained until the end of the experiments.

8. Conclusions

This study investigated pH-sensitive cyclodextrin nanosponges as a novel nanotechnological approach to the delivery of proteins through oral administration, using insulin as a case study.

The research was carried with several goals in mind, from the characterization *in vitro* with a comparison between the three prototypes carefully chosen for this study to finally test them *in vivo* to see if this kind of drug delivery system is suitable for the oral administration of insulin to overcome hyperglycaemia in diabetic mice. The focus was on oral administration as it is so advantageous but, as it presents numerous challenges, the formulations were studied under multiple aspects paying particular attention, for example, to pH-dependent release, the ability to form hydrogels, mucoadhesion, colloidal stability in gastric and intestinal fluids, all fundamental properties for this route.

The physicochemical characterization demonstrated that the top-down approach was successful in obtaining stable nanosuspensions of a comparable size and zeta potential in all three prototypes. The loading capacity and encapsulation efficiency were also similar and the incorporation inside the polymer matrices was confirmed also by DSC and ATR-FTIR analyses.

Their ability to swell at intestinal pH, enabling a sustained release of insulin, and to limit their swelling at gastric pH, as well as insulin release, gave valuable information on their behaviour in simulated GI media. The NS formulations promoted the absorption of insulin at the intestinal level, which was evaluated both *in vitro* and *in vivo*, and proved to be pharmacologically effective on two diabetic animal models.

It could be therefore deduced that the formulation process did not affect insulin, which was preserved in time inside the polymer matrix without being damaged and released at the absorption site after oral administration in its active form.

These results suggest that NSs are suitable DDSs for the oral delivery of insulin and are encouraging for future studies on the adjustment of the dosage *in vivo* and for a comparison of the response to treatment of the various prototypes.

We also believe that this approach could prove extremely useful for carrying other proteins and peptides, antibodies and enzymes of pharmaceutical interest considering the outstanding advantages of NS technology, such as low cost, environmental compatibility, non-toxicity and tunable structure for a targeted and sustained delivery.

Acknowledgements

References

1. Robinson, D. & Mauger, J. Drug delivery systems. *Am J Hosp Pharm.* **10**, S14-23 (1991).
2. Parepalli, Y. & Chavali, M. Polysaccharide nanoparticles based drug delivery – An overview. *Int. J. Nanosci. Technol.* (2013). doi:10.1021/bk-1987-0348.ch014
3. Hoti, G. *et al.* Strategies to Develop Cyclodextrin-Based Nanosponges for Smart Drug Delivery. in *IntechOpen* (2021). doi:10.5772/intechopen.100182
4. Montoto, S. S. *ADME Processes in Pharmaceutical Sciences. ADME Processes in Pharmaceutical Sciences* (2018). doi:10.1007/978-3-319-99593-9
5. Hoffman, A. S. The origins and evolution of 'controlled' drug delivery systems. *J. Control. Release* **132**, 153–163 (2008).
6. MG, K., V, K. & F, H. History and Possible Uses of Nanomedicine Based on Nanoparticles and Nanotechnological Progress. *J. Nanomed. Nanotechnol.* **06**, (2015).
7. Bayda, S., Adeel, M., Tuccinardi, T., Cordani, M. & Rizzolio, F. The history of nanoscience and nanotechnology: From chemical-physical applications to nanomedicine. *Molecules* **25**, 1–15 (2020).
8. Kutova, O. M., Guryev, E. L., Sokolova, E. A., Alzeibak, R. & Balalaeva, I. V. Targeted delivery to tumors: Multidirectional strategies to improve treatment efficiency. *Cancers (Basel).* **11**, (2019).
9. Dang, Y. & Guan, J. Nanoparticle-based drug delivery systems for cancer therapy. *Smart Mater. Med.* **1**, 10–19 (2020).
10. Bobo, D., Robinson, K. J., Islam, J., Thurecht, K. J. & Corrie, S. R. Nanoparticle-Based Medicines: A Review of FDA-Approved Materials and Clinical Trials to Date. *Pharm. Res.* **33**, 2373–2387 (2016).
11. Liu, Z., Jiao, Y., Wang, Y., Zhou, C. & Zhang, Z. Polysaccharides-based nanoparticles as drug delivery systems. *Adv. Drug Deliv. Rev.* **60**, 1650–1662 (2008).
12. Chamundeeswari, M., Jeslin, J. & Verma, M. L. Nanocarriers for drug delivery applications. *Environ. Chem. Lett.* **17**, 849–865 (2019).
13. dos Santos, M. A. & Grenha, A. *Polysaccharide Nanoparticles for Protein and Peptide Delivery: Exploring Less-Known Materials. Advances in Protein Chemistry and Structural Biology* **98**, (Elsevier Inc., 2015).
14. A. P. Anwunobi, M. O. E. Recent Applications of Natural Polymers in Nanodrug Delivery. *J. Nanomed. Nanotechnol.* **s4**, 2–7 (2011).
15. Beneke, C. E., Viljoen, A. M. & Hamman, J. H. Polymeric plant-derived excipients in drug delivery. *Molecules* **14**, 2602–2620 (2009).
16. Mizrahy, S., & Peer, D. Polysaccharides as building blocks for nanotherapeutics. *Chem. Soc. Rev.* **41**, 2623–2640 (2012).
17. Odeniyi, M., Omoteso, O., Adepoju, A. & Jaiyeoba, K. Starch nanoparticles in drug delivery: A review. *Polym. Med.* **48**, 41–45 (2019).
18. Appleton, S. L. *et al.* Cyclodextrins as anti-inflammatory agents: Basis, drugs and perspectives. *Biomolecules* **11**, 1–15 (2021).
19. Crini, G. Review : A History of Cyclodextrins. *Chem. Rev.* **114**, 10940–10975 (2014).
20. European Medicines Agency. *Background review for cyclodextrins used as excipients. Ema* **44**, (2014).
21. Hădărugă, N. G., Bandur, G. N., David, I. & Hădărugă, D. I. A review on thermal analyses of cyclodextrins and cyclodextrin complexes. *Environ. Chem. Lett.* **17**, 349–373 (2019).
22. Brewster, M. E. & Loftsson, T. Cyclodextrins as pharmaceutical solubilizers. *Adv. Drug Deliv. Rev.* **59**, 645–666 (2007).
23. Shimpi, S., Chauhan, B. & Shimpi, P. Cyclodextrins: Application in different routes of drug administration. *Acta Pharm.* **55**, 139–156 (2005).
24. Otero-Espinar, F. J., Torres-Labandeira, J. J., Alvarez-Lorenzo, C. & Blanco-Méndez, J. Cyclodextrins in drug delivery systems. *J. Drug Deliv. Sci. Technol.* **20**, 289–301 (2010).

25. Trotta, F., Zanetti, M. & Cavalli, R. Cyclodextrin-based nanosponges as drug carriers. *Beilstein J. Org. Chem.* **8**, 2091–2099 (2012).

26. Krabicov, I. *et al.* History of Cyclodextrin Nanosponges. *Polymers (Basel).* **12**, 1122 (2020).

27. Cavalli, R., Trotta, F. & Tumiatti, W. Cyclodextrin-based nanosponges for drug delivery. in *Journal of Inclusion Phenomena and Macrocyclic Chemistry* **56**, 209–213 (2006).

28. Trotta, F. Cyclodextrin Nanosponges and their Applications. in *Cyclodextrins in Pharmaceutics, Cosmetics, and Biomedicine* 323–342 (John Wiley & Sons, Inc., 2011). doi:10.1002/9780470926819.ch17

29. Caldera, F., Tannous, M., Cavalli, R., Zanetti, M. & Trotta, F. Evolution of Cyclodextrin Nanosponges. *Int. J. Pharm.* **531**, 470–479 (2017).

30. Solms, J. & Egli, R. . Harze mit Einschlusshohlräumen von Cyclodextrin-Struktur. *Helv Chim Acta* **48**, 1225–1228 (1965).

31. Hoffman, J. . Chromatography of nucleic acids on cross-linked cyciodextrin gels having inclusion-forming capacity. *J Macromol Sci Part A - Chem* **7**, 1147–1157 (1973).

32. Sugiura, I., Komiyama, M., Toshima, N. & Hirai, H. Immobilized β-Cyclodextrins. Preparation with Various Crosslinking Reagents and the Guest Binding Properties. *Bull Chem Soc Jpn* **62**, 1643–1651 (1989).

33. Su, C. & Yang, C. Partial removal of various food components from aqueous solution using crosslinked polymers of cyclodextrins with epichlorohydrin. *J Sci Food Agric* **54**, 635–643 (1991).

34. Li, D. . & Ma, M. Nanosponges: From inclusion chemistry to water purifying technology. *Chemtech* **29**, 31–37 (1999).

35. Swaminathan, S., Cavalli, R. & Trotta, F. Cyclodextrin-based nanosponges: a versatile platform for cancer nanotherapeutics development. *Wiley Interdiscip. Rev. Nanomedicine Nanobiotechnology* **8**, 579–601 (2016).

36. A. Ansari, K., J. Torne, S., Pradeep R. Vavia, P., Trotta, F. & Cavalli, R. Paclitaxel Loaded Nanosponges: In-Vitro Characterization and Cytotoxicity Study on MCF-7 Cell Line Culture. *Curr. Drug Deliv.* **8**, 194–202 (2011).

37. Mognetti, B. *et al.* In vitro enhancement of anticancer activity of paclitaxel by a Cremophor free cyclodextrin-based nanosponge formulation. *J. Incl. Phenom. Macrocycl. Chem.* **74**, 201–210 (2012).

38. Minelli, R. *et al.* Nanosponge-encapsulated camptothecin exerts anti-tumor activity in human prostate cancer cells. *Eur. J. Pharm. Sci.* **47**, 686–694 (2012).

39. Ramírez-Ambrosi, M., Caldera, F., Trotta, F., Berrueta, L. & Gallo, B. Encapsulation of apple polyphenols in β-CD nanosponges. *J. Incl. Phenom. Macrocycl. Chem.* **80**, 85–92 (2014).

40. Ansari, K. A., Vavia, P. R., Trotta, F. & Cavalli, R. Cyclodextrin-based nanosponges for delivery of resveratrol: In vitro characterisation, stability, cytotoxicity and permeation study. *AAPS PharmSciTech* **12**, 279–286 (2011).

41. Anandam, S. & Selvamuthukumar, S. Fabrication of cyclodextrin nanosponges for quercetin delivery: Physicochemical characterization, photostability, and antioxidant effects. *J. Mater. Sci.* **49**, 8140–8153 (2014).

42. Sapino, S. *et al.* Photochemical and antioxidant properties of gamma-oryzanol in beta-cyclodextrin-based nanosponges. *J. Incl. Phenom. Macrocycl. Chem.* **75**, 69–76 (2013).

43. Shende, P. K., Gaud, R. S., Bakal, R. & Patil, D. Effect of inclusion complexation of meloxicam with β-cyclodextrin- and β-cyclodextrin-based nanosponges on solubility , in vitro release and stability studies. *Colloids Surfaces B Biointerfaces* **136**, 105–110 (2015).

44. Ferro, M. *et al.* Anomalous diffusion of ibuprofen in cyclodextrin nanosponge hydrogels: An HRMAS NMR study. *Beilstein J. Org. Chem.* **10**, 2715–2723 (2014).

45. Swaminathan, S., Vavia, P. R., Trotta, F. & Cavalli, R. Nanosponges encapsulating dexamethasone for ocular delivery: Formulation design, physicochemical characterization, safety and corneal permeability assessment. *J. Biomed. Nanotechnol.* **9**, 998–1007 (2013).

46. Bastiancich, C. *et al.* Cyclodextrin-Based Nanosponges as a Nanotechnology Strategy for Imiquimod Delivery in Pathological Scarring Prevention and Treatment. *J. Nanopharmaceutics Drug Deliv.* **2**, 311–324 (2015).

47. Conte, C. *et al.* β-cyclodextrin nanosponges as multifunctional ingredient in water-containing semisolid formulations for skin delivery. *J. Pharm. Sci.* **103**, 3941–3949 (2014).

48. Lembo, D. *et al.* Encapsulation of Acyclovir in new carboxylated cyclodextrin-based nanosponges improves the agent's antiviral efficacy. *Int. J. Pharm.* **443**, 262–272 (2013).

49. Trotta, F. *et al.* Cyclodextrin nanosponges as effective gas carriers. *J. Incl. Phenom. Macrocycl. Chem.* **71**, 189–194 (2011).

50. Cavalli, R. *et al.* Nanosponge formulations as oxygen delivery systems. *Int. J. Pharm.* **402**, 254–257 (2010).

51. Dora, C. P. *et al.* Potential of erlotinib cyclodextrin nanosponge complex to enhance solubility, dissolution rate, in vitro cytotoxicity and oral bioavailability. *Carbohydr. Polym.* **137**, 339–349 (2016).

52. Gigliotti, C. L. *et al.* In vitro and in vivo therapeutic evaluation of camptothecin-encapsulated β-cyclodextrin nanosponges in prostate cancer. *J. Biomed. Nanotechnol.* **12**, 114–127 (2016).

53. Gigliotti, C. L. *et al.* Enhanced cytotoxic effect of camptothecin nanosponges in anaplastic thyroid cancer cells in vitro and in vivo on orthotopic xenograft tumors. *Drug Deliv.* **24**, 670–680 (2017).

54. Pushpalatha, R., Selvamuthukumar, S. & Kilimozhi, D. Cyclodextrin nanosponge based hydrogel for the transdermal co-delivery of curcumin and resveratrol : Development , optimization , in vitro and ex vivo evaluation. *J. Drug Deliv. Sci. Technol.* **52**, 55–64 (2019).

55. Pushpalatha, R., Selvamuthukumar, S. & Kilimozhi, D. Cross-linked, cyclodextrin-based nanosponges for curcumin delivery - Physicochemical characterization, drug release, stability and cytotoxicity. *J. Drug Deliv. Sci. Technol.* **45**, 45–53 (2018).

56. Gholibegloo, E. *et al.* Improved curcumin loading, release, solubility and toxicity by tuning the molar ratio of cross-linker to β-cyclodextrin. *Carbohydr. Polym.* **213**, 70–78 (2019).

57. Daga, M. *et al.* GSH-targeted nanosponges increase doxorubicin-induced toxicity 'in vitro' and 'in vivo' in cancer cells with high antioxidant defenses. *Free Radic. Biol. Med.* **97**, 24–37 (2016).

58. Trotta, F. *et al.* Glutathione Bioresponsive Cyclodextrin Nanosponges. *Chempluschem* **81**, 439–443 (2016).

59. Momin, M. M., Zaheer, Z., Zainuddin, R. & Jaiprakash, N. Extended release delivery of erlotinib glutathione nanosponge for targeting lung cancer. *Artif. Cells, Nanomedicine, Biotechnol.* **46**, 1064–1075 (2017).

60. Argenziano, M. *et al.* Glutathione/pH-responsive nanosponges enhance strigolactone delivery to prostate cancer cells. *Oncotarget* **9**, 35813–35829 (2018).

61. Fontana, R. M. *et al.* Cyclodextrin-Calixarene Nanosponges as Potential Platforms for pH-Dependent Delivery of Tetracycline. *ChemistrySelect* **4**, 9743–9747 (2019).

62. Singh, P. *et al.* Biofunctionalization of β -cyclodextrin nanosponges using cholesterol. *Carbohydr. Polym.* **190**, 23–30 (2018).

63. Pei, M., Pai, J. Y., Du, P. & Liu, P. Facile Synthesis of Fluorescent Hyper-Cross-Linked β-Cyclodextrin-Carbon Quantum Dot Hybrid Nanosponges for Tumor Theranostic Application with Enhanced Antitumor Efficacy. *Mol. Pharm.* **15**, 4084–4091 (2018).

64. Gholibegloo, E. *et al.* Folic acid decorated magnetic nanosponge : An efficient nanosystem for targeted curcumin delivery and magnetic resonance imaging. *J. Colloid Interface Sci.* **556**, 128–139 (2019).

65. Gangadharappa, H. V., Chandra Prasad, S. M. & Singh, R. P. Formulation, in vitro and in vivo evaluation of celecoxib nanosponge hydrogels for topical application. *J. Drug Deliv. Sci. Technol.* **41**, 488–501 (2017).

66. Patel, C. J., Pragna, K. S., Archita, J. P., Dharmik, M. M. & Arunkumar, S. RP-HPLC Method for Simultaneous Estimation of a Hydrophilic Drug Gemcitabine Hydrochloride in Combination with Paclitaxel, Bicalutamide and Letrozole in Nanosponges. *Int. J. Pharm. Res. Sch. (IJPRS)* **5**, 32–39 (2016).

67. Shende, P., Chaphalkar, R., Deshmukh, K. & Gaud, R. S. Physicochemical Investigation of Engineered Nanosuspensions Containing Model Drug, Lansoprazole. *J. Dispers. Sci. Technol.* **37**, 504–511 (2016).

68. Garcia-Fernandez, M. J. *et al.* New multifunctional pharmaceutical excipient in tablet formulation based on citric acid-cyclodextrin polymer. *Int. J. Pharm.* **511**, 913–920 (2016).

69. Zainuddin, R. *et al.* Enhancement of oral bioavailability of anti- HIV drug rilpivirine HCl through nanosponge formulation. *Drug Dev. Ind. Pharm.* **0**, 2076–2084 (2017).

70. Rao, M. R. P. & Shirsath, C. Enhancement of Bioavailability of Non-nucleoside Reverse Transciptase Inhibitor Using Nanosponges. *AAPS PharmSciTech* **18**, 1728–1738 (2017).

71. Sundararajan, M., Thomas, P. A., Venkadeswaran, K., Jeganathan, K. & Geraldine, P. Synthesis and characterization of chrysin-loaded β-cyclodextrin-based nanosponges to enhance in-vitro solubility, photostability, drug release, antioxidant effects and antitumorous efficacy. *J. Nanosci. Nanotechnol.* **17**, 8742–8751 (2017).

72. Pushpalatha, R., Selvamuthukumar, S. & Kilimozhi, D. Carbonyl and carboxylate crosslinked cyclodextrin as a nanocarrier for resveratrol : in silico , in vitro and in vivo evaluation. *J. Incl. Phenom. Macrocycl. Chem.* **92**, 261–272 (2018).

73. Dhakar, N. K. *et al.* Comparative evaluation of solubility, cytotoxicity and photostability studies of resveratrol and oxyresveratrol loaded nanosponges. *Pharmaceutics* **11**, 1–15 (2019).

74. Mady, F. M., Ragab, S. & Ibrahim, M. Cyclodextrin-based nanosponge for improvement of solubility and oral bioavailability of Ellagic acid. *Pak. J. Pharm. Sci.* **31**, 2069–2076 (2018).

75. Dhakar, N. K. *et al.* Evaluation of solubility enhancement , antioxidant activity , and cytotoxicity studies of kynurenic acid loaded cyclodextrin nanosponge. *Carbohydr. Polym.* **224**, (2019).

76. Trotta, F. *et al.* Molecularly imprinted cyclodextrin nanosponges for the controlled delivery of L-DOPA: perspectives for the treatment of Parkinson's disease. *Expert Opin. Drug Deliv.* **13**, 1671–1680 (2016).

77. Kumar, S. & Rao, R. Analytical tools for cyclodextrin nanosponges in pharmaceutical field: a review. *J. Incl. Phenom. Macrocycl. Chem.* **94**, 11–30 (2019).

78. Zhao, F. *et al.* EDTA-Cross-Linked β-Cyclodextrin: An Environmentally Friendly Bifunctional Adsorbent for Simultaneous Adsorption of Metals and Cationic Dyes. *Environ. Sci. Technol.* **49**, 10570–10580 (2015).

79. Venuti, V. *et al.* Combining Raman and infrared spectroscopy as a powerful tool for the structural elucidation of cyclodextrin-based polymeric hydrogels. *Phys. Chem. Chem. Phys.* **17**, 10274–10282 (2015).

80. Salgin, S., Salgin, U. & Vatansever, Ö. Synthesis and Characterization of β-Cyclodextrin Nanosponge and Its Application for the Removal of p-Nitrophenol from Water. *Clean - Soil, Air, Water* **45**, (2017).

81. Junthip, J., Promma, W., Sonsupap, S. & Boonyanusith, C. Adsorption of paraquat from water by insoluble cyclodextrin polymer crosslinked with 1,2,3,4-butanetetracarboxylic acid. *Iran. Polym. J. (English Ed.* **28**, 213–223 (2019).

82. Berto, S. *et al.* Synthesis of new ionic β-cyclodextrin polymers and characterization of their heavy metals retention. in *Journal of Inclusion Phenomena and Macrocyclic Chemistry* **57**, 631–636 (2007).

83. Hayiyana, Z. *et al.* Ester-Based Hydrophilic Cyclodextrin Nanosponges for Topical Ocular Drug Delivery. *Curr. Pharm. Des.* **22**, 6988–6997 (2017).

84. Pawar, S., Shende, P. & Trotta, F. Diversity of β -cyclodextrin-based nanosponges for transformation of actives. *Int. J. Pharm.* **565**, 333–350 (2019).

85. Singireddy, A. & Subramanian, S. Cyclodextrin nanosponges to enhance the dissolution profile of quercetin by inclusion complex formation. *Part. Sci. Technol.* **34**, 341–346 (2016).

86. Silva, F., Caldera, F., Trotta, F., Nerín, C. & Domingues, F. C. Encapsulation of coriander essential oil in cyclodextrin nanosponges: A new strategy to promote its use in controlled-release active packaging. *Innov. Food Sci. Emerg. Technol.* **56**, (2019).

87. Trotta, F. & Cavalli, R. Characterization and applications of new hyper-cross-linked cyclodextrins. *Compos. Interfaces* **16**, 39–48 (2009).

88. Morin-Crini, N. *et al.* Water-insoluble β-cyclodextrin–epichlorohydrin polymers for removal of pollutants from aqueous solutions by sorption processes using batch studies: A review of inclusion mechanisms. *Progress in Polymer Science* **78**, 1–23 (2018).

89. Ferro, M. *et al.* Dynamics and interactions of ibuprofen in cyclodextrin nanosponges by solid-state NMR spectroscopy. *Beilstein J. Org. Chem.* **13**, 182–194 (2017).

90. Deshmukh, K., Tanwar, Y. S., Sharma, S., Shende, P. & Cavalli, R. Functionalized nanosponges for controlled antibacterial and antihypocalcemic actions. *Biomed. Pharmacother.* **84**, 485–494 (2016).

91. Russo, M., Saladino, M. L., Chillura Martino, D., Lo Meo, P. & Noto, R. Polyaminocyclodextrin nanosponges: Synthesis, characterization and pH-responsive sequestration abilities. *RSC Adv.* **6**, 49941–49953 (2016).

92. Swaminathan, S. *et al.* Cyclodextrin-based nanosponges encapsulating camptothecin: Physicochemical characterization, stability and cytotoxicity. *Eur. J. Pharm. Biopharm.* **74**, 193–201 (2010).

93. Shringirishi, M. *et al.* Fabrication and characterization of nifedipine loaded β-cyclodextrin nanosponges: An in vitro and in vivo evaluation. *J. Drug Deliv. Sci. Technol.* **41**, 344–350 (2017).

94. Dubey, P. *et al.* Formulations and evaluation of Cyclodextrin complexed Ceadroxil loaded nanosponges. *Int. J. Drug Deliv.* **9**, 84 (2017).

95. Rana, Z., Zahid, Z. & Jaiprakash, N. Sangshetti Mufassir, M. Enhancement of oral bioavailability of anti-HIV drug rilpivirine HCl through nanosponge formulation. *Drug Dev. Ind. Pharm.* **43**, 2076–2084 (2017).

96. R. P. Rao, M. *et al.* Self-nanoemulsifying Drug Delivery System of Mebendazole for Treatment of Lymphatic Filariasis. *Indian J. Pharm. Sci.* **80**, 1057–1068 (2018).

97. Deshmukh, K. & Shende, P. Toluene diisocyanate cross-linked β-cyclodextrin nanosponges as a pH-sensitive carrier for naproxen. *Mater. Res. Express* **5**, 7 (2018).

98. Rao, M. R. P., Chaudhari, J., Trotta, F. & Caldera, F. Investigation of Cyclodextrin-Based Nanosponges for Solubility and Bioavailability Enhancement of Rilpivirine. **19**, 2358–2369 (2018).

99. Zidan, M. F., Ibrahim, H. M., Afouna, M. I. & Ibrahim, E. A. *In vitro* and *in vivo* evaluation of cyclodextrin-based nanosponges for enhancing oral bioavailability of atorvastatin calcium. *Drug Dev. Ind. Pharm.* **44**, 1243–1253 (2018).

100. Mendes, C. *et al.* Cyclodextrin based nanosponge of norfloxacin : Intestinal permeation enhancement and improved antibacterial activity. **195**, 586–592 (2018).

101. Nait Bachir, Y., Nait Bachir, R. & Hadj-Ziane-Zafour, A. Nanodispersions stabilized by β-cyclodextrin nanosponges: application for simultaneous enhancement of bioactivity and stability of sage essential oil. *Drug Dev. Ind. Pharm.* **45**, 333–347 (2019).

102. Kamble, M., Zaheer, Z., Mokale, S. & Zainuddin, R. Formulation Optimization and Biopharmaceutical Evaluation of Imatinib Mesylate Loaded β-Cyclodextrin Nanosponges. *Pharm. Nanotechnol.* **07**, 343–361 (2019).

103. Rezaei, A., Varshosaz, J., Fesharaki, M., Farhang, A. & Jafari, S. M. Improving the solubility and in vitro cytotoxicity (anticancer activity) of ferulic acid by loading it into cyclodextrin nanosponges. *Int. J. Nanomedicine* **14**, 4589–4599 (2019).

104. Sherje, A. P., Surve, A. & Shende, P. CDI cross-linked β-cyclodextrin nanosponges of paliperidone: synthesis and physicochemical characterization. *J. Mater. Sci. Med.* **30**, (2019).

105. Argenziano, M. *et al.* In Vitro Enhanced Skin Permeation and Retention of Imiquimod Loaded in β -Cyclodextrin Nanosponge Hydrogel. *Pharmaceutics* **11**, (2019).

106. Mashaqbeh, H., Obaidat, R. & Al-Shar'i, N. Evaluation and characterization of curcumin-β-cyclodextrin and cyclodextrin-based nanosponge inclusion complexation. *Polymers (Basel).* **13**, (2021).

107. Kumar, A. & Rao, R. Enhancing efficacy and safety of azelaic acid via encapsulation in cyclodextrin nanosponges: development, characterization and evaluation. *Polym. Bull.* **78**, 5275–5302 (2021).

108. Jasim, I. K., Abdulrasool, A. A. & Abd-Alhammid, S. N. Nanosponge based gastroretentive drug delivery system of 5-fluorouracil for gastric cancer targeting. *Int. J. Drug Deliv. Technol.* **11**, 958–963 (2021).

109. Shoaib, Q.-U.-A., Latif, S., Ijaz, Q.A., Bukhari, N.I., Abbas, N. Solubility and dissolution rate enhancement of ibuprofen by cyclodextrin based carbonate nanosponges. *Pak. J. Pharm. Sci.* **34**, 1045–1055 (2021).

110. Allahyari, S. *et al.* In-vitro characterization and cytotoxicity study of flutamide loaded cyclodextrin nanosponges. *J. Drug Deliv. Sci. Technol.* **61**, 102275 (2021).

111. Kumar, S., Prasad, M. & Rao, R. Topical delivery of clobetasol propionate loaded nanosponge hydrogel for effective treatment of psoriasis: Formulation, physicochemical characterization, antipsoriatic potential and biochemical estimation. *Mater. Sci. Eng. C* **119**, 111605 (2021).

112. Pivato, R. V. *et al.* β-Cyclodextrin Nanosponge Hydrogels as Drug Delivery Nanoarchitectonics for Multistep Drug Release Kinetics. *ACS Appl. Polym. Mater.* **3**, 6562–6571 (2021).

113. Palminteri, M. *et al.* Cyclodextrin nanosponge for the gsh-mediated delivery of resveratrol in human cancer cells. *Nanotheranostics* **5**, 197–212 (2021).

114. Iriventi, P., Gupta, N. V., Osmani, R. A. M. & Balamuralidhara, V. Design & development of nanosponge loaded topical gel of curcumin and caffeine mixture for augmented treatment of psoriasis. *DARU, J. Pharm. Sci.* **28**, 489–506 (2020).

115. Appleton, S. L. *et al.* Nanosponges as protein delivery systems: Insulin, a case study. *Int. J. Pharm.* **590**, 119888 (2020).

116. Singireddy, A., Pedireddi, S. R. & Subramanian, S. Optimization of reaction parameters for synthesis of Cyclodextrin nanosponges in controlled nanoscopic size dimensions. *J. Polym. Res.* **26**, (2019).

117. Pushpalatha, R., Selvamuthukumar, S. & Kilimozhi, D. Hierarchy analysis of different cross-linkers used for the preparation of cross-linked cyclodextrin as drug nanocarriers. *Chem. Eng. Commun.* **205**, 759–771 (2018).

118. Pedrazzo, A. R. *et al.* Mechanochemical green synthesis of hyper-crosslinked cyclodextrin polymers. 1554–1563 (2020). doi:10.3762/bjoc.16.127

119. Benjamin J Bruno, Geoffrey D Miller, and C. S. L. Basics and recent advances in peptide and protein drug delivery.

120. Lau, J. L. & Dunn, M. K. Bioorganic & Medicinal Chemistry Therapeutic peptides : Historical perspectives , current development trends , and future directions. **26**, 2700–2707 (2018).

121. Dan, N., Samanta, K. & Almoazen, H. An Update on Pharmaceutical Strategies for Oral Delivery of Therapeutic Peptides and Proteins in Adults and Pediatrics. *Children* **7**, 307 (2020).

122. Fosgerau K, H. T. Peptide therapeutics: current status and future directions. *Drug Discov Today* **20**, 122±8 (2015).

123. http://www.actip.org/products/monoclonal-antibodies-approved-by-the-ema-and-fda-for-therapeutic-use/.

124. Alain Beck and Janice M Reichert. Therapeutic Fc-fusion proteins and peptides as successful alternatives to antibodies. *MAbs* **3**, 415–416 (2011).

125. Davinder S. Gill. Protein Pharmaceuticals. Discovery and Preclinical Development.

126. Ashaben Patel, Mitesh Patel, Xiaoyan Yang, and A. K. M. Recent Advances in Protein and Peptide Drug Delivery: A Special Emphasis on Polymeric Nanoparticles. *Protein Pept Lett.* **21**, 1102–1120 (2014).

127. Sonia, T. A. & Sharma, C. P. *Oral Delivery of Insulin. Oral Delivery of Insulin* (2015). doi:10.1016/C2013-0-18177-9

128. Jitendra, Sharma PK, Bansal S, B. A. Noninvasive routes of proteins and peptides drug delivery. *Indian J Pharm Sci.* **73**, 367–75 (2011).

129. Smart, AL; Gaisford, S; Basit, A. Oral peptide and protein delivery: Intestinal obstacles to delivery and commercial prospects. *Expert Opin. Drug Deliv.* **11**, 1323–1335 (2014).

130. Homayun, B., Lin, X. & Choi, H. J. Challenges and recent progress in oral drug delivery systems for biopharmaceuticals. *Pharmaceutics* **11**, (2019).

131. Fuccella, L. ., Perucca, E. & Sirtori, C. *Farmacologia clinica*. (2006).

132. Couvreur P, P. F. Nano- and microparticles for the delivery of polypeptides and proteins. *Adv Drug Del Rev* **10**, 141–62 (1993).

133. Rowland, M. & Tozer, T. N. *Clinical Pharmacokineticsand Pharmacodynamics Concepts and Applications*. (2011).

134. Reis, C. P. & Neufeld, R. J. Nanoencapsulation II . Biomedical applications and current status of peptide and protein nanoparticulate delivery systems. **2**, 53–65 (2006).

135. Clemente, N. *et al.* Immunotherapy of experimental melanoma with ICOS-Fc loaded in biocompatible and biodegradable nanoparticles. *J. Control. Release* **320**, 112–124 (2020).

136. Varewijck, A. J. & Janssen, J. A. M. J. L. Insulin and its analogues and their affinities for the IGF1 receptor. *Endocr. Relat. Cancer* **19**, 63–75 (2012).

137. Guariguata, L. *et al.* Global estimates of diabetes prevalence for 2013 and projections for 2035. *Diabetes Res. Clin. Pract.* **103**, 137–149 (2014).

138. Wong, C. Y., Martinez, J. & Dass, C. R. Oral delivery of insulin for treatment of diabetes : status quo , challenges and opportunities. **68**, 1093–1108 (2016).

139. Pillai, O. & Panchagnula, R. Insulin therapies - Past, present and future. *Drug Discov. Today* **6**, 1056–1061 (2001).

140.
    https://www.scopus.com/term/analyzer.uri?sid=6c80a240c965027d44236b6a36d97566&origin=resultslist&src=s&s=TITLE-ABS-KEY%28oral+administration+insulin

141. Woitiski , C.B. , Sarmento , B. , Carvalho , R.A. , Neufeld , R.J. and Veiga, F. Facilitated nanoscale delivery of insulin across intestinal membrane models. *Int. J. Pharm.* **412**, 123 – 31 (2011).

142. Sarmento, B. *et al.* Alginate/chitosan nanoparticles are effective for oral insulin delivery. *Pharm. Res.* **24**, 2198–2206 (2007).

143. Krauland, A. H. & Alonso, M. J. Chitosan/cyclodextrin nanoparticles as macromolecular drug delivery system. *Int. J. Pharm.* **340**, 134–142 (2007).

144. Mi , F.-L. , Wu , Y.-Y. , Lin , Y.-H. , Sonaje , K. , Ho , Y.-C., et al . Oral delivery of peptide drugs using nanoparticles self- assembled by poly(γ -glutamic acid) and a chitosan derivative functionalized by trimethylation. *Bioconjug. Chem.* **19**, 1248 – 55 (2008).

145. Qian, F., Cui, F., Ding, J., Tang, C. & Yin, C. Chitosan graft copolymer nanoparticles for oral protein drug delivery: Preparation and characterization. *Biomacromolecules* **7**, 2722–2727 (2006).

146. Shi, L. & Caldwell, K. D. Mucin adsorption to hydrophobic surfaces. *J. Colloid Interface Sci.* **224**, 372–381 (2000).

147. Sarmento, B., Ribeiro, A., Veiga, F., Ferreira, D. & Neufeld, R. Oral bioavailability of insulin contained in polysaccharide nanoparticles. *Biomacromolecules* **8**, 3054–3060 (2007).

148. Chalasani, K. B., Russell-Jones, G. J., Yandrapu, S. K., Diwan, P. V. & Jain, S. K. A novel vitamin B12-nanosphere conjugate carrier system for peroral delivery of insulin. *J. Control. Release* **117**, 421–429 (2007).

149. Clemente, N. *et al.* Paclitaxel-loaded nanosponges inhibit growth and angiogenesis in melanoma cell models. *Front. Pharmacol.* **10**, 1–13 (2019).

150. Pedrazzo, A. R. *et al.* Eco-Friendly -cyclodextrin and Linecaps Polymers for the Removal of Heavy Metals. 1–14 (2019).

151. Juluri, A. *et al.* Taste Masking of Griseofulvin and Caffeine Anhydrous Using Kleptose Linecaps DE17 by Hot Melt Extrusion. *AAPS PharmSciTech* **17**, 99–105 (2016).

152. Anceschi, A., Magnacca, G., Trotta, F. & Zanetti, M. Preparation and characterization of microporous carbon spheres from high amylose pea maltodextrin. *RSC Adv.* **7**, 36117–36123 (2017).

153. Torne, S. J., Ansari, K. A., Vavia, P. R., Trotta, F. & Cavalli, R. Enhanced oral paclitaxel bioavailability after administration of paclitaxel-loaded nanosponges. *Drug Deliv.* **17**, 419–425 (2010).

154. Fernanda M. Carbinatto, Ana Do´ris de Castro, Raul C. Evangelista, B. S. F. C. Insights into the swelling process and drug releasemechanisms from cross-linked pectin/highamylose starch matrices. *Asian J. Pharm. Sci.* **9**, 27–34 (2014).

155. Shende, P. *et al.* Acute and Repeated Dose Toxicity Studies of Different β-Cyclodextrin-Based Nanosponge Formulations. *J. Pharm. Sci.* **104**, 1856–1863 (2015).

156. Filipe, V., Hawe, A. & Jiskoot, W. Critical evaluation of nanoparticle tracking analysis (NTA) by NanoSight for the measurement of nanoparticles and protein aggregates. *Pharm. Res.* **27**, 796–810 (2010).

157. Presas, E. *et al.* Physicochemical, pharmacokinetic and pharmacodynamic analyses of amphiphilic cyclodextrin-based nanoparticles designed to enhance intestinal delivery of insulin. *J. Control. Release* **286**, 402–414 (2018).

158. Gatti, T. H. H. *et al.* Insulin-loaded polymeric mucoadhesive nanoparticles: Development, characterization and cytotoxicity evaluation. *Brazilian J. Pharm. Sci.* **54**, 1–10 (2018).

159. Dzwolak, W., Ravindra, R., Lendermann, J. & Winter, R. Aggregation of bovine insulin probed by DSC/PPC calorimetry and FTIR spectroscopy. *Biochemistry* **42**, 11347–11355 (2003).

160. Mendes, C. *et al.* Cyclodextrin based nanosponge of norfloxacin: Intestinal permeation enhancement and improved antibacterial activity. *Carbohydr. Polym.* **195**, 586–592 (2018).

161. Boddupalli, B. M., Mohammed, Z. N. K. & Ravinder Nath A.1, D. B. Mucoadhesive drug delivery system: An overview. *J. Adv. Pharm. Tech. Res.* (2010).

162. Ahuja, A., Khar, R. K. & Ali, J. Mucoadhesive drug delivery systems. *Drug Dev. Ind. Pharm.* **23**, 489–515 (1997).

163. Byrne, M. E., Park, K. & Peppas, N. A. Molecular imprinting within hydrogels. *Adv. Drug Deliv. Rev.* **54**, 149–161 (2002).

164. Omidian, H. & Park, K. Swelling agents and devices in oral drug delivery. *J. Drug Deliv. Sci. Technol.* **18**, 83–93 (2008).

165. Roberts C.J. Protein Aggregation and Its Impact on Product Quality. *Curr Opin Biotechnol* 211–217 (2014). doi:10.1016/j.copbio.2014.08.001.Protein

166. Derewenda, U., Derewenda, Z., Dodson, G. ., Hubbard, R. . & Korber, F. Molecular structure of insulin: the insulin monomer and its assembly. *Br Med Bull* **45**, 4–18 (1989).

167. Farrell, A., Bones, J. & Cook, K. Optimizing Protein Aggregate Analysis by SEC. *BioPharm Int.* **30**, 46–47, 50–51 (2017).

168. Palaniswamy, M. . & Coffey, A. Size Exclusion Chromatography of Biosimilar and Innovator Insulin. *Agilent Technologies, Inc.,* (2021). Available at: https://www.agilent.com/cs/library/applications/5991-6872EN.pdf.

169. Sambuy Y, De Angelis I, Ranaldi G, Scarino ML, Stammati A, Z. F. The Caco-2 cell line as a model of the intestinal barrier: influence of cell and culture-related factors on Caco-2 cell functional characteristics. *Cell Biol Toxicol.* **21**, 1–26 (2005).

170. Sosnik, A., Neves, J. & Sarmento, B. Mucoadhesive polymers in the design of nano-drug delivery systems for administration by non-parenteral routes: A review. *Prog. Polym. Sci.* **39**, 2030–2075 (2014).

171. Zara, G. P. *et al.* Pharmacokinetics and Tissue Distribution of Idarubicin-Loaded Solid Lipid Nanoparticles After Duodenal Administration to Rats. *J. Pharm. Sci.* **91**, 1324–133 (2002).

172. Cavalli, R. et al. Transmucosal transport of tobramycin incorporated in SLN after duodenal administration to rats. Part I—A pharmacokinetic study. *Pharmacol. Res.* **42**, 541–545 (2000).

173. Bargoni, A. *et al.* Transmucosal transport of tobramycin incorporated in solid lipid nanoparticles (SLN) after duodenal administration to rats. Part II - Tissue distribution. *Pharmacol. Res.* **43**, 497–502 (2001).

174. King, A. J. F. The use of animal models in diabetes research. *Br. J. Pharmacol.* **166**, 877–894 (2012).

175. B.L, F. Streptozotocin-Induced Diabetic Models in Mice and Rats. *Curr. Protoc.* (2015).

176. Chen, Y. G., Mathews, C. E. & Driver, J. P. The role of NOD mice in type 1 diabetes research: Lessons from the past and recommendations for the future. *Front. Endocrinol. (Lausanne).* **9**, 1–13 (2018).

177. Makino, S. *et al.* Breeding of a Non-Obese, Diabetic Strain of Mice. *J-STAGE* **29**, 1–13 (1890).

178. Pearson, J. ., Wong, F. . & Wen, L. The importance of the Non Obese Diabetic (NOD) mouse model in autoimmune diabetes. *J Autoimmun* **66**, 76–88 (2016).

179. Szkudelski, T. The mechanism of alloxan and streptozotocin action in B cells of the rat pancreas. *Physiol. Res.* **50**, 537–546 (2001).

Annexe

Table A1. List of experiments carried out on group 1 NOD mice.

NOD mice	Sample	Route of administration	Dose	Purpose
Mouse 2	Industrial NS insulin-loaded	Oral gavage	60 IU/kg	Evaluation of efficacy
	Saline solution	Oral gavage	---	Control
Mouse 1,2,3,4,5,6,7,8,9	Saline solution	Oral gavage	---	Control
Mouse 1,2,3,4,5,6,9	Industrial NS insulin-loaded	Oral gavage	60 IU/kg	Evaluation of efficacy
Mouse 7,8	Saline solution	Oral gavage	---	Control
Mouse 1,2,4,5,8,9 Mouse 10,11,12,13,14	Saline solution	Oral gavage	---	Control
Mouse 1,2,4,5,8*,9	Industrial NS insulin-loaded	Oral gavage	60 IU/kg	Evaluation of efficacy
Mouse 10,11,12,13,14	Industrial NS insulin-loaded	Oral gavage	60 IU/kg	Evaluation of efficacy
Mouse 1,2,4,5,9	Industrial NS insulin-loaded	Oral gavage	60 IU/kg	Evaluation of efficacy
Mouse 10,11,12,13,14,15	Saline solution	Oral gavage	---	Control
Mouse 1,2,4	Industrial NS insulin-loaded	Oral gavage	90 IU/kg	Evaluation of efficacy
Mouse 10,11,12,13,14,15	Industrial NS insulin-loaded	Oral gavage	60 IU/kg	Evaluation of efficacy
Mouse 10,11,12,13,14,15	Industrial NS insulin-loaded	Oral gavage	60 IU/kg	Evaluation of efficacy

Table A1. List of experiments carried out on group 1 NOD mice (*continued*).

NOD mice	Sample	Route of administration	Dose	Purpose
Mouse 1,2,9	Industrial NS insulin-loaded	Oral gavage	90 IU/kg	Evaluation of efficacy
Mouse 4,5	Saline solution	Oral gavage	---	Control
Mouse 10,11,12	Industrial NS insulin-loaded	Oral gavage	60 IU/kg	Evaluation of efficacy
Mouse 1,2,9	Industrial NS insulin-loaded	Oral gavage	90 IU/kg	Evaluation of efficacy
Mouse 4,5	Saline solution	Oral gavage	---	Control
Mouse 13,14,15	LC CITR insulin-loaded	Oral gavage	60 IU/kg	Evaluation of efficacy

Table A2. List of experiments carried out on group 2 NOD mice.

NOD mice	Sample	Route of administration	Dose	Purpose
Mouse 4, 9, 19, 25	Saline solution	Oral gavage	---	Control
Mouse 4, 9, 19, 25	Industrial NS insulin-loaded	Oral gavage	60 IU/kg	Evaluation of efficacy
Mouse 4, 9, 19, 25	Industrial NS insulin-loaded	Oral gavage	60 IU/kg	Evaluation of efficacy
Mouse 4, 9, 19, 25	Industrial NS insulin-loaded	Oral gavage	60 IU/kg	Evaluation of efficacy
Mouse 4, 7, 9	Bovine insulin	Subcutaneous injection	1.5 IU/kg	Control
Mouse 11, 19, 25	Industrial NS insulin-loaded	Subcutaneous injection	1.5 IU/kg	Evaluation of efficacy

Table A3. List of experiments carried out on group 3 NOD mice diabetic (D) and non-diabetic (ND).

No. NOD mice	Sample	Route of administration	Dose	Purpose
4 D 4 ND	Saline solution	Oral gavage	---	Control
4 D	Bovine insulin solution	Oral gavage	60 IU/kg	Control
4 D 4 ND	Bovine insulin solution	Subcutaneous injection	1.5 IU/kg	Control
5 D 6 ND	Bovine insulin solution	Oral gavage	60 IU/kg	Control
6 D 7 ND	Bovine insulin solution	Subcutaneous injection	1.5 IU/kg	Control
6 D 6 ND	Industrial NS insulin-loaded	Oral gavage	60 IU/kg	Evaluation of efficacy
6 D 6 ND	Industrial NS insulin-loaded	Oral gavage	60 IU/kg	Evaluation of the efficacy
4 D 4 ND	Industrial NS insulin-loaded	Oral gavage	60 IU/kg	Evaluation of the efficacy
6 D 6 ND	Industrial NS insulin-loaded	Subcutaneous injection	1.5 IU/kg	Evaluation of the efficacy
6 D 6 ND	Industrial NS insulin-loaded	Subcutaneous injection	1.5 IU/kg	Evaluation of the efficacy
5 D 5 ND	Industrial NS insulin-loaded	Oral gavage	60 IU/kg	Evaluation of the efficacy
7 D	Bovine insulin solution	Oral gavage	60 IU/kg	Control
6 D 5 ND	Bovine insulin solution	Oral gavage	60 IU/kg	Control

Table A4. Monitoring of weight and blood sugar levels (BSL) in group 1 NOD mice.

	Date	20/05/19		27/05/19		03/06/19		10/06/19		17/06/19		25/06/19		01/07/19		08/07/19	
	Mouse Identification code	Weight (g)	BSL (mg/dl)	Weight (g)	BSL (mg/dl)	Weight (g)	BSL (mg/dl)	Weight (g)	BSL (mg/dl)	Weight (g)	BSL (mg/dl)	Weight (g)	BSL (mg/dl)	Weight (g)	BSL (mg/dl)	Weight (g)	BSL (mg/dl)
cage 1	mouse 1	17.0	91	22.5	110	23.0	98	22.5	103	23.0	84	23.5	100	23.5	102	23.5	102
	mouse 2	15.5	84	20.5	106	21.5	97	20.5	112	22.5	176	21.6	283	22.0	506	21.7	580
	mouse 3	20.5	95	25.0	111	27.0	108	25.0	94	25.0	92	25.5	109	25.3	101	26.3	112
	mouse 4	20.8	82	25.5	119	27.0	116	26.5	101	26.5	107	26.0	96	25.3	109	25.0	120
	mouse 5	20.8	98	24.5	97	27.0	124	25.5	106	25.0	119	25.5	162	25.5	195	27.0	186
	mouse 6	19.5	377	23.2	570	24.5	>600	20.3	>600	20.3	>600	18.0	>600	17.0	>600	16.5	>600
cage 2	mouse 7	22.3	111	23.0	101	25.0	104	24.3	94	24.5	110	25.5	140	27.0	131	26.0	115
	mouse 8	22.3	102	22.8	89	25.0	104	24.0	98	24.0	135	24.0	101	25.0	126	24.5	105
	mouse 9	20.5	105	20.9	121	21.0	98	20.5	115	21.0	119	20.0	169	21.5	410	22.0	437
	mouse 10	23.4	116	24.8	92	26.0	99	25.7	99	26.0	107	26.5	120	26.5	104	25.0	118
	mouse 11	20.5	108	21.9	91	22.0	103	23.3	104	25.0	112	23.3	196	23.0	420	22.0	426
	mouse 12	21.5	116	22.5	106	23.0	86	22.3	94	23.0	88	24.0	110	24.2	84	24.0	110
cage 3	mouse 13	25.1	83	26.0	94	27.5	97	27.5	106	27.0	110	28.0	99	---*			
	mouse 14	24.0	102	24.0	107	25.0	98	24.1	110	24.0	93	25.0	110	25.5	133	25.5	136
	mouse 15	21.5	102	22.5	131	23.5	106	22.4	105	23.5	107	24.0	91	23.5	86	23.0	117
	mouse 16	20.5	92	22.7	96	23.8	90	22.8	102	23.2	83	23.2	130	---*			
	mouse 17	21.0	99	21.5	108	25.0	102	23.9	117	25.0	128	23.5	98	23.6	96	23.5	113
	mouse 18	23.0	113	22.5	93	24.5	160	24.3	121	25.5	200	26.0	177	25.0	234	25.0	147
cage 4	mouse 19	23.0	117	23.0	111	25.0	96	23.4	104	25.5	108	24.9	95	24.0	101	25.0	122
	mouse 20	24.0	101	24.5	119	26.5	104	25.3	128	25.0	106	26.0	120	25.5	100	26.0	126
	mouse 21	22.5	105	23.0	119	24.4	120	25.0	102	25.0	115	25.0	132	24.5	175	24.5	154
	mouse 22	22.5	119	23.5	129	24.7	173	24.3	217	24.3	534	24.4	571	23.4	>600	25.0	>600
	mouse 23	23.0	108	23.0	125	25.0	89	23.3	117	24.3	99	25.2	83	23.5	104	26.0	115
	mouse 24	22.5	97	23.0	104	25.6	123	24.5	105	25.0	103	25.2	132	25.0	143	25.5	138

*died naturally

Table A5.Monitoring of weight and blood sugar levels (BSL) in group 2 NOD mice.

	Date	20/01/20		27/01/20		03/02/20		10/02/20		17/02/20		25/02/20		02/03/20		09/03/20	
	Mouse identification code	Weight (g)	BSL (mg/dl)	Weight (g)	BSL (mg/dl)	Weight (g)	BSL (mg/dl)	Weight (g)	BSL (mg/dl)	Weight (g)	BSL (mg/dl)	Weight (g)	BSL (mg/dl)	Weight (g)	BSL (mg/dl)	Weight (g)	BSL (mg/dl)
Cage 1	mouse 1	22	92	26	100	24	105	26	100	24	104	27	115	27	106	26	110
	mouse 2	25	94	25	107	24	120	25	107	26	144	26	116	26	135	26	160
	mouse 3	25	101	28	121	25	90	28	121	27	111	27	94	27	122	27	120
	mouse 4	25	93	28	409	27	211	28	409	28	574	21	>600	18	>600	24	>600
	mouse 5	23	80	24	103	23	100	24	103	24	94	25	120	24	87	24	106
Cage 2	mouse 6	22	91	24	95	22	97	24	95	24	110	24	114	24	87	24	97
	mouse 7	23	104	24	114	24	109	24	114	25	129	26	173	23	120	25	210
	mouse 8	23	90	24	109	24	98	24	109	26	123	24	112	24	92	24	117
	mouse 9	22	98	24	502	22	316	24	502	22	544	21	>600	16	>600	21	>600
	mouse 10	22	108	23	121	23	100	23	121	24	103	25	124	25	116	25	133
Cage 3	mouse 11	25	99	26	122	26	112	26	122	24	126	29	234	26	233	27	381
	mouse 12	24	110	24	94	23	118	24	94	23	110	26	110	26	105	26	90
	mouse 13	25	103	26	90	24	90	26	90	24	113	27	127	28	102	27	95
	mouse 14	26	90	27	110	25	84	27	110	28	109	27	127	27	112	28	113
	mouse 15*	26	85								---*						
Cage 4	mouse 16	24	109	24	105	23	105	24	105	26	94	26	159	25	101	26	106
	mouse 17	22	78	21	94	21	97	21	94	24	123	24	104	24	98	24	108
	mouse 18	24	93	27	117	25	103	27	117	25	107	29	105	28	103	27	98
	mouse 19	21	135	23	420	22	222	23	420	22	563	21	>600	15	>600	18	>600
	mouse 20	22	88	24	90	23	105	24	90	25	102	25	118	25	106	25	111
Cage 5	mouse 21	24	79	26	116	24	95	26	116	29	150	26	133	27	103	27	102
	mouse 22	24	87	25	131	24	115	25	131	25	107	25	90	25	114	25	123
	mouse 23	22	91	23	140	23	142	23	140	24	116	24	114	24	109	25	87
	mouse 24	22	87	22	103	22	114	22	103	23	113	25	107	23	104	25	111
	mouse 25	25	92	27	377	26	201	27	377	27	>600	24	>600	18	>600	20	>600

*died naturally

Table A6. Monitoring of weight and blood sugar levels in group 3 NOD mice.

	Date	21/09/20		28/09/20		5/10/20		12/10/20		19/10/20		26/10/20		02/11/20	
	Mouse identification code	Weight (g)	BSL (mg/dl)	Weight (g)	BSL (mg/dl)	Weight (g)	BSL (mg/dl)	Weight (g)	BSL (mg/dl)	Weight (g)	BSL (mg/dl)	Weight (g)	BSL (mg/dl)	Weight (g)	BSL (mg/dl)
Cage 1	mouse 1	21	>600	20	>600	19	>600	17	>600	13	>600	15	>600	14	>600
	mouse 2	24	114	23	117	23	119	25	133	27	105	26	129	25	144
	mouse 3	24	106	24	123	24	124	25	128	26	107	25	105	24	125
	mouse 4	24	113	25	108	25	112	26	111	25	96	26	106	26	114
	mouse 5	22	125	23	123	24	119	24	101	24	106	24	145	23	107
Cage 2	mouse 6	22	103	22	110	24	122	23	113	24	117	24	100	23	125
	mouse 7	20	88	21	95	20	133	23	132	23	113	23	169	22	235
	mouse 8	26	123	26	126	27	124	27	128	27	115	26	111	27	138
	mouse 9	24	115	24	116	25	116	26	114	25	106	26	114	25	131
	mouse 10	23	100	23	100	23	110	25	115	26	98	25	124	25	119
Cage 3	mouse 11	25	121	24	113	26	120	25	107	26	116	25	115	25	129
	mouse 12	22	123	22	104	22	108	23	109	23	124	23	109	24	132
	mouse 13	25	101	24	104	25	110	25	98	26	109	26	107	25	134
	mouse 14	25	114	25	128	27	121	25	126	27	102	27	119	26	143
	mouse 15	22	116	24	125	25	121	24	115	25	103	24	110	24	140
Cage 4	mouse 16	24	120	25	116	26	117	25	131	27	119	27	129	25	126
	mouse 17	24	107	25	111	25	117	26	125	25	107	25	111	24	103
	mouse 18	24	115	25	115	24	115	25	116	27	125	27	130	25	104
	mouse 19	21	115	21	102	23	106	25	113	23	112	23	120	24	96
	mouse 20	24	114	24	103	25	114	26	107	25	97	25	146	25	379
Cage 5	mouse 21	24	114	24	101	24	98	25	96	24	123	26	243	23	359
	mouse 22	24	106	23	114	25	131	25	125	25	130	24	112	25	129
	mouse 23	21	108	22	114	23	114	24	118	24	120	25	121	24	127
	mouse 24	25	115	25	112	25	115	26	112	25	111	25	104	24	112
	Mouse 25	22	113	23	123	23	105	25	135	24	143	25	144	24	130

Table A6. Monitoring of weight and blood sugar levels in group 3 NOD mice (*continued*).

	Date	09/11/20		16/11/20		23/11/20		30/11/20		09/12/20		14/12/20	
	Mouse identification code	Weight (g)	BSL (mg/dl)	Weight (g)	BSL (mg/dl)	Weight (g)	BSL (mg/dl)	Weight (g)	BSL (mg/dl)	Weight (g)	BSL (mg/dl)	Weight (g)	BSL (mg/dl)
Cage 1	mouse 1	13	>600	14	>600			---*					
	mouse 2	25	106	25	111	25	134	26	144	26	108	26	121
	mouse 3	24	106	26	101	25	136	26	106	28	118	28	134
	mouse 4	26	144	25	127	25	354	26	584	25	>600	25	>600
	mouse 5	26	105	24	120	25	121	25	126	25	107	26	132
Cage 2	mouse 6	23	98	24	137	23	107	26	128	25	127	25	99
	mouse 7	24	367	24	560	23	>600	24	>600	23	>600	21	>600
	mouse 8	26	98	27	140	27	129	30	127	27	109	29	111
	mouse 9	26	102	26	122	26	122	27	115	26	116	27	120
	mouse 10	25	110	25	135	27	129	27	159	25	179	27	238
Cage 3	mouse 11	26	156	25	117	26	151	25	143	26	140	26	140
	mouse 12	25	117	25	146	25	124	26	158	26	160	26	153
	mouse 13	26	120	25	135	24	109	26	119	27	107	27	116
	mouse 14	28	176	27	418	28	302	27	424			---*	
	mouse 15	27	263	25	255	26	314	23	209	25	255	24	174
Cage 4	mouse 16	26	133	28	122	27	138	27	113	27	126	28	119
	mouse 17	25	109	26	111	26	106	27	114	27	109	27	131
	mouse 18	26	106	27	100	26	106	27	154	27	129	28	129
	mouse 19	22	121	26	136	22	124	24	129	24	132	24	417
	mouse 20	26	530	26	>600	25	>600	25	>600	24	>600	23	>600
Cage 5	mouse 21	24	510	24	535	23	540	23	>600	23	>600	20	>600
	mouse 22	25	136	24	120	25	134	25	121	25	112	26	114
	mouse 23	25	122	26	140	27	133	28	134	27	134	27	140
	mouse 24	23	142	24	116	24	110	24	100	24	102	25	102
	Mouse 25	26	134	24	194	26	179	28	175	26	147	28	152

*died naturally

Table A7. Blood sugar levels (BSL) of NOD mice in group 1 used as a control (oral administration of saline solution).

NOD mice	Time (minutes)		0	15	30	45	60	90	120	180
Mouse 6	BSL	(mg/dl)	76	149	217	---*	289	303	308	202
	BSL	(%)	100	196	285		380	398	405	265
Mouse 6	BSL	(mg/dl)	71	263	403	419	363	350	343	251
	BSL	(%)	100	370	568	590	511	493	483	354
Mouse 22	BSL	(mg/dl)	120	326	324	303	279	271	225	164
	BSL	(%)	100	272	270	253	233	226	188	137
Mouse 6	BSL	(mg/dl)	53	193	221	216	260	269	252	130
	BSL	(%)	100	364	417	408	491	508	475	245
Mouse 22	BSL	(mg/dl)	105	316	121	317	256	194	188	84
	BSL	(%)	100	301	115	302	244	185	179	80
Mouse 9	BSL	(mg/dl)	85	195	186	150	122	107	85	63
	BSL	(%)	100	229	219	176	144	126	100	74
Mouse 11	BSL	(mg/dl)	120	287	318	287	277	241	194	143
	BSL	(%)	100	239	265	239	231	201	162	119
Mouse 11	BSL	(mg/dl)	210	471	476	465	496	468	422	290
	BSL	(%)	100	224	227	221	236	223	201	138

*not determined

Table A8. Blood sugar levels (BSL) of NOD mice in group 1 treated orally with industrial NS insulin-loaded at a dose of 60 IU/kg.

NOD mice	Time (minutes)		0	15	30	45	60	90	120	180
Mouse 6	BSL	(mg/dl)	150	310	315	---*	241	155	101	72
	BSL	(%)	100	206	210		160	103	67	49
Mouse 6	BSL	(mg/dl)	60	266	268	252	222	157	122	76
	BSL	(%)	100	443	447	420	370	262	203	127
Mouse 22	BSL	(mg/dl)	139	326	316	308	263	174	99	96
	BSL	(%)	100	235	227	222	189	125	71	69
Mouse 6	BSL	(mg/dl)	106	176	86	64	43	33	40	29
	BSL	(%)	100	166	81	60	41	31	38	27
Mouse 22	BSL	(mg/dl)	120	402	440	426	390	330	289	121
	BSL	(%)	100	335	367	355	325	275	241	101
Mouse 2	BSL	(mg/dl)	143	385	383	339	361	255	249	110
	BSL	(%)	100	269	268	237	252	178	174	77
Mouse 6	BSL	(mg/dl)	112	249	291	326	378	266	202	129
	BSL	(%)	100	222	260	291	338	238	180	115
Mouse 11	BSL	(mg/dl)	83	301	312	292	264	202	148	96
	BSL	(%)	100	363	376	352	318	243	178	116

*not determined

Table A8. Blood sugar levels (BSL) of NOD mice in group 1 treated orally with industrial NS insulin-loaded at a dose of 60 IU/kg (*continued*).

NOD mice	Time (minutes)		0	15	30	45	60	90	120	180
Mouse 22	BSL	(mg/dl)	277	522	459	382	351	206	162	102
	BSL	(%)	100	188	166	138	127	74	58	37
Mouse 9	BSL	(mg/dl)	94	148	99	107	108	106	98	77
	BSL	(%)	100	157	105	114	115	113	104	82

Table A9. Blood sugar levels (BSL) of NOD mice in group 1 treated orally with industrial NS insulin-loaded at a dose of 90 IU/kg.

NOD mice	Time (minutes)		0	15	30	45	60	90	120	180
Mouse 2	BSL	(mg/dl)	256	547	483	477	483	356	350	250
	BSL	(%)	100	214	189	186	189	139	137	98
Mouse 6	BSL	(mg/dl)	184	346	213	107	65	45	33	23
	BSL	(%)	100	188	116	58	35	24	18	13
Mouse 11	BSL	(mg/dl)	127	369	436	375	330	239	160	89
	BSL	(%)	100	291	343	295	260	188	126	70
Mouse 6	BSL	(mg/dl)	285	482	519	450	411	342	212	77
	BSL	(%)	100	169	182	158	144	120	74	27
Mouse 22	BSL	(mg/dl)	509	>600	584	584	>600	575	519	396
	BSL	(%)	100	>118	115	115	>118	113	102	78
Mouse 2	BSL	(mg/dl)	501	600	600	558	577	568	526	530
	BSL	(%)	100	120	120	111	115	113	105	106
Mouse 6	BSL	(mg/dl)	357	335	308	308	325	257	205	114
	BSL	(%)	100	94	86	86	91	72	57	32
Mouse 22	BSL	(mg/dl)	505	>600	>600	>600	>600	559	520	342
	BSL	(%)	100	>119	>119	>119	>119	111	103	68

Table A10. Blood sugar levels (BSL) of NOD mice in group 1 treated orally with CTR-LC-1:8 insulin-loaded at a dose of 60 IU/kg.

NOD mice	Time (minutes)		0	15	30	45	60	90	120	180
Mouse 21	BSL	mg/dl	118	351	264	273	188	124	109	101
	BSL	%	100	297	224	231	159	105	92	86
Mouse 24	BSL	mg/dl	75	230	159	122	84	72	43	45
	BSL	%	100	307	212	163	112	96	57	60
Mouse 14	BSL	mg/dl	64	87	78	67	46	53	31	43
	BSL	%	100	136	122	105	72	83	48	67

Table A11 Blood sugar levels (BSL) of NOD mice in group 2 used as a control (oral administration of saline solution).

NOD mice	Time (minutes)		0	15	30	45	60	90	120	180
Mouse 4	BSL	mg/dl	115	286	293	301	306	315	274	187
	BSL	%	100	249	255	262	266	274	238	163
Mouse 9	BSL	mg/dl	449	>600	>600	596	>600	594	536	420
	BSL	%	100	>134	>134	133	>134	132	119	94
Mouse 19	BSL	mg/dl	401	564	600	568	600	580	600	561
	BSL	%	100	141	150	142	150	145	150	140
Mouse 25	BSL	mg/dl	498	>600	>600	>600	>600	>600	560	543
	BSL	%	100	>121	>121	>121	>121	>121	112	109

Table A12. Blood sugar levels (BSL) of NOD mice in group 2 treated orally with Industrial NS insulin-loaded at a dose of 60 IU/kg.

NOD mice	Time (minutes)		0	15	30	45	60	90	120	180
Mouse 4	BSL	mg/dl	332	389	454	491	478	456	391	315
	BSL	%	100	117	137	148	144	137	118	95
Mouse 9	BSL	mg/dl	418	597	573	546	485	403	365	367
	BSL	%	100	143	137	131	116	96	87	88
Mouse 19	BSL	mg/dl	434	441	315	308	285	328	292	254
	BSL	%	100	102	73	71	66	76	67	59
Mouse 25	BSL	mg/dl	552	>600	582	>600	580	566	514	497
	BSL	%	100	>109	105	>109	105	103	93	90
Mouse 4	BSL	mg/dl	212	211	162	126	117	109	60	58
	BSL	%	100	100	76	59	55	51	28	27
Mouse 9	BSL	mg/dl	412	469	409	292	212	182	99	50
	BSL	%	100	114	99	71	52	44	24	12
Mouse 19	BSL	mg/dl	493	477	399	335	269	237	160	117
	BSL	%	100	97	81	68	55	48	33	24

Table A12. Blood sugar levels (BSL) of NOD mice in group 2 treated orally with Industrial NS insulin-loaded at a dose of 60 IU/kg (*continued*).

NOD mice	Time (minutes)		0	15	30	45	60	90	120	180
Mouse 25	BSL	mg/dl	391	412	405	403	309	263	200	57
	BSL	%	100	105	104	103	79	67	51	15
Mouse 4	BSL	mg/dl	291	448	419	344	290	174	101	57
	BSL	%	100	154	144	118	100	60	35	20
Mouse 9	BSL	mg/dl	443	556	472	488	429	395	348	258
	BSL	%	100	126	107	110	97	89	79	58
Mouse 19	BSL	mg/dl	488	>600	516	>600	576	563	535	481
	BSL	%	100	>123	106	>123	118	115	110	99
Mouse 25	BSL	mg/dl	87	163	100	68	76	54	30	28
	BSL	%	100	187	115	78	87	62	35	32

Table A13. Blood sugar levels (BSL) of NOD mice in group 2 treated subcutaneously with bovine insulin-loaded at a dose of 1.5 IU/kg.

NOD mice	Time (minutes)		0	15	30	45	60	90	120
Mouse 4	BSL	mg/dl	355	475	288	129	63	55	41
	BSL	%	100	134	81	36	18	16	12
Mouse 9	BSL	mg/dl	362	381	315	150	96	38	27
	BSL	%	100	105	87	41	27	11	8
Mouse 7	BSL	mg/dl	111	89	40	32	40	85	150
	BSL	%	100	80	36	29	36	77	135

Table A14. Blood sugar levels (BSL) of NOD mice in group 2 treated subcutaneously with Industrial NS insulin-loaded at a dose of 1.5 IU/kg.

NOD mice	Time (minutes)		0	15	30	45	60	90	120
Mouse 19	BSL	mg/dl	308	339	174	76	51	30	22
	BSL	%	100	110	57	25	17	10	7
Mouse 25	BSL	mg/dl	44	33	20	18	20	---*	
	BSL	%	100	75	46	41	46	---*	
Mouse 11	BSL	mg/dl	103	71	33	25	18	16	16
	BSL	%	100	69	32	24	18	16	16

*interruption of the experiment

Table A15. Blood sugar levels (BSL) of NOD mice in group 3 used as a control (oral administration of saline solution).

DIABETIC NOD mice	Mouse 1		Mouse 7		Mouse 20		Mouse 21	
Time (minutes)	BSL							
	mg/dl	%	mg/dl	%	mg/dl	%	mg/dl	%
0	49	100	109	100	78	100	96	100
15	236	482	148	136	186	239	300	313
30	332	678	106	97	140	180	274	285
45	351	716	117	107	124	159	240	250
60	295	602	134	123	148	190	208	217
90	221	451	112	103	114	146	126	131
120	204	416	105	96	106	136	90	94
NON-DIABETIC NOD mice	Mouse 11		Mouse 13		Mouse 22		Mouse 24	
Time (minutes)	BSL							
	mg/dl	%	mg/dl	%	mg/dl	%	mg/dl	%
0	88	100	85	100	103	100	112	100
15	116	132	155	182	114	111	111	99
30	124	141	173	204	122	118	137	122
45	132	150	166	195	143	139	141	126
60	123	140	165	194	123	119	131	117
90	116	132	147	173	100	97	111	99
120	92	105	113	133	83	81	91	81

Table A16. Blood sugar levels (BSL) of NOD mice in group 3 used as a control (oral administration of insulin solution at a dose of 60 IU/kg).

DIABETIC NOD mice	Time (minutes)		0	15	30	45	60	90	120
Mouse 4	BSL	mg/dl	>600	>600	>600	>600	>600	>600	467
	BSL	%	>100	>100	>100	>100	>100	>100	78
Mouse 7	BSL	mg/dl	526	>600	>600	>600	>600	>600	>600
	BSL	%	100	>114	>114	>114	>114	>114	>114
Mouse 20	BSL	mg/dl	550	>600	>600	>600	>600	>600	>600
	BSL	%	100	>109	>109	>109	>109	>109	>109
Mouse 21	BSL	mg/dl	221	448	474	423	442	299	158
	BSL	%	100	203	215	191	200	135	72
Mouse 15	BSL	mg/dl	117	201	234	177	157	141	121
	BSL	%	100	172	200	151	134	121	103
Mouse 10	BSL	mg/dl	119	345	252	265	204	177	144
	BSL	%	100	290	212	223	171	149	121
Mouse 4	BSL	mg/dl	511	>600	>600	>600	>600	>600	578
	BSL	%	100	>117	>117	>117	>117	>117	113

Table A16. Blood sugar levels (BSL) of NOD mice in group 3 used as a control (oral administration of insulin solution at a dose of 60 IU/kg) (*continued*).

DIABETIC NOD mice	Time (minutes)		0	15	30	45	60	90	120
Mouse 7	BSL	mg/dl	154	573	>600	>600	>600	>600	552
	BSL	%	100	372	>390	>390	>390	>390	358
Mouse 20	BSL	mg/dl	357	590	594	>600	>600	>600	535
	BSL	%	100	165	166	>168	>168	>168	150
Mouse 21	BSL	mg/dl	101	203	290	308	213	130	73
	BSL	%	100	201	287	305	211	129	72
Mouse 15	BSL	mg/dl	113	334	316	246	220	177	133
	BSL	%	100	296	280	218	195	157	118
Mouse 10	BSL	mg/dl	96	279	298	306	239	183	162
	BSL	%	100	291	310	319	249	191	169
Mouse 19	BSL	mg/dl	126	283	296	314	290	268	249
	BSL	%	100	225	235	249	230	213	198
Mouse 1	BSL	mg/dl	32	242	286	250	225	163	103
	BSL	%	100	756	894	781	703	509	322
Mouse 7	BSL	mg/dl	99	419	365	351	333	266	175
	BSL	%	100	423	369	355	336	269	177
Mouse 20	BSL	mg/dl	121	256	232	218	226	167	111
	BSL	%	100	212	192	180	187	138	92
Mouse 21	BSL	mg/dl	82	222	137	105	96	73	68
	BSL	%	100	271	167	128	117	89	83
Mouse 15	BSL	mg/dl	90	254	219	181	166	125	92
	BSL	%	100	282	243	201	184	139	102
Mouse 1	BSL	mg/dl	31	169	237	264	210	133	81
	BSL	%	100	545	765	852	677	429	261
Mouse 7	BSL	mg/dl	125	433	449	417	412	314	196
	BSL	%	100	346	359	334	330	251	157
Mouse 20	BSL	mg/dl	98	230	157	128	121	95	83
	BSL	%	100	235	160	131	124	97	85
Mouse 21	BSL	mg/dl	90	105	100	93	86	103	113
	BSL	%	100	117	111	103	96	114	126

Table A16. Blood sugar levels (BSL) of NOD mice in group 3 used as a control (oral administration of bovine insulin solution at a dose of 60 IU/kg) (*continued*).

NON-DIABETIC NOD mice	Time (minutes)		0	15	30	45	60	90	120
Mouse 11	BSL	mg/dl	116	183	120	131	115	104	96
	BSL	%	100	158	103	113	99	90	83
Mouse 22	BSL	mg/dl	95	114	97	81	67	64	70
	BSL	%	100	120	102	85	71	67	74
Mouse 13	BSL	mg/dl	92	137	108	79	78	71	74
	BSL	%	100	149	117	86	85	77	80
Mouse 24	BSL	mg/dl	70	107	82	50	41	40	50
	BSL	%	100	153	117	71	59	57	71
Mouse 5	BSL	mg/dl	114	134	103	112	99	84	90
	BSL	%	100	118	90	98	87	74	79
Mouse 11	BSL	mg/dl	82	178	144	133	123	99	100
	BSL	%	100	217	176	162	150	121	122
Mouse 13	BSL	mg/dl	79	86	74	87	82	86	82
	BSL	%	100	109	94	110	104	109	104
Mouse 22	BSL	mg/dl	64	98	112	131	106	79	67
	BSL	%	100	153	175	205	166	123	105
Mouse 23	BSL	mg/dl	74	172	132	122	120	94	81
	BSL	%	100	232	178	165	162	127	110
Mouse 24	BSL	mg/dl	80	137	141	124	121	91	90
	BSL	%	100	171	176	155	151	114	113
Mouse 25	BSL	mg/dl	73	178	146	161	159	112	100
	BSL	%	100	244	200	221	218	153	137

Table A17. Blood sugar levels (BSL) of NOD mice in group 3 treated subcutaneously with bovine insulin at a dose of 1.5 IU/kg.

DIABETIC NOD mice	Time (minutes)		0	15	30	45	60	90	120	NON-DIABETIC NOD mice	Time (minutes)		0	15	30	45	60	90	120
Mouse 1	BSL	mg/dl	36	165	137	88	83	33	30	Mouse 11	BSL	mg/dl	100	89	48	33	28	31	40
	BSL	%	100	458	381	244	231	92	83		BSL	%	100	89	48	33	28	31	40
Mouse 7	BSL	mg/dl	162	267	88	72	75	104	125	Mouse 13	BSL	mg/dl	61	74	49	35	28	48	78
	BSL	%	100	165	54	44	46	64	77		BSL	%	100	121	80	57	46	79	128
Mouse 20	BSL	mg/dl	103	173	70	65	76	81	88	Mouse 22	BSL	mg/dl	82	63	33	29	25	23	30
	BSL	%	100	168	68	63	74	79	85		BSL	%	100	77	40	35	31	28	37
Mouse 21	BSL	mg/dl	106	137	65	60	52	66	71	Mouse 24	BSL	mg/dl	76	73	39	35	33	26	70
	BSL	%	100	129	61	57	49	62	67		BSL	%	100	96	51	46	43	34	92
Mouse 1	BSL	mg/dl	35	240	164	72	46	30	25	Mouse 11	BSL	mg/dl	108	76	35	23	---*		
	BSL	%	100	686	469	206	131	86	71		BSL	%	100	70	32	21			
Mouse 7	BSL	mg/dl	158	145	74	47	40	88	128	Mouse 22	BSL	mg/dl	85	73	40	31	29	31	---*
	BSL	%	100	92	47	30	25	56	81		BSL	%	100	86	47	37	34	37	
Mouse 20	BSL	mg/dl	150	334	140	110	80	77	81	Mouse 13	BSL	mg/dl	104	79	31	29	28	28	
	BSL	%	100	223	93	73	53	51	54		BSL	%	100	76	30	28	27	27	
Mouse 21	BSL	mg/dl	94	111	64	37	29	26	33	Mouse 24	BSL	mg/dl	109	56	23	21	22	27	
	BSL	%	100	118	68	39	31	28	35		BSL	%	100	51	21	19	20	25	
Mouse 14	BSL	mg/dl	123	91	49	34	27	27	64	Mouse 23	BSL	mg/dl	101	78	38	30	26	27	54
	BSL	%	100	74	40	28	22	22	52		BSL	%	100	77	38	30	26	27	54
Mouse 15	BSL	mg/dl	97	66	28	---*				Mouse 25	BSL	mg/dl	128	BSL	42	27	25	22	22
	BSL	%	100	68	29						BSL	%	100	BSL	33	21	20	17	17
										Mouse 12	BSL	mg/dl	113	96	48	36	BSL	29	36
											BSL	%	100	85	43	32	BSL	26	32

*interruption of the experiment

Table A18. Blood sugar levels (BSL) of NOD mice in group 3 treated orally with Industrial NS insulin-loaded at a dose of 60 IU/kg.

DIABETIC NOD mice	Time (minutes)		0	15	30	45	60	90	120
Mouse 1	BSL	mg/dl	40	260	330	241	174	57	29
	BSL	%	100	650	825	603	435	143	73
Mouse 7	BSL	mg/dl	201	418	407	364	357	264	192
	BSL	%	100	208	203	181	178	131	96
Mouse 20	BSL	mg/dl	369	>600	>600	576	532	509	417
	BSL	%	100	>163	>163	156	144	138	113
Mouse 21	BSL	mg/dl	86	178	128	83	70	69	49
	BSL	%	100	207	149	97	81	80	57
Mouse 14	BSL	mg/dl	135	249	203	156	139	109	102
	BSL	%	100	184	150	116	103	81	76
Mouse 15	BSL	mg/dl	80	191	95	71	69	61	58
	BSL	%	100	239	119	89	86	76	73
Mouse 1	BSL	mg/dl	79	54	37	53	24	21	16
	BSL	%	100	68	47	67	30	27	20
Mouse 7	BSL	mg/dl	251	461	390	349	326	301	206
	BSL	%	100	184	155	139	130	120	82
Mouse 20	BSL	mg/dl	488	>600	>600	>600	598	576	526
	BSL	%	100	>123	>123	>123	>123	118	108
Mouse 21	BSL	mg/dl	98	326	320	289	249	168	102
	BSL	%	100	333	327	295	254	171	104
Mouse 14	BSL	mg/dl	154	103	108	97	99	95	94
	BSL	%	100	67	70	63	64	62	61
Mouse 15	BSL	mg/dl	125	294	273	231	219	126	103
	BSL	%	100	235	218	185	175	101	82
Mouse 4	BSL	mg/dl	160	325	230	200	181	184	177
	BSL	%	100	203	144	125	113	115	111
Mouse 7	BSL	mg/dl	394	562	598	539	554	562	482
	BSL	%	100	143	152	137	141	143	122
Mouse 15	BSL	mg/dl	102	149	110	105	102	77	50
	BSL	%	100	146	108	103	100	76	49

Table A18. Blood sugar levels (BSL) of NOD mice in group 3 treated orally with Industrial NS insulin-loaded at a dose of 60 IU/kg (*continued*).

DIABETIC NOD mice	Time (minutes)		0	15	30	45	60	90	120
Mouse 21	BSL	mg/dl	79	205	155	91	68	68	46
	BSL	%	100	260	196	115	86	86	58
Mouse 4	BSL	mg/dl	565	>600	>600	>600	>600	522	483
	BSL	%	100	106	106	106	106	92	86
Mouse 7	BSL	mg/dl	421	>600	>600	>600	>600	568	518
	BSL	%	100	>143	>143	>143	>143	135	123
Mouse 20	BSL	mg/dl	275	518	485	475	450	348	309
	BSL	%	100	188	176	173	164	127	112
Mouse 21	BSL	mg/dl	91	296	326	267	179	87	65
	BSL	%	100	325	358	293	197	96	71
Mouse 15	BSL	mg/dl	86	217	187	156	127	107	91
	BSL	%	100	252	217	181	148	124	106
NON-DIABETIC NOD mice	Time (minutes)		0	15	30	45	60	90	120
Mouse 11	BSL	mg/dl	90	253	195	129	119	98	72
	BSL	%	100	281	217	143	132	109	80
Mouse 13	BSL	mg/dl	73	90	54	65	42	56	48
	BSL	%	100	123	74	89	58	77	66
Mouse 22	BSL	mg/dl	81	122	116	88	92	75	59
	BSL	%	100	151	143	109	114	93	73
Mouse 24	BSL	mg/dl	73	152	89	81	77	74	65
	BSL	%	100	208	122	111	106	101	89
Mouse 2	BSL	mg/dl	103	225	157	142	110	102	78
	BSL	%	100	218	152	138	107	99	76
Mouse 3	BSL	mg/dl	85	165	145	117	110	73	61
	BSL	%	100	194	171	138	129	86	72
Mouse 11	BSL	mg/dl	115	211	184	148	133	159	124
	BSL	%	100	184	160	129	116	138	108
Mouse 22	BSL	mg/dl	112	115	133	128	115	105	92
	BSL	%	100	103	119	114	103	94	82

Table A18. Blood sugar levels (BSL) of NOD mice in group 3 treated orally with Industrial NS insulin-loaded at a dose of 60 IU/kg (*continued*).

NON-DIABETIC NOD mice	Time (minutes)		0	15	30	45	60	90	120
Mouse 13	BSL	mg/dl	87	131	80	68	87	57	57
	BSL	%	100	151	92	78	100	66	66
Mouse 24	BSL	mg/dl	97	110	128	138	109	91	72
	BSL	%	100	113	132	142	112	94	74
Mouse 2	BSL	mg/dl	114	132	176	124	120	83	88
	BSL	%	100	116	154	109	105	73	77
Mouse 3	BSL	mg/dl	77	96	132	99	82	78	64
	BSL	%	100	125	171	129	107	101	83
Mouse 11	BSL	mg/dl	92	152	133	115	100	83	83
	BSL	%	100	165	145	125	109	90	90
Mouse 22	BSL	mg/dl	82	128	125	109	106	95	65
	BSL	%	100	156	152	133	129	116	79
Mouse 13	BSL	mg/dl	69	114	106	70	60	50	49
	BSL	%	100	165	154	101	87	73	71
Mouse 24	BSL	mg/dl	67	145	110	101	84	65	59
	BSL	%	100	216	164	151	125	97	88
Mouse 11	BSL	mg/dl	71	122	115	110	102	86	74
	BSL	%	100	172	162	155	144	121	104
Mouse 22	BSL	mg/dl	56	128	82	82	76	70	51
	BSL	%	100	229	146	146	136	125	91
Mouse 13	BSL	mg/dl	62	92	70	62	62	56	44
	BSL	%	100	148	113	100	100	90	71
Mouse 24	BSL	mg/dl	59	163	103	94	70	63	65
	BSL	%	100	276	175	159	119	107	110
Mouse 5	BSL	mg/dl	74	143	115	112	104	82	61
	BSL	%	100	193	155	151	141	111	82

Table A19. Blood sugar levels (BSL) of NOD mice in group 3 treated subcutaneously with industrial NS insulin-loaded at a dose of 1.5 IU/kg.

DIABETIC NOD mice	Time (minutes)		0	15	30	45	60	90	120
Mouse 4	BSL	mg/dl	347	243	123	68	54	62	114
	BSL	%	100	70	35	20	16	18	33
Mouse 7	BSL	mg/dl	493	486	125	96	87	121	184
	BSL	%	100	99	25	20	18	25	37
Mouse 20	BSL	mg/dl	102	255	73	67	46	38	43
	BSL	%	100	250	72	66	45	37	42
Mouse 21	BSL	mg/dl	106	111	51	33	21	22	25
	BSL	%	100	105	48	31	20	21	24
Mouse 14	BSL	mg/dl	142	97	60	32	27	23	33
	BSL	%	100	68	42	23	19	16	23
Mouse 15	BSL	mg/dl	138	64	47	23	17	14	22
	BSL	%	100	46	34	17	12	10	16
Mouse 4	BSL	mg/dl	435	324	117	69	40	46	106
	BSL	%	100	75	27	16	9	11	24
Mouse 7	BSL	mg/dl	457	>600	316	168	91	67	55
	BSL	%	100	131	69	37	20	15	12
Mouse 20	BSL	mg/dl	362	547	252	130	64	24	29
	BSL	%	100	151	70	36	18	7	8
Mouse 21	BSL	mg/dl	109	299	113	73	34	18	20
	BSL	%	100	274	104	67	31	17	18
Mouse 15	BSL	mg/dl	128	91	33	---*			
	BSL	%	100	71	26	---*			
Mouse 14	BSL	mg/dl	190	172	35	20	19	---*	
	BSL	%	100	91	18	11	10	---*	

*interruption of the experiment

Table A19. Blood sugar levels (BSL) of NOD mice in group 3 treated subcutaneously with industrial NS insulin-loaded at a dose of 1.5 IU/kg (*continued*).

NON-DIABETIC NOD mice	Time (minutes)		0	15	30	45	60	90	120
Mouse 11	BSL	mg/dl	78	90	47	31	23	23	22
	BSL	%	100	115	60	40	30	30	28
Mouse 22	BSL	mg/dl	84	66	28	21	18	19	24
	BSL	%	100	79	33	25	21	23	29
Mouse 13	BSL	mg/dl	73	67	30	19	23	18	20
	BSL	%	100	92	41	26	32	25	27
Mouse 24	BSL	mg/dl	67	62	31	22	25	14	20
	BSL	%	100	93	46	33	37	21	30
Mouse 2	BSL	mg/dl	76	84	42	30	23	23	35
	BSL	%	100	111	55	40	30	30	46
Mouse 3	BSL	mg/dl	60	70	36	26	23	16	19
	BSL	%	100	117	60	43	38	27	32
Mouse 11	BSL	mg/dl	119	97	40	22	19	---*	
	BSL	%	100	82	34	19	16	---*	
Mouse 22	BSL	mg/dl	105	71	24	16	17	17	14
	BSL	%	100	68	23	15	16	16	13
Mouse 13	BSL	mg/dl	93	77	29	19	19	20	21
	BSL	%	100	83	31	20	20	22	23
Mouse 24	BSL	mg/dl	57	51	19	14	15	19	19
	BSL	%	100	90	33	25	26	33	33
Mouse 5	BSL	mg/dl	107	59	35	32	29	29	35
	BSL	%	100	55	33	30	27	27	33
Mouse 2	BSL	mg/dl	75	63	34	24	23	21	22
	BSL	%	100	84	45	32	31	28	29
Mouse 3	BSL	mg/dl	86	60	27	25	23	22	27
	BSL	%	100	70	31	29	27	26	31

*interruption of the experiment

Table A20. Blood sugar levels of STZ-induced diabetic mice in the efficacy study.

	Blood sugar levels (mg/dl)						Blood sugar levels (%)					
Time (minutes)	0	15	30	60	90	120	0	15	30	60	90	120
Saline solution Control (diabetic mice)	347	504	442	493	490	509	100	145	127	142	141	147
	411	>600	>600	580	511	548	100	>146	>146	141	124	133
	303	>600	517	545	476	426	100	>198	171	180	157	141
	386	>600	>600	498	489	466	100	>155	>155	129	127	121
	464	>600	>600	>600	>600	>600	100	>129	>129	>129	>129	>129
	494	>600	>600	>600	>600	>600	100	>122	>122	>122	>122	>122
	382	524	>600	507	572	470	100	137	>157	133	150	123
	302	553	>600	507	510	480	100	183	>199	168	169	159
	451	517	>600	553	650	550	100	115	>133	123	144	122
	528	>600	>600	>600	>600	>600	100	>114	>114	>114	>114	>114
Insulin solution Control (diabetic mice)	514	>600	578	564	>600	541	100	>117	113	110	>117	105
	>600	>600	>600	>600	>600	>600	>100	>100	>100	>100	>100	>100
Control (healthy mice)	159	300	268	186	269	182	100	189	169	117	169	115
	131	197	152	150	134	149	100	150	116	115	102	114
	175	215	177	180	185	147	100	123	101	103	106	84
	149	355	289	266	197	156	100	238	194	179	132	105
	141	276	219	191	182	164	100	196	155	136	129	116
	150	315	207	190	179	180	100	210	138	127	119	120
	137	348	357	320	206	169	100	254	261	234	150	123
	155	321	257	304	222	191	100	207	166	196	143	123
	162	309	259	241	181	165	100	191	160	149	112	102
	146	358	295	217	179	151	100	245	202	149	123	103

Table A20. Blood sugar levels of STZ-induced diabetic mice in the efficacy study (*continued*).

	Blood sugar levels (mg/dl)						Blood sugar levels (%)					
Time (minutes)	0	15	30	60	90	120	0	15	30	60	90	120
Insulin SC injection 1.5 IU/Kg	374	>600	310	130	110	126	100	>160	83	35	29	34
	350	554	223	106	77	53	100	158	64	30	22	15
	500	383	129	120	85	76	100	77	26	24	17	15
	445	567	230	60	70	63	100	127	52	14	16	14
	388	525	242	93	70	61	100	135	62	24	18	16
	446	420	240	131	115	101	100	94	54	29	26	23
	438	482	238	120	70	66	100	110	54	27	16	15
Industrial NS insulin-loaded oral gavage 90 IU/Kg	391	593	395	348	386	459	100	152	101	89	99	117
	480	539	528	491	449	464	100	112	110	102	94	97
	433	535	447	391	408	425	100	124	103	90	94	98
	435	510	540	411	439	525	100	117	124	95	101	121
	444	588	187	95	83	119	100	132	42	21	19	27
	309	570	533	480	413	507	100	185	173	155	134	164
	455	584	575	552	559	510	100	128	126	121	123	112
	324	544	164	138	150	169	100	168	51	43	46	52
	349	514	518	488	412	395	100	147	148	140	118	113
	478	576	344	220	267	320	100	121	72	46	56	67
	451	>600	595	522	560	520	100	>133	132	116	124	115
	472	570	455	361	298	298	100	121	96	77	63	63
	474	597	566	594	509	530	100	126	119	125	107	112
	432	>600	565	375	533	505	100	>139	131	87	123	117
	526	>600	210	142	163	54	100	>114	40	27	31	10
	348	526	362	138	110	102	100	151	104	40	32	29
	414	>600	520	569	560	510	100	>145	126	137	135	123
	441	510	406	346	368	334	100	116	92	79	83	76
	504	>600	557	546	499	478	100	>119	111	108	99	95

Table A20. Blood sugar levels of STZ-induced diabetic mice in the efficacy study (*continued*).

Time (minutes)	Blood sugar levels (mg/dl)						Blood sugar levels (%)					
	0	**15**	**30**	**60**	**90**	**120**	**0**	**15**	**30**	**60**	**90**	**120**
Industrial NS insulin-loaded oral gavage 120 IU/Kg	407	503	528	>600	469	488	100	124	130	>147	115	120
	341	489	559	478	403	396	100	143	164	140	118	116
	326	516	312	111	82	77	100	158	96	34	25	24
	321	>600	519	555	464	494	100	>187	162	173	145	154
	232	41	440	540	247	244	100	18	190	233	107	105
	383	479	510	535	473	468	100	125	133	140	124	122
Industrial NS insulin-loaded S.C injection 1.5 IU/Kg	554	450	221	105	99	96	100	81	40	19	18	17
	449	535	254	141	103	97	100	119	57	31	23	22
	451	533	254	116	122	103	100	118	56	26	27	23
Insulin-loaded LC Oral gavage 90 IU/kg	440	420	377	380	389	384	100	96	86	86	88	87
	418	519	555	447	328	157	100	124	133	107	79	38
	474	>600	>600	>600	529	538	100	>127	>127	>127	112	114
	305	479	487	481	399	401	100	157	160	158	131	132
	279	521	484	437	400	377	100	187	174	157	143	135
	539	>600	>600	564	516	486	100	>111	>111	105	96	90
	461	>600	543	540	516	486	100	>130	118	117	112	105
	529	>600	596	600	541	534	100	>113	>113	>113	102	101
	485	596	497	433	335	241	100	123	103	89	69	50
	481	>600	>600	582	513	562	100	>125	>125	121	107	117
Insulin LC CITR S.C injection 1.5 IU/Kg	461	>600	>600	>600	>600	>600	100	>130	>130	>130	>130	>130
	471	599	291	124	76	95	100	127	62	26	16	20
	394	600	303	136	118	122	100	152	77	35	30	31

Training activities

During my PhD, alongside the scientific activity, I attended a number of training activities. These include the courses present in the Table 1.

Table 34. List of courses

Course title	Instructor	University / Department	Hours	CFU
Introduction to Scientific Programming (in Python)	Dr. Alessandro Erba	Department of chemistry/ University of Turin	20	5
2019_Food-omics: integrated analytical strategies for in-depth chemical characterization of food	Prof.ssa Chiara Cordero Dott.ssa Erica Liberto	Department of Science and Pharmaceutical Technology/ University of Turin	16	4
2019 Structure and function of natural and engineered enzymes	Prof. Gianfranco Gilardi Dott.ssa Giovanna Di Nardo	Department of Science and Pharmaceutical Technology/ University of Turin	16	4
Training course "Bibliography and bibliometrics like pros" 2019	-	Department of Medicine/ University of Turin	8	2
English for Scientific Academic purposes – PhD students	Jemma Robinson	University of Turin in collaboration with the University Institute of European Studies	30	7.5
General training course for workers on hygiene and safety	-	University of Turin	4	1

The conferences, seminars and workshops attended are in Table 2.

Table 35. list of conferences, seminars and workshops

Title	Kind of activity	Hours	University
PhD Program in Chemical and Materials Sciences-The students of XXXIII Cycle presented their research activities	Workshop	11.5	University of Turin
PhD thesis defenses Dr. Rubin Pedrazzo , Dr. Kumar Dhakar	Thesis defense	1.5	
Open Science and Fair Data	Workshop	7	
Horizon Europe and Project Writing	Seminar	4	
1st EIT Food Italy Workshop	Workshop	8	
The story of four APIs: from bench to plant_ Dr. V. Farina	Seminar	4	

Table 36. list of conferences, seminars and workshops (*continued*).

Title	Kind of activity	Hours	University
Bio-soft nanomaterials based on amphiphilic cyclodextrins	Seminar	1.5	University of Turin
Workshop sulla ricerca bibliografica_2019	Workshop	8	
Alimenti a fini medici speciali, integratori alimentari, dispositivi medici: Aggiornamenti normativi	Workshop	8	
Machine Learning meets chemistry	Seminar	6.5	
Synthesis of cyclodextrin derivatives	Seminar	1.5	
ACS Career Day Young Chemist Committee (YCC)	Seminar	4	Young Chemist Committee
Microcalorimetria delle nanoparticelle: bio e nano insieme per la medicina del futuro	Webinar	1.5	Alfatest
I vaccini necessitano di controlli accurati. Come verificare lo stato di aggregazione per evitare risposte immunogeniche	Webinar	1.5	
From Stimuli Responsive and Shape Memory Materials to Algorithmic Materials that Mimic Behaviorists´ Classical Conditioning	Virtual DCMIC seminar #1	1	University of Turin
Supramolecular Broad-Spectrum Antivirals	Virtual DCMIC seminar #2	1	
Understanding Gene Transcription and Genome Organization using Electron Microscopy	Virtual DCMIC seminar #3	1	
Signal and Data Processing Workflows for Untargeted Chemical Analysis: Sensor Array and Mass Spectrometry Analysis of Complex Gas Samples	Virtual DCMIC seminar #4	1	
Additive manufacturing and bioprinting techniques used for the creation of tissue and organ constructs	Virtual DCMIC seminar #7	1	
Crystalline-nanoporous polymers and their possible industrial applications	Seminar	1	
High resolution separation of nanoparticles and macromolecules	Workshop	10	
Challenges in Protein drug formulation: From stability prediction to protein excipient interaction studies	Seminar	1	

I attended also the Summer Schools below:

- 4th International Cyclodextrins Summer School, Politecnico di Milano, Milano (Italia), 10/06/19-12/06/19 **CFU: 3**

- Green Chemistry Postgraduate Summer School, Italy, 06/07/20-10/07/20. **CFU: 5,** with the following poster: "β-cyclodextrin nanosponges for the delivery of insulin"
Silvia Lucia Appleton, Maria Tannous, Monica Argenziano, Arianna Carolina Rosa, Davide Rossi, Fabrizio Caldera, Anna Scomparin, Francesco Trotta, Roberta Cavalli.

I was involved in the following papers:

- I. Krabicová, S.L Appleton, M. Tannous, G. Hoti, F. Caldera, A.R Pedrazzo, C. Cecone, R. Cavalli and F. Trotta "History of Cyclodextrin Nanosponges", *Polymers* **2020**; 12 (5), 1122.

- S. Acquadro, S.L Appleton, A. Marengo, C. Bicchi, B. Sgorbini, M. Mandrone, F. Gai, P.G Peiretti, C. Cagliero and P. Rubiolo "Grapevine Green Pruning Residues as a Promising and Sustainable Source of Bioactive Phenolic Compounds" *molecules* **2020**; 25(3): 464.

- A.R Pedrazzo, F. Caldera, M. Zanetti, S.L Appleton, N.K Dhakar, and F. Trotta "Mechanochemical green synthesis of hyper-crosslinked cyclodextrin polymers" *Beilstein J Org Chem*. **2020**; 16: 1554–1563.

- C. Cecone, G. Hoti, I. Krabicová, S.L Appleton, F. Caldera, P. Bracco, M. Zanetti and F. Trotta "Sustainable synthesis of cyclodextrin-based polymers by exploiting natural deep eutectic solvents" *Green chemistry* **2020**; 17, 5806-5814.

- S.L Appleton, M. Tannous, M. Argenziano, E. Muntoni, A.C Rosa, D. Rossi, F. Caldera, A. Scomparin, F. Trotta, R. Cavalli, "Nanosponges as protein delivery systems: insulin, a case study" *International Journal of pharmaceutics* **2020**; 590.

- G. Hoti, F. Caldera, C. Cecone, A. Pedrazzo, A. Anceschi, S.L. Appleton, Y.K. Monfared, and F. Trotta. **2021**. "Effect of the Cross-Linking Density on the Swelling and Rheological Behavior of Ester-Bridged β-Cyclodextrin Nanosponges." *Materials* 14 (3): 1–20. https://doi.org/10.3390/ma14030478.

- S.L. Appleton, S. Navarro-Orcajada, F.J. Martínez-Navarro, F. Caldera, J.M. López-Nicolás, F. Trotta, A. Matencio. "Cyclodextrins as Anti-inflammatory Agents: Basis, Drugs and Perspectives". *Biomolecules* **2021**, *11*, 1384.

- G. Hoti, S.L. Appleton, A.R. Pedrazzo, C. Cecone, A. Matencio, F. Trotta and F. Caldera **2021**. "Strategies to Develop Cyclodextrin-Based Nanosponges for Smart Drug Delivery", *IntechOpen,* DOI: 10.5772/intechopen.100182.